University of Tennessee, Knoxville

TRACE: Tennessee Research and Creative Exchange

Doctoral Dissertations

Graduate School

12-2000

ENU-induced mutations reveal quaking functions in embryogenesis and postnatal myelination

Janice K. Noveroske

Follow this and additional works at: https://trace.tennessee.edu/utk_graddiss

Recommended Citation

Noveroske, Janice K., "ENU-induced mutations reveal quaking functions in embryogenesis and postnatal myelination. " PhD diss., University of Tennessee, 2000.
https://trace.tennessee.edu/utk_graddiss/8372

This Dissertation is brought to you for free and open access by the Graduate School at TRACE: Tennessee Research and Creative Exchange. It has been accepted for inclusion in Doctoral Dissertations by an authorized administrator of TRACE: Tennessee Research and Creative Exchange. For more information, please contact trace@utk.edu.

To the Graduate Council:

I am submitting herewith a dissertation written by Janice K. Noveroske entitled "ENU-induced mutations reveal quaking functions in embryogenesis and postnatal myelination." I have examined the final electronic copy of this dissertation for form and content and recommend that it be accepted in partial fulfillment of the requirements for the degree of Doctor of Philosophy, with a major in Biochemistry and Cellular and Molecular Biology.

Jeff A. MacCabe, Major Professor

We have read this dissertation and recommend its acceptance:

Monica J. Justice, Jim D. Godkin, Ranjan Ganguly

Accepted for the Council:

Carolyn R. Hodges

Vice Provost and Dean of the Graduate School

(Original signatures are on file with official student records.)

To the Graduate Council:

I am submitting herewith a dissertation written by Janice K. Noveroske entitled "ENU-Induced Mutations Reveal *Quaking* Functions in Embryogenesis and Postnatal Myelination." I have examined the final copy of this dissertation for form and content and recommend that it be accepted in partial fulfillment of the requirements for the degree of Doctor of Philosophy, with a major in Biochemistry, Cellular and Molecular biology.

Jeff A. MacCabe

Jeff A. MacCabe, Major Professor

We have read this dissertation
and recommend its acceptance:

Monica J. Justice

J D Godkin

Ranjan Ganguly

Accepted for the Council:

Associate Vice Chancellor and
Dean of The Graduate School

ENU-INDUCED MUTATIONS REVEAL *QUAKING* FUNCTIONS IN EMBRYOGENESIS AND POSTNATAL MYELINATION

A Dissertation
Presented for the
Doctor of Philosophy
Degree
The University of Tennessee, Knoxville

Janice K. Noveroske
December 2000

DEDICATION

This thesis is dedicated to the two most generous people in the world who taught me everything I ever really needed to know.

To my Dad, who taught me how to fish (but still bates my hooks).

To my Mom, who taught me to be perceptive to people in need of a friend.

ACKNOWLEDGEMENTS

I would like to thank my committee members, Dr. Ranjan Ganguly, and Dr. Jim Godkin for their time and input on this project. I especially thank Dr. Jeff MacCabe and Dr. Monica Justice for their support in my graduate career and for the amazing scientific opportunities they have given me. I also extend the highest of thanks to Dr. Mary Ann Handel for being a wonderful scientific mentor and model of dignity for myself and other women in science. I thank my scientific collaborators, Dr. Rebecca Hardy, Dr. Jeff Noebels, Caleb Davis, Dr. Vinciane Gaussin and Dr. Hannes Vogel for their time and scientific expertise.

Thanks goes out to my family for keeping me grounded like no one but family can. I also extend the warmest of thanks to my extended family and dearest friends Jerilyn Swann, Beverly Stanford and Sylvia McLain for their warm hearts and free spirit influence. A very special thanks also goes to Sharon Thomas for her unending support and for keeping me doubled over laughing throughout this project. Lastly, I thank Andrew Salinger, Hisashi Nakamura and Diego Lorenzetti for their support, scientific advice and all around good natures that have been such a pleasure to work with.

ABSTRACT

Since the discovery of the mouse *quaking viable* allele (qk^{v}) in 1964, researchers have attempted to elucidate the function of *quaking* in postnatal brain myelination. More recently, a critical role for *quaking* in embryogenesis was revealed, but little has been determined on how the loss of *quaking* function leads to embryonic death. In the work presented here, we report that the defect in the embryonic lethal qk^{k2} allele is a T to A transversion in the KH domain, and that homozygous qk^{k2} mutant embryos die from cardiovascular defects. Antibodies against the vascular endothelial marker PECAM-1 reveal that qk^{k2} homozygous mutants completely lack the yolk sac vascular network present in wild-type embryos.

Hearts of qk^{k2}/qk^{k2} embryos lack the looping morphogenesis of their wild-type littermates, but *Nkx2.5*, a gene that functions in cardiac looping, is expressed in a wild-type pattern. Cardiac myocytes in mutant embryos also express α–sarcomeric actin protein and whole hearts in organ culture were found to beat at wild-type rates. Real-time quantitative RT-PCR reveals that cardiac developmental markers are expressed at normal levels in qk^{k2} mutant hearts but that expression of the vascularization gene, *Vegf*, is increased two-fold compared to wild-type. In addition, the cell cycle genes *Ccnd1*, *Cdkn1a* and *Cdkn1c* have abnormal expression compared to wild-type embryonic hearts.

The neural associated genes *Shh*, *Foxa2*, *Fgf8*, and *Pax6* as well as the notochord marker *T*, are all expressed in wild-type patterns in qk^{k2} embryos at the time of death. However, adult carriers of the qk^{k2} allele are significantly more susceptible to chemically induced seizures with the convulsant drug pentylenetetrazole than wild-type animals.

In an effort to further dissect the function of *quaking*, we performed a single generation ENU mutagenesis screen to create new alleles. We report here, the generation of the qk^{e5} allele which, unlike the previous induced alleles of *quaking*, is homozygous viable.

The qk^{e5} phenotype consists of postnatal *quaking* and seizures, which progresses to severe ataxia and early death. Ultrastructural analysis reveals an almost complete lack of myelin compared to both wild-type and qk^{v}/qk^{v} brains. Protein expression analysis in the postnatal brain shows that like qk^{v}/qk^{v}, qk^{e5}/qk^{e5} mice have low QKI-5 and no QKI-6 and QKI-7 proteins in developing oligodendrocytes. However, oligodendrocytes of both qk^{e5} and qk^{v} homozygous mice express a full range of developmental marker genes indicating that *quaking* may function relatively late in oligodendrocyte development. We determined by electroencephalogram recordings, that qk^{e5}/qk^{e5} surface cortex activity is abnormal and that seizures result in electrical activity characteristic of a decrimental response.

Together these results reveal a previously unsuspected and critical role for *quaking* in cardiovascular development as well as a more important role in postnatal brain myelination then had been determined from 40 years of studies utillizing the qk^{v} allele.

TABLE OF CONTENTS

CHAPTER PAGE

I. LITERATURE REVEIW

ENU Mutagenesis 1
Quaking Allelic Series 4
Quaking Function 5
Project Goals 10

II. EMBRYONIC FUNCTION OF QUAKING

Abstract 12
Introduction 13
Materials and Methods 14
Results 18
Discussion 22

III. NEUROLOGICAL FUNCTION OF QUAKING

Abstract 32
Introduction 32
Materials and Methods 34
Results 38
Discussion 45

IV. SUMMARY AND FUTURE DIRECTIONS 52
REFERENCES 54
APPENDIX 75
VITA 137

LIST OF TABLES

TABLE PAGE

1. Expression and functional evolution of *quaking* 82

2. Whole mount *in situ* genetic markers 102

3. Pentylenetetrazole seizure susceptibility 107

4. Homozygous and compound heterozygous phenotypes of qk^{e5} 111

5. Pentylenetetrazole seizure susceptibility at 42.5 mg/kg 120

6. Pentylenetetrazole seizure susceptibility at 45.5 mg/kg 120

LIST OF FIGURES

FIGURE PAGE

1. Mutagenic action of *N*-ethyl-*N*-nitrosourea 76
2. Mispairing of ENU ethylated bases 78
3. Structure of the *quaking* protein product QKI 80
4. Genomic structure and transcripts of the *quaking* gene 83
5. The Model of *quaking* function 85
6. Molecular defect in the qk^{k2} allele 87
7. Embryo lethality of the qk^{k2} allele 89
8. Vascular differentiation defects in qk^{k2} mutants 91
9. Expression of *quaking* in the yolk sac 93
10. Histological sections of E10.5 embryos 94
11. Expression of heart markers during embryo development 96
12. Embryonic heart rates in organ culture 98
13. Cardiac gene expression by quantitative RT-PCR 99
14. Cell cycle gene expression by quantitative RT-PCR 101
15. Whole mount *in situ* hybridization at E9.5 with *Shh*, *Fgf8* and *Foxa2* ... 103
16. Whole mount *in situ* hybridization at E9.5 with *Pax6* and *T* 105
17. ENU mutagenesis screen for new *qkI* alleles 108
18. *Quaking* allelism test crosses 109
19. Histology of qk^{e5} homozygous brains 112
20. Dysmyelination in qk^{e5} homozygotes 114
21. Electroencephalogram recording apparatus 116
22. Cortical surface electroencephalogram recordings 118
23. Adult brain *qkI* expression 121
24. Oligodendrocyte development 122

LIST OF FIGURES CONTINUED

FIGURE PAGE

25. Postnatal brain QKI-5 and O4 expression 124

26. Postnatal brain QKI-6 and MBP expression 126

27. Postnatal brain QKI-7 and O4 expression 128

28. Postnatal brain PDGFαR and NG2 expression 130

29. Postnatal brain QKI-5 and CNP expression 131

30. Postnatal brain QKI expression 133

31. The *quaking* mutant allele series 135

LIST OF ABBREVIATIONS

bp	Base pair
cDNA	Complementary deoxyribonucleic acid
CNS	Central nervous system
DNA	Deoxyribonucleic acid
E	Embryonic
ENU	*N*-ethyl-*N*-nitrosourea
kb	Kilobase
LFB	Luxol fast blue
μg	Microgram (10^{-6} gram)
μl	Microliter (10^{-6} liter)
N	Sample number
ng	Nanogram (10^{-9} gram)
P	Postnatal
PBS	Phosphate buffered saline
PNS	Peripheral nervous system
PCR	Polymerase chain reaction
PTZ	Pentylenetetrazole
RFLP	Restriction fragment length polymorphism
RNA	Ribonucleic acid
RT	Reverse transcriptase
UTR	Untranslated region

I. LITERATURE REVIEW

ENU MUTAGENESIS

N-ethyl-*N*-nitrosourea (ENU) has become one of the most powerful tools in mammalian genetics. It has the highest mutation rate of any germline mutagen tested in the mouse, allowing phenotype-driven approaches to isolate mutations in any gene of interest. Its ability to produce single base pair mutations *in vivo* allows for a detailed analysis of a gene's normal functions and the physiological consequences when mutated, making it ideal for modeling human diseases.

ENU is a laboratory-synthesized compound that causes random single base pair mutations in a wide variety of organisms (Figure 1) (All figures and tables are found in an appendix at the end of this dissertation). It acts directly through alkylation of nucleic acids without any metabolic processing required for its activation (Justice, 1999; Singer and Dosahjh, 1990). The ethyl group of ENU can be transferred to oxygen or nitrogen radicals at a number of reactive sites that have been identified *in vivo* and *in vitro*. These include the N1, N3 and N7 groups of adenine, the O6, N3 and N7 of guanine, the O2, O4 and N3 of thymine, and the O2 and N3 of cytosine (Justice, 1999; Shibuya and Morimoto, 1993). These transferred ethyl groups are DNA adducts which alone do not constitute a mutation, however, their presence can cause mistaken identity of the ethylated base during DNA replication, which results in mispairing (Figure 2). After two rounds of replication, a single base pair substitution exists that is unidentifiable to cellular repair systems. Although ENU primarily induces point mutations, a few small deletions have been reported (Shibuya and Morimoto, 1993). The most common reported mutations for the mouse germline are AT to TA transversions and AT to GC transitions, which together comprise 82% of the total lesions sequenced. It is generally accepted that these base pair changes are due to the mispairing of alkylated O4-thymine and O2-thymine respectively (Justice, 1999).

ENU and similar compounds that alkylate oxygens, particularly at O4-thymine, O2-thymine and O2-cytosine, tend to be more efficient at mutagenizing pre-meiotic cells (Vogel and Natarajan, 1995) while compounds that induce higher levels of N-alkylations tend to effectively mutagenize post-meiotic cell stages. In addition, promutagens that require metabolic activation for alkylation are more efficient at mutating mid- to late-spermatids but have little if any mutagenic effect in spermatogonial stem cells or metabolically inactive spermatozoa (Vogel *et al.*, 1983; Zijlstra *et al.*, 1989; Zijlstra *et al.*, 1987). In the mouse testis, the action of ENU is most potent in spermatogonial stem cells with its optimal dose producing about one mutation per gene in every 175 to 655 gametes (Hitotsumachi *et al.*, 185; Shedlovsky *et al.*, 1993; Noveroske, Weber and Justice unpublished).

At its optimal mutagenic dose, ENU drastically reduces the number of spermatogonial stem cells in the seminiferous tubules (Russell *et al.*, 1979). As a result, treated males usually undergo a temporary sterile period after which surviving stem cells repopulate the testis through mitosis and meiosis, eventually giving rise to clones of mutagenized sperm. Due to the clonal nature of the sperm produced, an adequate number of offspring need to be observed to ensure enough gametes are sampled but without high risk of re-isolating the same mutation. The appropriate gamete sample size varies with the dose of ENU but an adequate sample for the high doses used in most mutagenesis experiments (300 mg/kg) is 30 – 50 gametes per male.

Various genetic strategies including one-, two- and three-generation screens can be used to isolate new ENU induced mutations with phenotypes of interest (Justice, 1999). A single generation screen is useful when the desired goal is to rapidly generate viable and fertile mutants that represent single gene allele series, modifiers or dominant mutations. Recessive lethal mutations in a defined region of the genome can be identified using two-generation deletion screens. Three-generation pedigree screens may be used to scan the entire genome for a viable mutation of interest or to isolate lethal or sterile alleles in combination with linked markers or balancer chromosomes.

In the mouse germline studies to date, the mutations in 61 ENU induced alleles from 24 loci have been identified (Noveroske *et al.*, 2000). These include 39 missense mutations, 6 nonsense mutations and 16 splice-site mutations. A large number of these lesions result in amorphic proteins that lack function and allow assessment of the null phenotype. The loss-of-function missense mutations are extremely valuable for identifying single amino acids crucial for protein structure or function. This was the case for the isolation of $qk^{kt3/4}$, a recessive embryo lethal allele of the *quaking* locus selected from an ENU mutagenesis screen (Justice and Bode, 1988). This allele revealed an unexpected embryo lethal (null) phenotype resulting from a missense mutation (Ebersole *et al.*, 1996). ENU mutations can also result in the very informative hypomorphic (partial loss of function), antimorphic (opposing/ dominant negative function), and hypermorphic (exaggerated function) protein changes. Hypomorphic changes can allow later acting functions to be revealed as in the case of the mouse *eed* gene. The null allele of this gene causes early embryonic death but an ENU-induced hypomorphic allele allows the mouse to survive embryogenesis and exhibit skeletal transformations along the vertebral column, providing insight into *eed* as a regulator of homeotic genes (Schumacher *et al.*, 1996). The ENU-induced allele of the mouse *Clock* gene produces an antimorphic protein product that antagonizes normal protein function (King *et al.*, 1997a; King *et al.*, 1997b), while the protein product of the β-globin allele (Hbb^{d4}) is an excellent example of a hypermorphic protein change. The Hbb^{d4} protein has an increased affinity for oxygen which causes a reduction of a stable heme-heme interaction, resulting in polycythemia (Peters *et al.*, 1985).

The ability of ENU to produce a range of different protein product effects and mutant phenotypes has made it useful in creating series of alleles at single loci to uncover multiple gene functions. An extensive ENU mutant allele series exists for the *MyoVA* (*dilute*) locus, which includes alleles with gradations of diluted (lightened) coat color, in combination with different levels of severity of neurological problems (Huang *et al.*, 1998a; Huang *et al.*, 1998b). The complete loss of function at *dilute* produces mice that have a very diluted coat color accompanied by severe neurological abnormalities. However, many intermediate alleles provide valuable information about the functional complexity of *MyoVA*.

The mutant mice that are being created from ongoing ENU mutagenesis projects are a valuable resource for analysis of gene functions on the molecular level and studies of the physiological consequences of mutations in the whole organism.

QUAKING ALLELIC SERIES

The *quaking viable* allele (*qk*^{v}) which originally defined the *quaking* locus, is the result of a spontaneous 1 Mb deletion (Ebersole *et al.*, 1992; Sidman *et al.*, 1964). In addition, there are four embryo lethal alleles that were induced by ENU mutagenesis. The *qk*^{kt1}, *qk*^{k2} and *qk*$^{kt3/4}$ alleles were produced in a single generation screen to create new alleles in the *t*-region of mouse chromosome 17 (Justice and Bode, 1986; Justice and Bode, 1988). The *qk*$^{l-1}$ allele was isolated during a two generation screen to identify embryonic lethal alleles in this same region (Shedlovsky *et al.*, 1986). These alleles not only identified a previously unknown role for *quaking* in embryonic development, but were critical resources for its cloning and confirmation as a candidate gene (Ebersole *et al.*, 1996).

No two *quaking* alleles are alike in the phenotypes that they produce as homozygotes, heterozygotes or compound heterozygotes. This range of phenotypes reflects the fact that the mutations responsible alter different points in the pathway of *quaking* function. In the *qk*^{v} allele, the coding region of *quaking* is intact but expression is lost specifically in myelinating cells of the CNS and PNS, implicating this allele as a regulatory mutation (Ebersole *et al.*, 1996; Hardy *et al.*, 1996). This results in a dysmyelination of the CNS causing severe *quaking* and seizures. The embryonic lethal allele *qk*$^{kt3/4}$ contains an A to G transition in the coding region of *quaking* that results in a glutamic acid to glycine amino acid change (Ebersole *et al.*, 1996). Functional studies of proteins containing this amino acid alteration reveal that it abolishes dimerization of *quaking* proteins (Chen and Richard, 1998). The *qk*$^{l\text{-}1}$ allele is the result of an A to G base pair change which causes the loss of a splice site necessary to produce the transcript coding for the nuclear isoform of *quaking* protein (Cox *et al.*, 1999). Thus, the loss of the nuclear isoform alone is sufficient to cause embryonic death. The defect in the embryonic lethal allele *qk*^{kt1} remains undetected and the defect in *qk*^{k2} will be discussed in the work presented here.

The variety of effects produced on the molecular/cellular level and the range of phenotypes created, have made the *quaking* allele series a useful resource for both embryonic and postnatal brain development studies.

QUAKING FUNCTION

The cloning of the *quaking* gene (*qkI*) revealed that it encodes a 319-327 amino acid RNA binding protein (Figure 3) (Ebersole *et al.*, 1996). *Quaking* proteins (QKI) contain a central KH (RNA binding) domain flanked by two highly conserved domains designated QUA1 and QUA2 which are necessary for high affinity RNA binding (Jacque *et al.*, 1983). They also contain RG boxes, which are indicative of RNA binding proteins, as well as features that suggest QKI acts downstream in a signal transduction pathway. These include proline rich regions containing putative SH3 binding sites and a tyrosine tail for phosphorylation/dephosphorylation activation. These features place QKI in the "STAR" (Signal Transduction and Activation of RNA) family of proteins (Vernet and Artzt, 1997).

Members of this family share high homology in the approximately 200 amino acid "STAR" domain that contains the KH domain and flanking QUA sequence. They also, almost without exception, contain the response elements for signal transduction activation. *Sam68, gld-1, SF1* and *Bbp1p* are the most thoroughly studied of the more than 30 STAR family members. *Sam68/SAM68* (SRC-associated in mitosis) from both mouse and human, codes for a nuclear phosphoprotein (Darnell *et al.*, 1994b; Fumagalli *et al.*, 1994; Taylor and Shalloway, 1994). This protein is expressed in mitotic cells and transformed 3T3 cells, functioning downstream of SRC signaling. The *C. elegans* gene *gld-1* is a tumor suppressor with wild-type function in oocyte differentiation (Jones *et al.*, 1996; Jones and Schedl, 1995). In *gld-1* null mutants, oocytes exit meiotic prophase and proliferate mitotically forming germ line tumors. Unlike the other STAR family members, however, *gld-1* does not contain features of signal transduction activation. Human *SF1* and its yeast homologue *Bbp1p* share the least sequence similarity with other STAR members but they retain RNA binding ability and contain proline rich regions and motifs for binding SRC-type kinases (Abovich and Roshbash, 1997; Arning *et al.*, 1996; Berglund *et al.*, 1997; Kramer, 1992). Human *SF1* is required for prespliceosome complex assembly and *Bbp1p* is also an essential splicing factor (Abovich and Roshbash, 1997; Arning *et al.*, 1996).

Quaking homologues have been cloned in human (*hqk*), *Xenopus* (*Xqua*), chicken (*qk*), Zebrafish (*zqk*) and *Drosophila* (*who/how/qkr93F*) (Baehrecke, 1997; Fyrberg *et al.*, 1997; Mezquita *et al.*, 1998; Tanaka *et al.*, 1997; Zaffran *et al.*, 1997; Zorn and Krieg, 1997). The expression patterns of each of these homologues and the loss of function phenotypes generated in *Drosophila, Xenopus* and mouse imply that primitive organisms require *quaking* for development of mesodermal structures while in higher organisms, *quaking* takes on a more specialized role in ectodermal neural development (Table 1). In *Drosophila, how* (*held out wings*) expression is exclusive to mesodermal tissue during development and is maintained in adult heart and muscle (Zaffran *et al.*, 1997). A functional role in muscle is evident from null alleles of *how*, which die prior to hatching, exhibiting reduced muscle movement and low heart rates (Zaffran *et al.*, 1997). *Drosophila* with partial loss of *how* function develop into adults but are immobile with wings that are held straight out due to improper muscle attachment. In *Xenopus*, *Xqua* transcripts are found in the heart, dorsal mesoderm and neural tube (Zorn and Krieg, 1997). Overexpression of *Xqua* causes reduced notochord and head development leading to embryonic death. *Xqua* is also expressed in the adult brain but its function there has not been assessed. In mice, the highest organism in which *quaking* function has been studied, *qkI* is expressed in embryonic heart and neural tissues, as well as at high levels in the postnatal brain (Ebersole *et al.*, 1996). Embryonic lethal *qkI* alleles result in neural and heart defects while partial loss of function in the viable allele causes adult CNS dysmyelination (Justice and Bode, 1986; Justice and Bode, 1988; Shedlovsky *et al.*, 1988; Sidman *et al.*, 1964). The majority of the human *quaking* sequence *hqk* has been determined from Expressed Sequence Tags (EST) database fragments (Zorn and Krieg, 1997). The *hqk* gene maps to the chromosomal location 6q25.7 in humans which is syntenic to that of mouse *quaking* in the proximal region of mouse chromosome 17 (Vernet and Artzt, 1997). The mouse *qkI* and human *hqk* are over 90% conserved at the amino acid level but no human defects associated with hqk mutations have yet been reported.

Analysis of mouse cDNA reveals five alternative *quaking* transcripts designated qkI-5a, qkI-5b, qkI-6, qkI-7 and qkIΔKH (Figure 4) that code for QKI-5, QKI-6, QKI-7 and QKIΔKH proteins respectively (Cox *et al.*, 1999; Kondo *et al.*, 1999). Although no expression or functional information has been determined for the QKIΔKH isoform, its loss of the KH domain is believed to result in a non-functional or possibly negative regulatory protein (Kondo *et al.*, 1999). KH motifs are usually present in multiple copies in RNA binding proteins from 2 to as many as 14 (Burd and Dreyfuss, 1994). *Quaking* is unusual in that it contains only a single KH motif but dimerization of QKI proteins essentially creates a functional protein unit with 2 KH domains (Zorn and Krieg, 1997). The importance of QKI dimerization is exemplified in the mouse *qk*$^{kt3/4}$ allele of *quaking*. In this mutant allele, a point mutation in the QUA2 domain abolishes self-association leading to loss of QKI function and death in homozygous *qk*$^{kt3/4}$ embryos (Chen and Richard, 1998).

Quaking transcripts are found in the developing head folds as early as E7.5 of development (Ebersole *et al.*, 1996). QKI-5, QKI-6, QKI-7 proteins are expressed in the developing central nervous system and heart at mid-gestation. This expression continues into postnatal life, with particularly high levels in the brain during myelination (Hardy, 1998b; Hardy *et al.*, 1996; Kondo *et al.*, 1999). QKI isoforms differ only in the carboxy terminus, a feature which results in the nuclear localization of QKI-5, and cytoplasmic localization of QKI-6 and QKI-7 (Hardy *et al.*, 1996). QKI-5 has however, been shown to have the ability to shuttle between the nucleus and cytoplasm *in vitro* (Wu *et al.*, 1999). In addition, *in vivo* studies of QKI-5 expression in the embryonic neural tube revealed that it moves from a nuclear to a cytoplasmic location in early glial cells as they differentiate and migrate away from the proliferative ventricular zone (Hardy, 1998b). This suggests that a change in cellular localization may alter QKI-5 function. A critical importance for the QKI-5 isoform is implied by the fact that its absence in *qk*$^{l-1}$ homozygous embryos, even in the presence of QKI-6 and QKI-7, results in embryonic death. Also, mouse QKI-5 is the only isoform that is ancestrally conserved in *Drosophila*. QKI-6 and QKI-7 proteins, whose corresponding transcripts share the same 3' UTR, are always expressed together both in the embryo and postnatal brain (Hardy, 1998b; Hardy *et al.*, 1996). Their importance is exemplified by the dysmyelination resulting from their loss in myelinating oligodendrocytes of *qk*^{v} /*qk*^{v} mice (Hardy *et al.*, 1996). However, decreased expression of QKI-5 in these same cells may also contribute to altered oligodendrocyte function. In wild-type mice all three QKI isoforms are expressed throughout the developing brain and neural tube prior to E12.5 of embryo development, at which time they become more restricted to the neural progenitors of the ventricular zone (Hardy, 1998b). At approximately this time, a small stripe of high QKI-5 expression occurs in the ventral lateral region of the neural tube where glial cells have been suggested to arise. Prior to this discovery, PDGFαR, which is expressed in this same region only slightly later than QKI-5, was considered the earliest marker of glial cell differentiation (Pringle and Richardson, 1993). Given the QKI-5 expression in this region at a slightly earlier time point, and its continued presence in glial cells as they differentiate, QKI now has the designation of being the earliest marker of glial cell differentiation (Hardy, 1998b). *In vitro* and *in vivo* studies show that QKI-6, like the related *GLD-1* from *C. elegans*, can suppress translation of transcripts containing TGEs (tra-2 and GLI elements) in their 3' UTRs (Jan *et al.*, 1999). More recently, QKI-7 has been shown to bind mRNA transcripts containing TGE consensus sequences *in vitro* (Li *et al.*, 2000). Since QKI-5 and QKI-7 differ from QKI-6 only in the very C-terminal end, they likely retain the same ability to suppress translation as QKI-6.

Efforts to determine the targets of QKI have focused primarily on postnatal brain myelin components. Numerous alterations have been reported for multiple myelin proteins, myelin lipids and even neurotransmitters in *qkv* homozygous animals but most are likely secondary effects of the overall breakdown in myelin formation (Hogan and Greenfield, 1984). However, two of the major myelin proteins, myelin associated glycoprotein (MAG) and myelin basic protein (MBP) stand out as potential QKI targets. MAG has an adhesive role in myelin and is found in two isoforms, L-MAG and S-MAG, which are produced by alternative splicing of a single transcript (Salzer *et al.*, 1990; Trapp *et al.*, 1989). In *qk^v /qk^v* brain, transcripts coding for L-MAG are present at abnormally low levels while S-MAG transcripts are present at higher than normal levels (Fujita *et al.*, 1988). In addition, the levels of both L-MAG and S-MAG protein products are reduced in *qk^v /qk^v* brain (Bartoszewicz *et al.*, 1995; Fujita *et al.*, 1990). Since these alterations are unique to *quaking* mice, it suggests a possible role for QKI in the binding and subsequent processing of MAG RNA.

MBP has a critical role in mediating compaction of myelin lamellae in wild-type animals (Privat *et al.*, 1979; Readhead *et al.*, 1987). Although levels of MBP transcripts are normal in qk^v/qk^v brain, MBP proteins are present at severely reduced levels (Delassalle *et al.*, 1981; Jacque *et al.*, 1983; Roth *et al.*, 1985). Also, *in vitro* studies have shown that MBP RNA is not transported away from the oligodendrocyte perikaryon in qk^v/qk^v cell cultures as they are in wild-type, even though transport of other RNAs is unaffected (Barbarese, 1991). Hence, *quaking* may function in transporting MBP transcripts to the active site of myelination prior to its translation. In support of this idea, QKI was recently shown to bind MBP transcripts *in vitro* (Li *et al.*, 2000).

The current model for *quaking* function suggests that its transcription and translation in both embryonic cells and postnatal oligodendrocytes is necessary for their proper development (Figure 5). QKI proteins subsequently require dimerization and are likely regulated via signal transduction to function in transport or splicing of RNA, or perhaps suppression of their translation. If *quaking* functions properly, embryonic development proceeds normally and the postnatal brain is successfully myelinated.

PROJECT GOALS

The following project was undertaken with two goals in mind. The first was to define, at the molecular level, a role for *quaking* in embryonic development utilizing the qk^{k2} embryo lethal allele. With these studies, we hope to determine what effect the loss of *quaking* function has on developing embryonic tissues and how this leads to early embryonic death. This would fill a large gap in our knowledge of *quaking* function since its role during embryonic development has never been assessed on a molecular level. *Quaking* function during embryogenesis could conceivably be completely different than in the postnatal brain where most QKI functional studies have been concentrated.

The second goal of this project was to generate new mutant mouse resources for *quaking* studies by ENU mutagenesis. Although an extensive allele series exists for the *quaking* locus, no two are alike in their phenotypes or in their affect on *quaking* function at the molecular/cellular level. Therefore, induction of novel point mutations could potentially generate new unique alleles for functional studies.

II. EMBRYONIC FUNCTION OF QUAKING

ABSTRACT

The qk^{k2} allele is an ENU-induced, recessive embryonic lethal allele of the mouse *quaking* gene (*qkI*). Homozygous qk^{k2} embryos die at mid-gestation and have been reported to exhibit neural abnormalities and heart defects (Justice and Bode, 1988). We report here that qk^{k2} lethality is due to a T to A transversion in the KH (RNA binding) domain which results in a non-conservative valine to glutamic acid amino acid change. In addition, we report the existence of a new transcript from wild-type embryos, qkIΔQUA2, which codes for a truncated, possible negative regulatory isoform of *quaking*.

Antibodies against the vascular endothelial marker PECAM-1 reveal that qk^{k2} homozygous mutants have defective vascular differentiation. The remodeling of the capillary plexus into the large vitelline network seen on the yolk sac of wild-type embryos is completely lacking in qk^{k2} homozygous mutants at E9.5-10.5. We determined that *quaking* is expressed in the yolk sac by RT-PCR. Histological sections indicate that qk^{k2} heart development is morphologically normal with the exception that they lack the more tightly looped appearance of wild-type hearts. However, *Nkx2.5*, which functions in cardiac looping, is expressed in a wild-type pattern. In addition, cardiac myocytes from qk^{k2} homozygotes express α–sarcomeric actin protein and whole hearts in organ culture beat at wild-type rates. Real-time quantitative RT-PCR revealed that qk^{k2} hearts have alterations in the levels of *Vegf*, which functions in vasculogenesis, and in the cell cycle genes *Ccnd1*, *Cdkn1a* and *Cdkn1c*. No significant alterations were detected in the heart developmental genes *Anf*, *βMhc*, and *Mef2c* or in the vascular marker *Angp1*.

The neural associated genes *Shh*, *Foxa2*, *Fgf8*, and *Pax6* as well as the notochord marker *T*, are all expressed in wild-type patterns in qk^{k2} embryos, implying neural development is unaffected at the time of death. However, a single copy of the mutant qk^{k2}

allele does appear to affect nervous system development in adult qk^{k2} heterozygous mice. These animals are significantly more susceptible than wild-type mice to chemically induced seizures with the convulsant drug pentylenetetrazole.

Together these results indicate that *quaking* has a critical role in cardiovascular development. When this function is disrupted as it is in qk^{k2} homozygous embryos, it results in embryonic death. In addition, the qk^{k2} lethality appears to precede any discernable morphological or molecular function of *quaking* in embryonic neural tissues.

INTRODUCTION

The discovery of the *quaking viable* allele (qk^v) first defined the mouse *quaking* locus (Sidman *et al.*, 1964). This allele was the result of a spontaneous 1 Mb deletion in the proximal region of mouse chromosome 17 (Ebersole *et al.*, 1992). Homozygous qk^v mice exhibit a quaking phenotype and tonic/clonic seizures as a result of central nervous system dysmyelination (Sidman *et al.*, 1964).

The qk^{k2} allele was induced with *N*-ethyl-*N*-nitrosourea (ENU) and identified by its failure to complement the qk^v phenotype of seizures and quaking in qk^{k2}/ qk^v compound heterozygotes (Justice and Bode, 1988). Unlike the qk^v allele, however, qk^{k2} was found to be recessive embryonic lethal. Homozygous mutants arrest at approximately E9.5 of development and commonly exhibit open head folds, kinky neural tubes, missing somites, and abnormal hearts. There are three other ENU induced alleles of *quaking*: qk^{kt1}, $qk^{kt3/4}$, and qk^{l-1} (Justice and Bode, 1986; Shedlovsky *et al.*, 1988). These alleles are similar to qk^{k2} in that they result in embryonic lethality at mid-gestation however, each is slightly different in the phenotypes they produce as homozygotes, heterozygotes and compound heterozygotes with qk^v.

The *quaking* gene (*qkI*) encodes a highly conserved 319-327 amino acid RNA binding protein (Ebersole *et al.*, 1996). Transcripts are expressed from E7.5 in the head folds and continue in the nascent brain neural tube and heart throughout embryonic development as well as in the post-natal brain. There are five *quaking* transcripts, qkI-5a, qkI-5b, qkI-6, qkI-7 and qkIΔKH (Figure 4), which code for four different protein isoforms designated QKI-5, QKI-6, QKI-7 and QKIΔKH (Cox *et al.*, 1999; Kondo *et al.*, 1999). QKI proteins are found in the neural tube and heart as well as in vessel endothelial cells during embryo development (Hardy, 1998b). In addition, expression occurs in the post-natal brain and in virtually all of the major organs in adult mice, with highest expression in the brain, lung and heart (Hardy *et al.*, 1996; Kondo *et al.*, 1999).

The work presented here was carried out in an effort to determine the function of *quaking* during embryonic development. We found that the *qk*^{k2} allele is the result of a single base pair mutation in the central RNA binding domain of *quaking*. In homozygous mutants, this results in deficient vascular differentiation and alterations in cardiac cell cycle gene expression. Although it is well established that *quaking* has a critical role in the post-natal brain, the lethality of *qk*^{k2} reveals a second apparently unrelated role for *quaking* in cardiovascular development which appears to precede any significant function in neural tissues.

MATERIALS AND METHODS

Mouse Maintenance and Genotyping. The *qk*^{k2} allele was induced in C57BL/6J DNA by ENU mutagenesis (Justice and Bode, 1988) but has since been maintained on a BTBR background linked to *tufted* (*tf*) for over 20 generations. Stocks are maintained by brother-sister matings and offspring are genotyped using the CA repeat primers D17MIT114 and D17MIT194 (Research Genetics, Huntsville, AL), which closely flank the *quaking* locus and are polymorphic between C57BL/6J and BTBR. Ear punches digested in 200 µl 1X PCR buffer with .01 mg/ml proteinase K (Gibco BRL, Grand Island, NY) at 56 °C for 3 hours followed by a 96 °C incubation for ten minutes were used as the DNA source for genotyping. PCR cycling was as follows: Each 25 µl reaction contained 100 ng primer, 1mM $MgCl_2$, 0.2mM dNTPs, 5 µl ear punch digest and 1.25 U Taq polymerase (Gibco BRL) in its corresponding buffer. After an initial denaturation step of 3 minutes at 94 °C, reactions were subjected to 30 cycles of 30 seconds at 94 °C, 2 minutes at 55 °C and 2 minutes at 72 °C with a final extension time of 7 minutes at 72 °C. PCR products were resolved on a 3.5 % Metaphor gel (FMC BioProducts, Rockland ME). Embryonic genotyping was performed by the same method except that yolk sacs digested in a volume of 50 µl 1.X PCR buffer were used as the DNA source.

qk^{v} mice were obtained from the Jackson Laboratory (Bar Harbor, ME) and are maintained by brother-sister matings. Heterozygous mice can be distinguished from wild type by Southern blotting of *EcoRI* digested tail DNA and subsequent probing with a pCOS2 fragment (a gift from Karen Artzt, University of Texas, Austin). This probe recognizes an restriction fragment length polymorphism between the *qk*^{v} and wild-type alleles. Probes were labeled with [α-^{32}P] dCTP using a random prime labeling kit (Stratagene, La Jolla, CA) using manufacturer's instructions.

qk^{kt1} mice were obtained from Karen Artzt and are maintained as balanced lethals with Brachyury (*T*). The *qk*^{kt1} allele was generated in *t*-chromatin which contains a resident *tct* mutation. When *tct* is compounded with *T*, it results in tailless mice. At each generation, + *qk*^{kt1} tct/T + + mice are selected based on a tailless phenotype and mated to BTBR Nevis (T/+). Homozygosity for *T* or *qk*^{kt1} is embryonic lethal and carriers of *T* without *tct* can be identified by tails which are slightly shorter than wild-type.

Sequencing. Embryos were obtained at E9.5, frozen in liquid nitrogen and genotyped by PCR of yolk sac DNA (see mouse maintenance above). Poly (A)+ mRNA was isolated from embryos using a Micro-FastTrack Kit (Invitrogen, Carlsbad, CA) and reverse transcribed with a SuperScript Preamplification Kit (Gibco BRL) according to manufacturers instructions. PCR amplification using 10 ng of cDNA and *quaking* specific primers P1F (AGCTGCGGAGCCTGGAATAT), and 1664R (GTTCCGTTTGGCATGACAGC) was performed using the same conditions as for genotyping (see above mouse maintenance). Resulting products were separated on 0.7% agarose gel (FMC BioProducts, Rockland ME) and purified using a GlassMAX DNA isolation spin cartridge system (Gibco BRL). Sequencing was performed using a Dye Terminator Sequencing kit (Perkin-Elmer/Applied Biosystems) according to the manufacturers instructions. Sequencing reaction conditions were as follows: 35 cycles of 30 seconds at 96 °C, 15 seconds at 50 °C and 4 minutes at 60 °C.

For cDNA sequencing of yolk sac transcripts, total RNA was isolated with RNAZol B (Tel-Test Inc.,Friendswood, TX) according to manufacturers instructions. Subsequent reverse transcription, PCR and sequencing were performed identical to sequencing of embryonic cDNA.

Histology. Embryos were fixed in Bouins solution (LabChem Inc, Pittsburgh, PA), dehydrated through an ethanol series and cleared in hemo-D (Fisher Scientific, Fairlawn, NJ). They were then embedded in paraffin and sectioned at 10 µm thickness. Sections were subsequently deparaffinized in hemo-D, rehydrated and stained with hemotoxylin (Fisher Scientific) and aqueous eosin (Sigma, St. Louis, MO). Stained sections were dehydrated, cleared in hemo-D and mounted with Permount (Fisher Scientific).

Immunohistochemistry. Embryos were fixed in 4% paraformaldehyde in phosphate buffered saline (PBS) for two hours and dehydrated in an ethanol series to 100%. For immunostaining of paraffin sections, embryos were cleared in hemo-D (Fisher Scientific), embedded in paraffin and sectioned at 5 µm thickness. Sections were then cleared, and rehydrated through an ethanol series prior to staining. Staining was performed using a

Vectastain Elite ABC kit with its corresponding peroxidase substrate Vector VIP kit (Vector laboratories, Burlingame, CA) according to manufacturer's instructions. Anti-α-sarcomeric actin antibody (clone 5C5, Sigma) was used at a 1:500 dilution. Slides were counter-stained in methyl green (Vector Laboratories), dehydrated through an ethanol series, cleared in hemo-D and mounted using Permount (Fisher Scientific). Immunostaining of whole embryos was performed as described in (Hogan *et al.*, 1994). Primary anti-mouse CD31 (PECAM-1) monoclonal antibody (PharMingen, San Diego, CA) was used at a dilution of 1:200 with a 1:500 dilution of anti-rat IgG-POD antibody (Boehringer Mannheim). Staining utilized the peroxidase substrate kit Vector VIP (Vector Laboratories).

Whole mount *in situ* hybridization. Antisense riboprobes were generated with a Digoxigenin-labeling kit (Gibco BRL) according to manufacturers instructions. Whole mount *in situ* hybridization was performed as previously described (Echelard *et al.*, 1993). Molecular probes were provided by: R. Schwartz (*Nkx2.5*), B. Hogan (*Shh*), B. Richards (*Foxa2*) P. H. Crossley (*Fgf8*) B. Herrmann (*T*) and T. M. Underhill (*Pax6*).

Heart organ culture. Embryos were dissected into PBS at E9.5 and hearts were removed and placed in culture in minimal essential media (Gibco BRL cat. # 11095-080) with 10% fetal bovine serum, 100 U/ml penicillin and 100 mg/ml streptomycin (Gibco BRL). The culture dish was assembled by placing a 70 um sterile cell strainer (Becton Dickenson, Franklin, Lakes, NJ) in a 60 mm petri dish. A layer of 1% agarose, made with culture media and 3% agarose in a 2:1 ratio, was placed in the bottom of the cell strainer to form a base on which heart tissues would not attach. Hearts were incubated at 37 °C with 5.0% CO_2. Heart beats per minute were counted each day for four days after which hearts were digested for PCR genotyping (see mouse maintenance above). The average beats per minute were compared using a two tailed t-test with $p = 0.05$ for significance.

Quantitative RT-PCR. Total RNA was extracted using RNAzol B (Tel-Test Inc., Friendswood, TX), from a pool of five hearts dissected from wild-type, heterozygous or qk^{k2} homozygous littermates. mRNA transcripts were quantified in triplicate by real-time RT-PCR using dual-labeled fluorogenic probes (Depre *et al.*, 1998). Reagents for the assay of *Anf*, and *βMhc* (Zhang *et al.*, 2000) as well as *Mef2c* (Depre *et al.*, 1998) and *36B4* (Ritter and Davies, 1998), as a constitutive control, have been reported. The sequences of the other primers and probes are available upon request.

Seizure susceptibility. Adult, 8-14 week old, qk^{k2} heterozygous mice and their wild-type littermates were given single intraperitoneal injections of pentylenetetrazole (Sigma, St. Louis, MO) in PBS at 42.5 mg PTZ/kg body weight. Mice were observed for 30 minutes for the occurrence of seizures. Results were analyzed using a fisher exact test at $p = 0.05$.

RESULTS

The qk^{k2} Molecular defect

Sequencing of homozygous qk^{k2} embryonic cDNA revealed a T to A transversion in the common coding region of the quaking gene at position 1118 (based on Genbank accession #AF090403). This base pair change was not present in cDNA from wild-type littermates or in the C57BL/6J strain in which the mutation arose (Figure 6). The T to A mutation results in a non-conservative amino acid change of a neutral non-polar valine to the acidic glutamic acid at amino acid position 157, within the KH domain of the QKI protein. We also report the discovery of a previously unknown transcript of quaking in wild-type mouse embryos. This transcript, which we have named qkIΔQUA2, contains the 40 base pair insert GAGTTCTTCTTTGCTTGATGGTCTATGGATTTGACTTATG at the 5' end of the QUA2 domain at position 1194 (based on Genbank accession #AF090403). This insert results in a FFFA amino acid sequence followed by an early stop codon (Figure 6).

Vascular development

Observation of E9.5-E10.5 embryos reveals that the majority of qk^{k2} homozygotes arrest at approximately E9.5 although some may arrest slightly earlier at E8.5-9.0 or develop further to E10.0-E10.5 as previously reported (Justice and Bode, 1988). Some mutants at E9.5 exhibit open head folds and kinky neural tubes (Figure 7) but often they are indistinguishable from their wild-type littermates in this regard. They do, however, commonly display hearts which appear less compacted than the plump hearts of their normal littermates. By E10.5, most homozygous qk^{k2} embryos are obviously developmentally delayed with some exhibiting a distorted puffy appearance (Figure 7). They also, almost without exception, have enlarged, fluid filled pericardial sacs (pericardial effusion) surrounding beating hearts. In addition, mutant embryos lack a well developed vitelline vessel network on the yolk sac, an observation that has never previously been reported for *quaking* mutants (Figure 8).

Immunohistochemical staining with antibodies against platelet endothelial cell adhesion molecule (PECAM-1), a marker of vascular endothelial cells (Baldwin *et al.*, 1994) was used to observe the development of embryonic blood vessels. Wild-type embryos at E9.5-10.5 have a very pronounced yolk sac vascular network which is formed from fusion and enlargement of the diffuse capillary plexus into larger vitelline vessels (Figure 8). Strikingly, in qk^{k2} embryos, these large vitelline vessels are absent on the yolk sac which consequently retains the less differentiated capillary network. Vessels within the mutant embryo proper also appear underdeveloped at this time although the effect is less dramatic than that seen on the yolk sac. Decreased size and branching of vessels are particularly visible in the head and intersegmental regions of the somites (Figure 8). To determine if *quaking* transcripts are expressed in the yolk sac, total RNA from yolk sacs at E8.5 and E9.5 was reverse transcribed. PCR of the resulting cDNA with *quaking* specific primers amplified the expected size product from both E8.5 and E9.5 (Figure 9). Subsequent sequencing of these products confirmed that they were *quaking* transcripts.

Cardiac Development

Histological sections stained with hemotoxylin and eosin at E9.5-10.5 reveal that qk^{k2} mutant hearts are normal except they lack the more compact morphology of the wild-type embryos (Figure 10). Whole mount *in situ* hybridization using a probe for *Nkx2.5*, which functions in cardiac looping (Tanaka *et al.*, 1999), showed normal expression throughout the heart in qk^{k2} mutant embryos (Figure 11). We also performed immunohistochemistry on E10.5 embryonic sections to assess the differentiation of cardiac muscle cells. Myocardial cells were shown to express α-sarcomeric actin, and the thickness of the myocardium appears normal throughout the heart (Figure 11).

The beating rates of hearts in organ culture were determined for qk^{k2} homozygous, heterozygous and wild-type embryos. The average beats per minute for each day in culture (Figure 12) were not significantly different between homozygous mutants and either heterozygous or wild-type hearts. On average, rates were 162 beats per minute on the first day in culture and decreased slightly each day to an average of 133 beats per minute on the fourth day. The overall averages for the entire four days were also calculated and, like the daily averages, revealed no significant differences between the three genotypes (data not shown). Although mutant and wild-type beating rates were similar, three out of seven qk^{k2} mutant hearts displayed a more focal beat that lacked the ability to traverse robustly across the entire heart as it did in wild-type hearts. This was not a feature of any of the wild-type or heterozygous qk^{k2} hearts observed in this experiment.

Real-time quantitative RT-PCR of heart RNA revealed the relative transcript levels of a selection of genes that function in cardiac development (*Anf*, and *βMhc*), myocyte specification (*Mef2c*), vascular development (*Vegf*, and *Angp1*) and cell cycling (*Ccnd1*, *Cdkn1a*, and *Cdkn1c*) (Ferrara *et al.*, 1996; Hunter and Pines, 1994; Lin *et al.*, 1997; Sherr, 1994; Sherr and Roberts, 1995; Suri *et al.*, 1996; Willie *et al.*, 1991; Zeller *et al.*, 1987). Levels were assessed prior to (E8.5) during (E9.5) and after (E10.5) the time of qk^{k2} mutant arrest. In each experiment, the level of the constitutive housekeeping gene for acidic ribosomal phosphoprotein PO, *36B4*, was determined as in internal control (Laborda, 1991).

Anf (atrial natriuretic factor) and *βMhc* (beta-myosin heavy chain) were present in qk^{k2} mutant hearts at wild-type levels (Figure 13). A transitory increase in both *Mef2c* (myocyte enhancer factor 2C) and *Angp1* (angiopoietin) that was detected in wild-type hearts at E9.5, was absent in qk^{k2}/qk^{k2} and $qk^{k2}/+$. At E8.5 and E10.5, however, the levels of *Mef2c* and *Angp1* in qk^{k2} mutants and heterozygotes were similar to wild-type. The expression of *Vegf* (vascular endothelial growth factor) was similar in mutant and wild-type heart at E8.5 but by E10.5, levels were two-fold higher in mutant hearts than in wild-type or heterozygotes. Transcript levels for each of the cell cycling genes assessed were altered in qk^{k2} mutant hearts (Figure 14). At E8.5, expression was similar to wild-type but by E10.5, cyclin D1 (*Ccnd1*), and cyclin-dependent kinase inhibitor 1C (*Cdkn1c)* were reduced compared to wild-type levels. At this same stage in development, cyclin-dependent kinase inhibitor 1A (*Cdkn1a)* expression was increased in qk^{k2} mutants relative to wild-type.

Neural Development

Whole mount *in situ* hybridization with probes for *Brachyury* (*T*), *Sonic hedgehog* (*Shh*), *Forked head box A2* (*Foxa2*), *fibroblast growth factor 8* (*Fgf8*), and *paired type homeobox 6* (*Pax6)* were used to assess the development of the neural tissues and associated mesodermal structures in qk^{k2} mutants. The normal expression patterns of these markers at E9.5 as well as their functions are shown in Table 2. Expression of each of these genes was determined to be normal in qk^{k2} mutant embryos (Figures 15 and 16). This was true for mutant embryos that reached E9.5 of development and those that were slightly more or less developed at the time of arrest (data not shown). We did, however, see one exception in 3 out of 9 qk^{k2} mutant embryos which showed a shortened domain of *Shh* expression in the anterior brain floor plate (Figure 15). These embryos arrested at approximately E9.0 but not all the mutant embryos that were stalled at this time showed the shortened pattern of expression.

In order to assess the affect of the qk^{k2} allele on adult mice, qk^{k2} heterozygous mice and their wild-type littermates were tested for susceptibility to chemically induced seizures with the convulsant drug pentylenetetrazole or (PTZ). Eighty four percent of qk^{k2} heterozygotes had full tonic/clonic seizures following PTZ injection while only 21% of their wild-type littermates succumb to seizures (Table 3).

DISCUSSION

Molecular defect

We have identified a T to A transversion in the KH (RNA binding) domain of the qk^{k2} embryo lethal allele. This base pair change results in a non-conservative amino acid change of valine to glutamic acid in a region that is common to all three isoforms of QKI protein. This valine is highly conserved, being found in all of the known homologues of *quaking* including human (*hqk*), *Xenopus* (*Xqua*), chicken (*qk*), Zebrafish (*zqk)* and *Drosophila* (*who/how/qkr93F*), as well as in the *quaking*-related human gene *Sam68* (Baehrecke, 1997; Darnell *et al.*, 1994a; Fumagalli *et al.*, 1994; Fyrberg *et al.*, 1997; Mezquita *et al.*, 1998; Tanaka *et al.*, 1997; Taylor and Shalloway, 1994; Zaffran *et al.*, 1997; Zorn and Krieg, 1997). This amino acid is not conserved in the other related STAR family members *gld-1, grr33, Bbplp* or *SF1* (Abovich and Roshbash, 1997; Agger and Freimuth, 1995; Berglund *et al.*, 1997; Cruz-Alvarez and Pellicer, 1987; Jones and Schedl, 1995; Kramer, 1992), likely reflecting diverging specificity of function of the related family members. In addition, the location of this particular amino acid is predicted to be part of a small, approximately 25 amino acid stretch of protein with a highly coiled coil conformation. This coiled coil structure is suggestive of a direct role in protein-protein interaction (Chen and Richard, 1998). A second predicted coiled coil motif lies in the QUA1 domain and is abolished by an ENU induced point mutation in the mouse $qk^{kt3/4}$ allele. The loss of this coiled coil domain prevents QKI protein dimerization and results in $qk^{kt3/4}$ homozygous embryo lethality (Chen and Richard, 1998; Justice and Bode, 1988). QKI proteins containing a deletion that includes the coiled coil domain mutated in qk^{k2}, can still dimerize (Chen and Richard, 1998) suggesting that some protein-protein interaction other than self association is affected in qk^{k2} mutants.

Unlike most KH domain containing proteins, *quaking* contains only a single KH motif (Ebersole *et al.*, 1996). However, even in proteins like Fragile X Syndrome gene (*FMR1*) which contain multiple KH domains, a single point mutation in one of these domains can significantly reduce RNA binding (Siomi *et al.*, 1994). Therefore, the mutation in qk^{k2} is highly likely to be responsible for the loss of *quaking* function, and embryonic death in qk^{k2} homozygotes.

We also report the presence of a previously unknown transcript of *quaking* from wild-type embryos. This transcript, which we have named qkIΔQUA2, contains an insertion at the 5' end of the QUA2 domain and results in an early stop codon and truncated protein product. A similar transcript which truncates at the same amino acid location has been identified in the chick homologue of *quaking* but is the result of a larger insert (Mezquita *et al.*, 1998). The insertion in qkIΔQUA2 in mouse and chicken is located in the analogous position of an intron-exon splice site in a transcript of the related *C. elegans* gene *gld-1*

(Jones and Schedl, 1995). In the case of *gld-1*, however, the splice site results in a functional transcript suggesting that qkIΔQUA2 in the mouse may be the non-functional remnant of an ancestrally conserved splice site. Alternatively, QKIΔQUA2 protein may have a very important role as negative regulator of *quaking* function. Another previously identified mouse transcript of *quaking* results in the truncated protein isoform QKIΔKH (Kondo *et al.*, 1999) and is similar to that found in the related human gene *Sam68* (Barlat *et al.*, 1997). These transcripts contain a stop codon in the middle of the KH domain resulting in truncated protein products. Studies with *Sam68* have shown that this truncated isoform can inhibit the function of full length *Sam68* isoforms (Barlat *et al.*, 1997) suggesting that QKIΔQUA2 may have a similar negative regulatory function.

Cardiovascular defects

Homozygous *qk*^{k2} embryos die at mid-gestation with reported abnormalities including open head folds and irregular neurocoels, often associated with abnormal and missing somites (Justice and Bode, 1988). Also, some mutant embryos were reported as having enlarged pericardial sacs. In an effort to determine the role(s) of *quaking* during development and the cause of lethality when *quaking* function is lost, we examined *qk*^{k2} embryos at the time of arrest and looked at the expression of a variety of markers for the developing circulatory system and neural tissues.

Using antibodies against the vascular endothelial marker PECAM-1, we found that *qk*^{k2} embryos completely lack the development of a vitelline vessel network on the yolk sac at the time of their arrest. Decreased vessel formation was also evident in the embryo itself, but was not as pronounced as that found in the yolk sac. We determined by RT-PCR that *quaking* transcripts were expressed in yolk sac at the time of *qk*^{k2} embryonic lethality, a finding that had not been reported in any previous *quaking* expression studies. Early wild-type embryos contain a diffuse capillary plexus both in the embryonic and extra-embryonic tissues. As the vessels differentiate during angiogenesis, some capillaries undergo atrophy while others expand and fuse, remodeling into a network of major veins and arteries (Hopper and Heart, 1985). In qk^{k2} mutants, this vascular differentiation fails to occur, resulting in a primitive capillary plexus that is insufficient for the developing embryo. Vascular defects have also been reported in loss of function mutants of *how* (*held out wings*), the *Drosophila* homologue of *quaking* (Zaffran *et al.*, 1997). Homozygous *how* mutants die prior to hatching and exhibit reduced muscle movements but appear morphologically normal with the exception of exhibiting narrow dorsal vessels. Loss of this critical angiogenic process has also been shown to be the cause of lethality in other mutant embryos including the mouse knock out of *Jagged1* (*Jag1*) which, like qk^{k2} mutants, lacks yolk sac vascular differentiation (Xue *et al.*, 1999). *Quaking* proteins were previously shown to be expressed in embryonic blood vessel endothelial cells (Hardy, 1998b), but the findings reported here demonstrate for the first time that *quaking* has a critical role in mouse vascular development.

During embryogenesis, vascular development depends on local hematopoetic influences from the rate and direction of cardiac blood flow (Hopper and Heart, 1985). This determines which capillaries undergo regression or expansion as well as whether they develop into the structurally distinct veins or arteries. In *Nkx2.5* null mice, cardiac and yolk sac vascular defects are present but since *Nkx2.5* is only expressed in the heart, the yolk sac abnormalities are considered secondary effects (Tanaka *et al.*, 1999). Some qk^{k2} mutant embryos at E9.5 and nearly all of those at E10.5 exhibit pericardial effusion which often coincides with visibly underdeveloped hearts. *Quaking* transcripts as well as QKI proteins have been identified in the heart of wild-type embryos at mid-gestation (Ebersole *et al.*, 1996 and Rebecca Hardy, unpublished results). Therefore, to determine if the loss of *quaking* function directly affects heart development, we performed a series of experiments to analyze qk^{k2} embryonic heart development and function.

Nkx2.5 null embryos, similar to qk^{k2}/qk^{k2}, arrest and die at E9.5-E10.5 with pericardial effusion and underdeveloped hearts that fail to undergo the looping required to form the right and left ventricle (Tanaka *et al.*, 1999). In addition, they lack vitelline vessel formation on the yolk sac and have a reduced blood vessel network within the embryo. Therefore, we wanted to determine if *Nkx2.5* expression was altered in qk^{k2} mutant embryos. Analysis of *Nkx2.5* expression by whole mount *in situ* hybridization revealed that it was present in a wild-type pattern in qk^{k2} mutant embryos, suggesting it does not function downstream of *quaking* in cardiac development. Assessment of cardiac myocyte differentiation by expression analysis of α-sarcomeric actin protein revealed that this contractile protein was present in qk^{k2} mutant hearts similar to wild-type. The contractility of myocytes was analyzed in whole heart organ cultures but no differences were observed in the average beating rates of qk^{k2} homozygote, heterozygote and wild-type hearts. This was an interesting finding given previous reports on the role of *quaking* in *Drosophila* development. The *Drosophila* homologue of *quaking* (*how*) was cloned in an effort to identify genes functioning in cardiac development (Zaffran *et al.*, 1997). Complete loss of function alleles die prior to hatching and although embryos at this stage appear normal with the exception of smaller dorsal aorta, they lack muscle movement and have lower heart rates than those of wild-type embryos. This could reflect a more important function for *how* in *Drosophila* heart development than *quaking* has in the mouse. Alternatively, it may simply reflect the fact that our assessment was carried out *in vitro* where there is no venous resistance while *Drosophila* studies were performed *in vivo*. The narrow dorsal vessels reported in *Drosophila* could conceivably result in increased pressure on the heart and affect beating rates (Zaffran *et al.*, 1997). We also found that the cardiac beating was less robust and failed to traverse across the whole heart in several of the qk^{k2}/qk^{k2} cultures. This is similar to the finding in *Drosophila*, where heart contractions had a smaller amplitude than in wild-type heart tissue (Zaffran *et al.*, 1997). Whether this is due to intrinsic electrical coupling problems, or simply reflects cardiac damage from high intraventricular pressure remains to be determined.

In order to assess the molecular development of qk^{k2}/qk^{k2} hearts, we determined the levels of a range of cardiac transcripts by real-time quantitative PCR. We found that the cardiac development gene *Anf* (Zeller *et al.*, 1987) and the cardiac contractile protein gene *βMhc* (Willie *et al.*, 1991) were expressed normally in qk^{k2} mutants. However, a previously unreported transitory increase of *Angp1* and *Mef2c* that was present in wild-type hearts at E9.5, was absent in qk^{k2} mutants. *Angp1* functions in vascular remodeling and mice homozygous for the *Angp1* null allele die from lack of yolk sac and embryonic blood vessel formation (Suri *et al.*, 1996). *Mef2c* null alleles have abnormal myocyte differentiation resulting in an inability to form the right and left ventricle chambers as well as a lack of yolk sac vascularization (Lin *et al.*, 1997; Subramanian and Nadalginard, 1996). The lack of *Angp1* and *Mef2c* upregulation at E9.5 is intriguing in light of the similarities in the null phenotypes of these genes compared to that of qk^{k2} homozygous embryos. However, the fact that $qk^{k2}/+$ hearts, which have no observable abnormalities, show nearly identical *Angp1* and *Mef2c* expression patterns to qk^{k2}/qk^{k2}; implies the alteration may not be significant. The missexpression of *Vegf*, however, is specific to qk^{k2}/qk^{k2} heart tissue. Unlike in wild-type and qk^{k2} heterozygotes, *Vegf* expression in qk^{k2} homozygous mutants does not decline after E9.5 but continues to increase up to E10.5 of development. The function of *Vegf* in the heart is unknown but it has been shown to have a critical function in early endothelial cell differentiation during the vasculogenesis process (Ferrara *et al.*, 1996). Vasculogenesis, the formation of the primitive capillary network, and angiogenesis, the remodeling of primitive capillaries into large and small vessels, are two distinct processes (Hanahan, 1997; Risua, 1997). Vasculogenesis, which requires *Vegf*, appears to be normal in qk^{k2} mutant embryos while angiogenic remodeling to create larger vessels is absent. In the absence of angiogenesis, *Vegf* does not decrease in qk^{k2} embryos as it does in wild-type, but it continues to rise. This could be a compensatory response to increase the capillary network in the absence of large vessel formation. The basis for this response mechanism has been documented *in vitro* using cardiac myocytes (Ladoux and Frelin, 1993). Hypoxic culture conditions were shown to induce high levels of *Vegf* expression in myocytes, suggestive of a response to promote cardiac capillary growth in the absence of sufficient oxygen levels. Cellular hypoxia can be the result of numerous physiological disorders including local or general circulatory deficiencies (Guyton and Hall, 1996) such as those present in qk^{k2} embryos.

The positive cell cycle regulator *Ccnd1*, and negative regulator *Cdkn1c*, are both down regulated in qk^{k2} mutant hearts. In contrast, the negative cell cycle regulator *Cdkn1a* is present at increased levels. These alterations were subtle at E9.5 but very distinct by E10.5. At E9.5, when qk^{k2}/qk^{k2} embryos arrest, cardiac development is undergoing a complex combination of processes (Hopper and Heart, 1985). Cardiac proliferation increases heart mass and facilitates looping morphogenesis while subsets of cardiac cells exit the cell cycle and terminally differentiate. Positive and negative regulation of cell proliferation for these processes relies on a complex network of signaling pathways coordinated by cyclins like *Ccnd1* and cyclin dependent kinases such as *Cdkn1a* and *Cdkn1b*. It is not uncommon to detect seemingly contrasting expression patterns of these regulatory proteins as we see in qk^{k2} hearts where *Cdkn1a* is upregulated, and *Cdkn1c* is downregulated. For example, *Cdkn1a* declines while *Cdkn1c* increases in human acute heart failure reflecting a reversion to a normal fetal expression pattern (Burton *et al.*, 1999). Although cyclin dependent kinases show tissue specific expression patterns, functional redundancy prevents analysis of their roles in development. Only *Cdkn1c* has been shown to have a significant role in multiple tissues. Loss of *Cdkn1c* function is responsible for Beckwith-Wiedemann syndrome, a human condition leading to complex overgrowth and cancer susceptibility (Zhang *et al.*, 1997).

Our results showing missexpression of *Cdkn1a* and *Cdkn1c* imply that cell cycling alterations exist in the hearts of qk^{k2} mutant embryos. Whether this results from direct loss of QKI function, a compensation response to vascular defects, or a general decrease in proliferation caused by embryonic arrest remains to be determined.

Neural tissue defects

The tremors and seizures exhibited in qk^{v} homozygous mice first defined a critical role for *quaking* in neural development (Sidman *et al.*, 1964). Based on the work reported here, however, the embryo lethality of the qk^{k2} allele precedes any discernable molecular or morphological defects in the developing neural tissues or underlying notochordal mesoderm. This is evident from both histological sectioning and the wild-type expression of *T*, *Shh*, *Foxa2*, *Fgf8* and *Pax6*. Since *quaking* transcripts are found in the neural tube from E7.5 of development (Ebersole *et al.*, 1996) several possibilities would explain why we do not see any molecular neurological development defects in qk^{k2} mutants. Most simply, *quaking* may not have a critical function in neural tissue until later in development (after E9.5 lethality). Alternatively, *quaking* may have an early embryonic function in a genetic pathway(s) that our selection of neurological markers would not detect. QKI proteins have been shown to have translational suppression ability *in vitro* (Jan *et al.*, 1999). Therefore, abnormalities in qk^{k2} mutants may be in the form of aberrantly expressed proteins rather than loss of expression of normal neural markers. It is not uncommon for embryos that arrest from circulatory defects at mid-gestation (a time of neural tube closure and embryo turning from an arched to a fetal position) to exhibit neural kinking and open head folds. The N-Cadherin knockout mouse is one example of this phenomenon (Radice *et al.*, 1997). Mice lacking N-Cadherin die from defective cell adhesion in cardiac tissues at mid-gestation, but often display open head folds and neural kinking as a consequence of the time of arrest. Although *quaking* is expressed in neural tissues, the morphological abnormalities observed in the headfolds and neural tube are not a consistent feature and they are not observed in embryos that survive later than E9.5. Therefore, we suggest that although there may be undetected defects on the molecular level, the morphological neural abnormalities observed in qk^{k2} mutants are secondary effects.

Heterozygous qk^{k2} mice are significantly more susceptible to PTZ induced seizures than their wild-type littermates. Thus, the qk^{k2} mutation has a compromising effect in neurological tissues of adult mice. PTZ antagonizes neuron GABA channels which are the primary inhibitory receptors of the central nervous system (Pellmar and Wilson, 1977) (Ramanjaneyula and Ticku, 1984). This antagonism leads to a loss of the normal, hyperpolarized state of the neuronal membranes and consequently, increased neuron excitability. Since *quaking* proteins are expressed in oligodendrocytes but not in neurons (Hardy *et al.*, 1996) where the GABA channels are located, it is likely that the PTZ susceptibility is due to effects of altered oligodendrocyte myelination of neuronal axons. This is supported by preliminary studies which show that qk^{k2} heterozygotes have decreased overall myelin lipid levels and in particular, that the ratios of specific lipid components are altered compared to wild-type (Justice, unpublished results). Heterozygous qk^{v} mice have also been tested for PTZ seizure susceptibility (Diego Lorenzetti, unpublished results) but unlike qk^{k2}, qk^{v} carriers are no more susceptible to seizures than their wild-type littermates. This may be the result of a significantly different effect that the qk^{k2} and qk^{v} alleles have on neural tissue, or it could be a result of the differences in the background strains on which they are kept. The C57BL/6 background strain, on which the qk^{v} allele is maintained, is more seizure resistant by a variety induction methods than a number of other background strains (Kosobud and Crabbe, 1990).

The PTZ susceptibility of qk^{k2} heterozygotes indicates that we have a mildly affected model of loss of *quaking* function in the brain. These models are particularly useful for functional biochemical studies in mutants with myelination disorders since secondary effects are abundant in severely affected mutants. A complete breakdown of the myelin system in mice like *jimpy* and *shiverer* make determination of single gene function difficult among the loss and alteration of numerous transcripts and proteins affected in these animals (Campagnoni and Macklin, 1988; Hogan and Greenfield, 1984; Lemke, 1986; Mikoshiba *et al.*, 1991).

Conclusions

We conclude that the qk^{k2} homozygous lethality is due to a T to A base pair change in the KH domain of the *quaking* gene. This mutation leads to embryonic death from cardiovascular defects including defective angiogenesis and pericardial effusion. Underdeveloped heart looping morphogenesis coincides with alterations in cell cycling genes and genes for vasculogenesis but no significant alterations heart developmental genes were observed. In addition, the qk^{k2} lethality appears to precede any discernable function in the developing neural tissue. Carriers of the qk^{k2} allele, however, show increased susceptibility to chemically induced seizures.

III: NEUROLOGICAL FUNCTION OF *QUAKING*

ABSTRACT

Until recently, the allele series of the mouse *quaking* gene consisted of a spontaneous qk^v allele, with a homozygous viable dysmyelination phenotype, and four ENU-induced alleles that are homozygous embryo lethal. We report here the isolation of qk^{e5} through ENU mutagenesis which, unlike the previous induced alleles of *quaking*, is homozygous viable. The qk^{e5}/qk^{e5} phenotype is strikingly more severe than that observed in qk^v homozygous mice. The qk^{e5} homozygous animals have a *quaking* phenotype which progresses to severe ataxia in adult mice, as well as early onset seizures which lead to early death. Ultrastructural analysis of qk^{e5}/qk^{e5} brains reveals a severe lack of myelin compared to both wild-type and qk^v/qk^v brains. Although sequencing and Northern analysis have not revealed the molecular defect in qk^{e5} mutants, protein expression analysis in the postnatal brain shows that the QKI-5 isoform is low and QKI-6 and QKI-7 are absent specifically in developing oligodendrocytes. Therefore, the qk^{e5} molecular defect appears to be a regulatory mutation. Protein expression experiments on postnatal brain also show that oligodendrocytes of qk^{e5}/qk^{e5} mice contain both early and late developmental marker genes indicating that *quaking* may function relatively late in oligodendrocyte development. We also report that electrical activity in the qk^{e5}/qk^{e5} brain is abnormal and that seizures display cortical patterns activity characteristic of a decremental response.

INTRODUCTION

The discovery of the *quaking viable* allele (qk^v) first defined the mouse *quaking* locus (Sidman *et al.*, 1964). This allele was the result of a spontaneous 1 Mb deletion in the proximal region of mouse chromosome 17 (Ebersole *et al.*, 1992). Homozygous qk^v mice exhibit *quaking* and spontaneous tonic/clonic seizures as the result of a severe central nervous system dysmyelination (Friedrich, 1974; Sidman *et al.*, 1964). Homozygous qk^v males are also sterile due to a failure of spermatid maturation (Bennett *et al.*, 1971). In addition to a role in postnatal brain function, *quaking* was determined to have a critical role in embryonic development. This was discovered upon recovery of three *N*-ethyl-*N*-nitrosourea (ENU) induced alleles of *quaking*. These alleles were selected based on their inability to complement the qk^v phenotype but were subsequently found to be homozygous embryo lethal (Justice and Bode, 1988).

The *quaking* gene encodes a highly conserved 319-327 amino acid RNA binding protein (Figure 3) (Ebersole *et al.*, 1996). Transcripts are expressed at E7.5 in the head folds and continue in the nascent brain, heart and neural tube during embryo development. They are also expressed in the postnatal brain with a peak at the most active time of CNS myelination (Ebersole *et al.*, 1996). There are five *quaking* transcripts, qkI-5a, qkI-5b, qkI-6, qkI-7 and qkIΔKH (Figure 4), which code for four different protein isoforms designated QKI-5, QKI-6, QKI-7 and QKIΔKH (Cox *et al.*, 1999; Kondo *et al.*, 1999). QKI-5, QKI-6, and QKI-7 differ from each other only in the C-terminal end of the protein, a feature that results in QKI-5 localization to the nucleus and QKI-6 and QKI-7 localization to the cytoplasm (Hardy *et al.*, 1996). QKI-5, QKI-6, QKI-7 proteins are expressed in the developing central nervous system and heart at mid-gestation. This expression continues into postnatal life, with particularly high levels in the brain during myelination (Hardy, 1998b; Hardy *et al.*, 1996; Kondo *et al.*, 1999).

The work reported here describes the induction of qk^{e5}, the first homozygous viable ENU allele of *quaking*. We also analyze the qk^{e5}/qk^{e5} phenotype with regard to behavior, brain histology, myelin ultrastructure and brain electrical activity, as well as the nature of the molecular and cellular qk^{e5} defect.

MATERIALS AND METHODS

Mouse maintenance. The *qk^{e5}* mutation was induced on 101 DNA and subsequently crossed to C57BL/6J at each generation. Mice are genotyped using the CA repeat primers D17MIT114 and D17MIT170 (Research Genetics, Huntsville, AL), which closely flank the *quaking* locus and are polymorphic between 101 and C57BL/6J. Ear punches digested in 200 µl 1X PCR buffer with 0.01 mg/ml proteinase K (Gibco BRL, Grand Island, NY) for 3 hours at 56 °C and 10 minutes at 96 °C were used as the DNA source. PCR cycling was as follows: Each 25 µl reaction contained 100 ng primer, 1 mM $MgCl_2$, 0.2mM dNTPs, 5 µl ear punch digest and 1.25 U Taq polymerase (Gibco BRL) in its corresponding buffer. After an initial denaturation step of 3 minutes at 94 °C, reactions were subjected to 30 cycles of 30 seconds at 94 °C, 2 minutes at 55 °C and 2 minutes at 72 °C with a final extension time of 7 minutes at 72 °C. PCR products were resolved on a 3.5 % Metaphor agarose gel (FMC BioProducts, Rockland, ME). Embryonic genotyping was performed by the same method except yolk sac digested in a volume of 50 µl 1 X PCR buffer was used as the DNA source.

The *qk^{v}* mice were obtained from the Jackson Laboratory (Bar Harbor, ME) and are maintained by brother-sister matings. Heterozygous mice can be distinguished from wild type by Southern blotting of *EcoRI* digested tail DNA and subsequent probing with a pCOS2 fragment (a gift from Karen Artzt, University of Texas, Austin). This probe recognizes an restriction fragment length polymorphism between the *qk^{v}* and wild type alleles. Probes were labeled with [α-^{32}P] dCTP using a random prime labeling kit (Stratagene, La Jolla, CA) using manufacturers procedures.

ENU mutagenesis. Adult (101 X C3H)F1 male mice mutagenized as previously described (Justice, 1999). Mice received an intraperitoneal dose of 100 mg ENU/kg body weight once a week for 4 consecutive weeks. Once fertility was regained, mutagenized males were mated to two new *qk^v* heterozygous females each week for seven weeks at which time they were cycled back through the same set of females. Up to 100 offspring per male were observed at weaning age (3 weeks) for a quaking-like phenotype.

Sequencing. Total RNA was isolated from adult brain using RNAzol B (Tel-Test Inc., Friendswood, TX) and reverse transcribed with a SuperScript Preamplification kit (Gibco BRL) according to the manufacturer's instructions. PCR amplification of brain cDNA using *quaking* specific primers, made against *qkI* Genbank sequence, was performed using the same cycling conditions as for genotyping (see above mouse maintenance). Resulting products were separated on 0.7% agarose gel (FMC BioProducts; Rockland, ME) and purified using a gel purification column (Qiagen Inc, Valencia, CA). The Resulting PCR products were sequenced using a Dye Terminator Sequencing Kit (Perkin-Elmer/Applied Biosystems) according to the manufacturers instructions. Reaction conditions were as follows: 35 cycles of 30 seconds at 96°C, 15 seconds at 50°C and 4 minutes at 60°C.

Northern analysis. Total brain RNA was isolated from 12 week old mice using RNAZol B (Tel-Test Inc) according to manufacturer's instructions. The resulting RNA was 1 X selected with a poly (A)+ selection column (Amersham Pharmacia Biotech, Inc., Piscataway, NJ). One to two micrograms of poly (A)+ RNA from each sample was separated on a 1.0% agarose gel with 7.0% formaldehyde and transferred to Magna Charge nylon membranes (Micron Separations Inc.). The membranes were prehybridized and hybridized as previously described (Church and Gilbert, 1984). The following primers were used to generate the indicated probes: Probe 1-QUA2: primers qK-1295F (5'GGGAGCATCTAAATGAAGAC3') and qK-1793R (5'CACCACTGGGTTCAATAGGG 3'). Probe 2-3'UTR: primers qk-5b-1576F

(5'GTGTTAGGTATGGCTTTCCC3') and qk-5b-2341R (5'ACACGCATATCGTGCCTTCG3'). The cDNA source for probe generation was the same as that used for wild-type cDNA sequencing (see above methods for sequencing). A GAPDH cDNA probe was used as a control for loading and migration. All probes were labeled with [α-^{32}P] dCTP using a random prime labeling kit (Stratagene, La Jolla, CA) using manufacturer's procedures.

Histology. Brains from twelve week old mice were fixed overnight in zinc formalin, dehydrated in an ethanol series and cleared in xylene. They were then embedded in paraffin in a 65 °C vacuum oven and subsequently sectioned at 5 um onto albumin coated glass slides. Sections were then deparaffinized in hemo-D and either rehydrated and stained with hemotoxylin (Fisher Scientific, Fairlawn, NJ) and eosin (Sigma, St. Louis, MO) or stained with luxol fast blue (Sigma) for myelin. Luxol staining required an overnight incubation at 65 °C in luxol fast blue/95%ethanol with subsequent destaining in alternating 0.05% lithium carbonate and 70% ethanol series. Both hemotoxylin and eosin, and luxol stained sections were subsequently dehydrated, cleared in hemo-D and mounted with Permount (Fisher Scientific).

Transmission electron microscopy. Mice were anesthetized with Avertin as previously described (Hogan et al., 1994) and perfused through the left ventricle with PBS followed by isotonic glutaraldehyde which consisted of 8% glutaraldehyde, 0.1M cacodylate buffer pH 7.4 and ddH2O in a 1:1:1 ratio. Brains were dissected into isotonic glutaraldehyde. Selected brain regions were rinsed in 0.1 M buffer prior to staining in 1% osmium tetroxide/PBS, and then dehydrated in a graded ethanol series to 100%. Tissues were placed in propylene oxide followed by a graded Araldite resin/propylene oxide series ending in 100% resin. Tissue blocks were polymerized overnight at 60 °C prior to ultra-thin sectioning.

Immunohistochemistry. Mice at P7, P14 and P30 days of age were perfused through the left ventricle with PBS followed by 4.0% paraformaldehyde/PBS. Brains were dissected out and placed in 4.0% paraformaldehyde/PBS for an additional 4 hours at 4 °C and then placed in PBS prior to dehydration to 30% sucrose. Brains were embedded in OCT and frozen in isopentane on dry ice. Sections 7 um thick were thaw mounted onto charged glass slides and frozen at –20 °C. Immunohistochemical staining of sections was performed according to Hardy et al., 1996 using a solution of 0.5M Tris pH 7.4, 10% goat serum, 1.0% BSA, and 0.1% gelatin for blocking and antibody incubation steps. QKI antibodies were a gift from Dr. Rebecca Hardy who obtained them from Dr. Karen Artzt.

Electroencephalogram recording. EEG recordings were obtained as previously described (Cox et al., 1997). Adult mice were anesthetized with Avertin according to (Hogan et al., 1994). A microminiature connector with four extending silver wire electrodes was glued to the exposed surface of the mouse skull. Electrodes were placed into the subdural space via small holes in the skull made with a dental drill on either side of the connector. Mice were allowed to rest for 1-2 days after which EEG and video recordings of 3-4 hours were taken for each mouse using a Grass model 6 electroencephalograph.

Seizure susceptibility testing. Adult (8-14 week old) *qk*^{e5} heterozygous and wild type mice at N8 of backcrossing to C57BL/6J were given single intraperitoneal injections of pentylenetetrazole (Sigma, St. Louis, MO) in PBS at 42.5 or 45.0 mg per kg body weight. Mice were observed for 30 minutes for the occurrence of seizures. Results were analyzed using a fisher exact test at p=0.05.

RESULTS

ENU mutagenesis

ENU mutagenized (101 X C3H)F1 males were mated to a series of *qk*^{v} heterozygous females in a single generation screen to produce new alleles of *quaking* (Figure 17). A total of 918 pups (459 gametes) were screened at weaning age and one male pup, which was small and quaked, was selected for heritability and allelism testing. This male was a potential carrier of a new *quaking* mutation compound with the *qk*^{v} allele (m/ *qk*^{v}). Subsequent matings to wild-type, *qk*^{v} heterozygous and *qk*^{v} homozygous females revealed the *quaking* phenotype was heritable and that it was only visible when compound with *qk*^{v} (Figure 18). Thus, the new mutation was recessive and allelic to *quaking*. We designated this allele *qk*^{e5} because it is the fifth ENU induced allele at the *quaking* locus.

Amplification of DNA from 101, C3H, and *qk*^{e5} carriers using primers for the CA repeat markers DMIT170 and DMIT114 revealed that the *qk*^{e5} mutation was induced in 101 DNA (data not shown). These markers closely flank the *quaking* locus proximally and distally and are polymorphic between the strains 101, C3H and C57BL/6J, on which the *qk*^{e5} mutation is being made congenic.

The *qk*^{e5} phenotype

Crosses of heterozygous *qk*^{e5} mice produced viable, fertile *qk*^{e5} homozygous offspring. This was an unexpected result given that the four previous ENU-induced alleles of *quaking* were all embryonic lethal. Homozygous qk^{e5} mice were recovered at the expected 25%, excluding the possibility that qk^{e5} homozygosity could be affecting viability during gestation (Table 4). Homozygous qk^{e5} mice begin quaking at approximately P10, similar to qk^{v} homozygotes. In qk^{v}/qk^{v} mice, quaking continues throughout the life of the mouse, along with adult onset tonic/clonic seizures. These mice are often underweight, compared to normal littermates, but commonly live to 1.5 years or longer. The qk^{e5} homozygotes, however, are much more severely affected. In these mice, seizures can onset as early as 3 weeks and the quaking phenotype progresses to a very severe ataxia by 2.5-3 months of age. Seizures are also more frequent in qk^{e5} mutants and very easily induced with slight noises and general mouse handling activities. Only approximately 35% of qk^{e5}/qk^{e5} mice survive to 5.0 months of age (N=37). This early death is presumably due to respiratory arrest during seizure episodes. Heterozygous qk^{e5} mice do not display any abnormal phenotype.

Crosses generating compound heterozygotes of qk^{e5} with qk^{kt1}, qk^{k2} and qk^{v} alleles showed that these mutants were all viable and born at the expected numbers (Table 4). Thus, qk^{e5} complements the lethality of the homozygous embryo lethal alleles to produce viable animals. A 25% recovery of compound heterozygous mutants was expected for all crosses except $qk^{e5}/+$ X $qk^{kt1}/+$ in which we expected 48%. This is due to the fact that qk^{kt1} is in *t*-chromatin which in males, causes an abnormally high (95%) transmission frequency of the chromosome bearing *t*-chromatin, and consequently the qk^{kt1} allele, to their offspring. Compound heterozygous qk^{kt1}/qk^{e5}, qk^{k2}/qk^{e5} and qk^{v}/qk^{e5} mice exhibit phenotypes of intermediate severity between qk^{v}/qk^{v} and qk^{e5}/qk^{e5} mice (Table 4). They display frequent seizures but their quaking does not progress to the early ataxia as it does in qk^{e5} homozygotes. Compound qk^{k2}/qk^{e5} mice all live beyond 5 months (N=37) while only 60% of qk^{v}/qk^{e5} mice survive to 5 months of age (N=35). The survival rate of qk^{kt1}/qk^{e5} mice was not determined.

Brain histology and ultrastructure

Coronal sections of adult brains stained with hemotoxylin and eosin show that structurally, *qk*^{e5} homozygous brains are normal. In a few cases, however, the ventricles in these mutants can be noticeably larger than in wild-type animals (Figure 19) but this is not an uncommon feature of myelination mutants (Rebecca Hardy, personal communication). There is, however, a visible lack of white matter in newly dissected unstained brain tissues. Luxol fast blue (LFB) staining, which is specific for myelin lipids, confirmed this observation (Figure 19). In wild-type brains, the corpus callosum and anterior commissure are the most highly myelinated tracts of the anterior brain. LFB staining in these regions in wild-type mice is very intense while these same regions in *qk*^{e5} homozygous brains completely lack staining. This appears a bit misleading, however, since brains from *qk*^{v} /*qk*^{v} mice which are known to have reduced, but significant amounts of myelin also completely lack any LFB staining in these regions (Figure 20). Alterations in myelin structure or composition may be affecting the ability of LFB to bind any myelin in these mutants, making assessment of relative myelin levels by this method indeterminable. Consequently, we assessed the levels of myelination on the ultrastructural level by transmission electron mycroscopy (TEM).

TEM of the corpus callosum reveals that *qk*^{e5}/*qk*^{e5} mice are severely deficient in myelin (Figure 20). The thick myelin sheaths composed of numerous lamellae that are abundant in wild-type animals are nearly completely absent in *qk*^{e5}/*qk*^{e5} mutants. Most axons are without any visible myelin and when myelin is seen, it consists only of a few lamellae that have abnormally dark interperiod lines. As a comparison of severity, we also performed TEM on the well characterized *qk*^{v} homozygotes. In these animals, there is a severe decrease in myelin compared to wild-type but notably more axons are surrounded by thin myelin sheaths than in *qk*^{e5} mutant mice. Myelin levels in the posterior brain stem were similarly myelin depleted in qk^{e5}/qk^{e5} and to a lesser extent in qk^{v}/qk^{v}. We also assessed the myelin levels in the peripheral nervous system (PNS) by observing sections of the sciatic nerve. Like qk^{v}/qk^{v} mice, qk^{e5}/qk^{e5} peripheral nerves are well myelinated and appear only slightly affected in their ability to produce wild-type levels of myelin (data not shown).

Electrical activity in the qk^{e5} brain

Electroencephalogram (EEG) recordings from the cortical surface of qk^{e5} homozygous mice display abnormal electrical activity both during and between ictal (seizure) events (Figures 21 and 22). A higher variability in electrical amplitude is commonly seen in qk^{e5}/qk^{e5} mice during normal activities than that observed in wild-type. Direct amplitude comparisons between mice are difficult to make due to slight variations in electrode placement and other uncontrollable features of the implants. However, amplitude changes for any given mouse as it displays different behaviors are relevant for characterization. Random, high amplitude, low frequency interictal spiking is common in qk^{e5} mutants but does not correlate to any behavioral abnormalities. In the case of one mouse, seizure episodes were repeatedly preceded by interictal spiking activity, allowing seizure events to be predicted approximately 5 seconds before onset. In other homozygous mutants, however, spiking occurred without related seizure episodes. Behavioral tonic/clonic seizure episodes in qk^{e5}/qk^{e5} mice result in increased frequency and reduced electrical amplitude relative to the electrical activity prior to seizures. This is in contrast to a classic epileptic seizure which usually results in increased frequency and higher amplitude activity. Seizure length in qk^{e5}/qk^{e5} mice is variable but generally lasts approximately 10-12 seconds after which electrical activity returns to a basal level characteristic of the individual mouse.

Heterozygous qk^{e5} mice and their wild-type littermates were tested for susceptibility to chemically induced seizures with the convulsant drug pentylenetetrazole (PTZ). At 42.5

mg/kg dose of PTZ, 23% of wild-type and 23% of qk^{e5} heterozygotes had full tonic/clonic seizures following injection (Table 5). At a higher does of 45.0 mg/kg, the occurrence increased to 38% in qk^{e5} heterozygotes and 34% in wild-type (Table 6). This difference in seizure frequency was not significant based on a two tailed t-test at p=0.05.

The qk^{e5} molecular defect

RT-PCR and sequencing of total brain RNA did not reveal any mutations in the coding regions of the *quaking* transcripts. We did identify one C to G base pair change in the 3' UTR of the qkI-5b transcript at position 2025. This base pair was different from the Genbank qkI-5b sequence (Accession #AF090403) and that of wild-type littermate cDNA. However, subsequent sequencing of homozygous 101 cDNA, the background strain on which qk^{e5} was induced, revealed that this C to G change was a naturally occurring polymorphism in the 101 strain.

Northern blot analysis of adult brain did not reveal any striking differences in transcript levels between qk^{e5} mutants and wild-type. The cDNA probe "1-QUA2" amplified from the 3' common coding region of *quaking*, recognized the 5, 6 and 7 kb transcripts in wild-type brain, as well as in $qk^{e5}/+$, qk^{e5}/qk^{e5}, and qk^{v}/qk^{v} (Figure 23). There is a subtle decrease in the level of qkI-6 and qkI-7 transcripts in qk^{e5}/qk^{e5} mice which is also apparent in qk^{v}/qk^{v} brain, however, no discernable difference exists between the two mutants. Another cDNA probe, "2-3'UTR", generated from the 3'UTR region common to qkI-5b, qkI-6 and qkI-7 transcripts, but not to qkI-5a, was used to probe the same brain Northern blot. In the absence of qk5a detection, the levels of qkI-5b could be assessed but no difference in expression was evident in wild-type, $qk^{e5}/+$, qk^{e5}/qk^{e5} and qk^{v}/qk^{v} brains (data not shown).

The *qk*^{e5} cellular defect

In an effort to determine the defect leading to dysmyelination in *qk*^{e5} homozygous mutants on a cellular level, we performed immunohistochemistry on postnatal brains with anti-QKI antibodies. To determine the differentiation state of oligodendrocytes, we also utilized antibodies against the markers platelet derived growth factor alpha receptor (PDGFαR), condroitin sulfate proteoglycan 2 (NG2/Cspg2), sulphatide/seminolipid antigen (O4), 2',3'-cyclic nucleotide 3'-phosphodiesterase (CNP) and myelin basic protein (MBP) which are each expressed in a stage specific manner during oligodendrocyte development (Figure 24). Our experiments to identify these antigens were performed on postnatal mouse brains prior to, during and after the most active time of myelination at P7, P14 and P90 respectively. Since the presence or absence of the antigens assessed was identical at all three ages within a given genotype, the results are only discussed in the context of a particular age when they pertain to myelin levels which increase from P7 to P90.

Double labeling with antibodies against QKI-5 and the oligodendrocyte specific marker O4 in wild-type brain reveal that oligodendrocytes (O4 positive cells) express QKI-5 at high levels (Figure 25). Cells that are O4 negative and have low levels of QKI-5 are either astrocytes or early oligodendrocyte progenitors. In *qk*^{e5}/*qk*^{e5} brains, O4 positive cells are detected indicating that oligodendrocytes are present, but they do not express QKI-5 at wild-type levels. Instead, QKI-5 is reduced to a level similar to that of O4 negative cells, many of which are astrocytes. The expression of QKI-5 in *qk*^{e5}/*qk*^{e5} astrocytes is low but unaltered from that of wild-type. This was confirmed by double staining of QKI-5 and the astrocyte specific marker glial fibrillary acidic protein (GFAP) (data not shown).

The cytoplasmic expression of QKI-6 observed in oligodendrocytes of wild-type animals, is completely absent in *qk*^{e5}/*qk*^{e5} brains (Figure 26). The low QKI-6 expression seen in *qk*^{e5} mutants is exclusive to astrocytes as was confirmed with antibodies against

GFAP (data not shown). So unlike QKI-5, which is expressed at low levels in qk^{e5}/qk^{e5} oligodendrocytes, QKI-6 is completely absent from these cells. Double labeling with MBP shows that this late marker of oligodendrocyte development is present in myelin of qk^{e5} mutants but at dramatically reduced levels (Figure 26).

Previous studies show that QKI-6 and QKI-7 have identical expression patterns, even when their expression is altered in qk^{v}/qk^{v} brain (Hardy *et al.*, 1996). We found this to be true for qk^{e5}/qk^{e5} brain as well. Double labeling with antibodies against QKI-7 and O4 shows that in wild-type brains, these proteins are both expressed in oligodendrocyte cytoplasm (Figure 27). In qk^{e5}/qk^{e5} mice, QKI-7 and O4 are mutually exclusive with O4 restricted to oligodendrocytes and QKI-7 restricted to astrocytes. Therefore, QKI-7 expression, like QKI-6, is absent in qk^{e5}/qk^{e5} oligodendrocytes.

In addition to the expression of O4 and MBP, we also determined the expression of the oligodendrocyte specific markers PDGFαR, NG2 and CNP. Although the polyclonal nature of the antibodies against PDGFαR and NG2 prevented double staining with QKI antibodies, these two early oligodendrocyte markers were both found to be present in qk^{e5}/qk^{e5} brains (Figure 28). The myelin protein CNP was also found to be present although at decreased levels, similar to MBP and likely due to a great extent, to the reduced amount of myelin (Figure 29).

In each of the immunohistochemistry experiments reported here on qk^{e5}/qk^{e5} and wild-type brains, we also included age-matched brains from qk^{v}/qk^{v} animals. The expression patterns of QKI proteins in qk^{v}/qk^{v} brain, which were reported previously (Hardy *et al.*, 1996) were indistinguishable from those determined for qk^{e5}/qk^{e5}. Expression of PDGFαR, NG2 and O4 in qk^{v}/qk^{v} oligodendrocytes was also similar to that of qk^{e5}/qk^{e5} (data not shown). The amount of CNP (Figure 29) and MBP (data not shown) however, were higher in qk^{v}/qk^{v} than in qk^{e5}/qk^{e5}.

DISCUSSION

The viable neurological phenotype of qk^{e5}

The ability of ENU to produce a range of effects on gene transcription, translation and protein product function has made it useful in creating series of mutant alleles at single loci to uncover multiple gene functions. We report here the production of a new allele of the mouse *quaking* gene, qk^{e5}, with a homozygous phenotype unlike any other ENU-induced *quaking* allele.

The qk^{e5} allele was selected from a single generation ENU screen by its failure to complement the qk^{v} phenotype of seizures and quaking in qk^{e5}/qk^{v} compound heterozygotes. This was the same method used to isolate qk^{k2}, $qk^{kt3/4}$ and qk^{kt1} in previous ENU screens (Justice and Bode, 1986; Justice and Bode, 1988). However, unlike these previously induced alleles that died as embryos when bred to homozygosity, the new qk^{e5} allele is homozygous viable. Furthermore, the phenotype of qk^{e5}/qk^{e5} mice is strikingly more severe than qk^{v}/qk^{v}; which was previously thought of as the loss of *quaking* function in the postnatal brain. Both qk^{e5}/qk^{e5} and qk^{v}/qk^{v} mice begin to quake just prior to the most active time of CNS myelination at P14. However, in qk^{e5} homozygotes this quaking progresses to a severe ataxia by 3 months of age rather than the continued quaking phenotype that is maintained by qk^{v}/qk^{v} mice. Seizures in qk^{e5} mutants onset much earlier and are more frequent than those of qk^{v}/qk^{v} mice and most qk^{e5}/qk^{e5} mice die between 3 and 6 months of age, presumably from seizure induced respiratory arrest.

Homozygous qk^{e5}/qk^{e5} mice are fertile, confirming that the sterility of qk^{v}/qk^{v} males is due to the alteration of a separate locus within or near the qk^{v} deletion. This was previously suspected to be case since the embryo lethal alleles of *quaking* rescue the qk^{v} sterility in compound heterozygotes (Justice and Bode, 1988).

Transmission electron microscopy and immunohistochemical staining with antibodies against the myelin proteins CNP and MBP reveal that the qk^{e5}/qk^{e5} neurological phenotype is the result of a severe lack of myelin sheath. This deficiency is much more severe than that observed for qk^{v}/qk^{v} CNS in this study and as previously reported (Friedrich, 1974). The thick myelin sheaths present in wild-type are completely absent in qk^{e5}/qk^{e5} mice with only the occasional thin myelin sheath present, often with abnormally dark interperiod lines. The qk^{e5}/qk^{e5} brain dysmyelination phenotype is very similar to that of the highly studied mouse mutant *shiverer* (Doolittle and Schweikart, 1977; Privat *et al.*, 1979b). Like qk^{e5}, *shiverer* mice have a trembling phenotype, seizures and early mortality due to an almost complete lack of CNS myelin. Homozygous qk^{e5} mutants are unique from *shiverer*, however, in that they become severely ataxic. This is an interesting finding in light of the fact that *shiverer* is the result of loss of MBP function, and MBP RNA is a suspected target of QKI protein (Privat *et al.*, 1979a; Readhead *et al.*, 1987). It suggests that if QKI is necessary for MBP function, that other targets of QKI must also be affected in qk^{e5} mutants and lead to the ataxic phenotypic.

The myelin deficiency of qk^{e5} mutants is evident in all regions of the brain from P7 to adulthood. Although the peripheral nervous system (PNS) shows a slight myelin decrease in qk^{e5}/qk^{e5} mice as has previously been shown for qk^{v}/qk^{v} (Sidman *et al.*, 1964), the effect there is very mild. QKI proteins are expressed in PNS myelinating Schwann cells similar to CNS oligodendrocytes and they are altered in an identical manner in qk^{v}/qk^{v} mice (Hardy, 1996). This suggests a less critical role for QKI in PNS myelination. It has been suggested that a putative transporter of myelin protein mRNAs such as QKI may not be as critical for Schwann cells which myelinate multiple axons in close proximity, as it would for oligodendrocytes myelinating single axons, often at greater distances (Hardy, 1998a). Alternatively, the targets of QKI proteins could be less critical for PNS myelin formation or compaction than in the CNS. In support of this idea, PNS myelin contains major myelin proteins which, although they have overlapping functions, are genetically distinct from those of the CNS (Reviewed in Scherer, 1995).

Cortical surface EEG recordings from qk^{e5} homozygous mice during seizure episodes display increased electrical frequency and reduced amplitude. This is in contrast to the classic epileptic seizure response that results in higher amplitude electrical impulses. Lower amplitude activity is characteristic of decrimental seizures and places qk^{e5}/qk^{e5} mice in a small subclass of epileptic syndromes which share this electrical response. Very little is known about this type of epilepsy but there are both human syndromes like West syndrome (Fusco and Vigevano, 1993) and mouse mutants like *shiverer* (Jeff Noebels, personal communication) which share this particular electrical phenomenon. Electroencephalographs record summations of large bursts of electrical activity from numerous neurons in a given brain region (Guyton and Hall, 1996). Increased amplitude, a common occurrence during seizure episodes, indicates synchronized bursts of many neurons. However, even when large bursts of neuronal firing occur during seizure events, the EEG signals can have low amplitude if neuron firing is desynchronized as it appears to be qk^{e5}/qk^{e5} mice.

Heterozygous qk^{e5} mice are no more susceptible to PTZ induced seizures than their wild-type littermates. This is in contrast to our findings for heterozygotes of the embryo lethal allele qk^{k2} (see chapter 2 of this thesis). This may reflect significant differences in the effect that these mutations have on the adult brain or, more simply, may reflect their seizure susceptibility on different mouse genetic backgrounds.

The qk^{e5} molecular and cellular defect

Sequencing of *quaking* cDNA did not reveal any base pair alterations responsible for the qk^{e5} defect. Northern analysis of adult brain showed a subtle decrease in the 6 kb and 7 kb transcripts in qk^{e5} homozygous brain, similar to qk^{v}/qk^{v}. Previously, the defect in qk^{v}/qk^{v} mice has been attributed to a loss of QKI-6 and QKI-7 specifically in oligodendrocytes (Hardy *et al.*, 1996). The observed decrease of qkI-6 and qkI-7 transcripts reported here likely reflects this loss of QKI-6 and QKI-7 in oligodendrocytes. A complete loss of these transcripts would not be expected in whole brain RNA preparations since astrocytes also express all three QKI isoforms in wild-type animals and their expression is unaltered in *qk*^{e5} and *qk*^{v} mutants. This suggests that the molecular defects in *qk*^{e5} and *qk*^{v} are regulatory mutations, but it does not give any clues as to why these alleles differ so greatly in their severity.

Previous studies have shown that the QKI-5 isoform is localized to the nucleus in wild-type oligodendrocytes, while QKI-6 and QKI-7 are present in the cytoplasm (Hardy *et al.*, 1996). During oligodendrocyte development, QKI-5 is expressed in progenitor cells while QKI-6 and QKI-7 are found in more mature oligodendrocytes which have stopped proliferating (Hardy, 1998b). All three isoforms are also expressed in supportive astrocytes but at a much lower levels (Hardy *et al.*, 1996). Expression analysis of the QKI isoforms in the postnatal brain revealed that like *qk*^{v}/*qk*^{v}, *qk*^{e5}/*qk*^{e5} oligodendrocytes have low nuclear QKI-5 compared to wild-type and a complete absence of QKI-6 and QKI-7 (Figure 30). Expression of all three isoforms in astrocytes was determined to be at low but unaltered levels compared to wild-type. These studies, even more so than those previously reported for the less severe *qk*^{v} allele, reveal the critical importance of QKI function in the myelination process. Prior studies suggested that the *qk*^{v} /*qk*^{v} defect was the result of a lack of up-regulation of QKI isoforms at P14. However, this study revealed that abnormal QKI expression and defective myelination is evident in both *qk*^{e5} and *qk*^{v} homozygous mutants as early as P7. Indeed an inability to properly myelinate axons likely extends back as early as E16.5 when myelin sheaths are first detected in the developing embryonic CNS (Hardy and Friedrich, 1996). Experiments to determine just how early QKI protein expression is altered are currently underway. Preliminary results indicate that at E12.5 and E15.5, QKI protein expression in the developing CNS is normal in *qk*^{e5} homozygous embryos. The nature of oligodendrocyte development, however, prevents the likelihood that we will identify a particular time point in development where the QKI missexpression responsible for the *qk*^{e5} and *qk*^{v} defect is initiated. Myelinating oligodendrocytes are generated throughout CNS development from E16.5 into adulthood (Hardy and Friedrich, 1996). Consequently, in any given region of the CNS throughout this time, oligodendrocytes at all stages of development are present. Quantitation of oligodendrocytes at different stages in their development from mid-gestation to postnatal life may therefore be necessary to determine the cellular basis for the difference in the *qk*^{e5} and *qk*^{v} phenotypes. The differing degrees to which *qk*^{e5} and *qk*^{v} can affect oligodendrocyte function makes them ideal resources for a oligodendrocyte development study of this kind. Our preliminary efforts to quantitate oligodendrocytes indicate that the overall number present in wild-type, *qk*^{v} /*qk*^{v} and *qk*^{e5}/*qk*^{e5} brain at P14 are the same. However, there is a higher number of immature "fuzzball" oligodendrocytes present in *qk*^{v}/*qk*^{v} brain compared to wild-type and an even higher number found in *qk*^{e5}/*qk*^{e5} brains. Consequently, we suggest that *quaking* is not affecting proliferation or apoptosis in oligodendrocytes, but rather some final critical stage in their development. Our experiments assessing the expression of the marker genes PDGFαR, NG2, O4, CNP, and MBP support this idea. PDGFαR is one of the earliest markers of oligodendrocyte differentiation. It is expressed in oligodendrocyte progenitors prior to migration from the ventricular zone of the neural tube and continues until oligodendrocyte maturation (Nishiyama, 1998; Pringle and Richardson, 1993). The proteoglycan NG2 is expressed in oligodendrocyte precursors and functions as a neural outgrowth inhibitor (Levine and Card, 1987; Levine *et al.*, 1993). O4 is a lipid antigen of unknown function that appears after migration has ceased and continues in post mitotic oligodendrocyte (Warrington *et al.*, 1993; Warrington and Pfeiffer, 1992). Both CNP and MBP are myelin proteins expressed relatively late in oligodendrocyte development. CNP expression begins in immature oligodendrocytes just prior to myelination (Trapp *et al.*,

1988) while MBP is targeted to the site of myelination in mature oligodendrocytes (Ainger *et al.*, 1993; Colman *et al.*, 1982; Trapp *et al.*, 1987). All of these markers, which are expressed at different times in oligodendrocyte, development are present in both qk^{e5} and qk^{v} homozygous brains. Therefore, *quaking* likely affects a relatively late event in oligodendrocyte development. We can not, however, rule out the possibility that *quaking* may affect alternative pathways for development than those assessed with this selection of markers.

Based on the findings presented here, it is highly likely that qk^{e5} is a regulatory mutation. We suggest that in addition to a primary *quaking* gene promoter necessary for cardiovascular development, a second promoter or critical regulatory element exists for *quaking* regulation in oligodendrocytes. An ENU-induced mutation in a regulatory region could conceivably prevent the proper transcriptional elements from binding, resulting in lost QKI expression in oligodendrocytes. Reports of undetectable ENU-induced mutations in presumptive regulatory regions are not uncommon in the literature. A series of ENU-induced *Bmp-5* mutations have been reported in which mutations presumed to be regulatory, remain undetectable by current methods (Marker *et al.*, 1997). The more severe myelin deficiency caused by qk^{e5} suggests that the qk^{v} deletion allele is not the result of the loss of a *quaking* regulatory element as was previously suggested (Hardy *et al.*, 1996) but rather an alteration which leads to partial loss of regulatory function. This is supported by experiments which showed that the qk^{v} allele, in addition to a large deletion, is associated with several smaller rearrangements near the *quaking* locus (Vernet and Artzt, unpublished results). Conceivably, a regulatory region that looses function when mutated in qk^{e5} , could be repositioned in qk^{v} such that its function is compromised but not eliminated.

Conclusions

In conclusion, we have a new hypomorphic, viable allele of the mouse quaking gene that exhibits an extreme lack of CNS myelination resulting in quaking, ataxia, seizures and early death. The molecular defect in *qk*^{e5} appears to be regulatory and results in low QKI-5 and absent QKI-6 and QKI-7 in the postnatal brain oligodendrocytes. Oligodendrocytes of *qk*^{e5}/*qk*^{e5} mice express both early and late developmental marker genes indicating that *quaking* may function relatively late in their development. Electrical activity in the *qk*^{e5}/*qk*^{e5} brain is abnormal and seizures display cortical patterns characteristic of a decremental response.

IV: SUMMARY AND FUTURE DIRECTIONS

The effects of the qk^{k2} and qk^{e5} alleles represent two extremes in the loss of *quaking* function. The work presented here reveals that *quaking* has a critical role in cardiovascular development as well as a more important role in myelination than previously suspected.

We conclude, that the qk^{k2} embryonic lethal allele is the result of a thymine to adenine base pair change in the KH domain of the *quaking* gene. This mutation results in homozygous embryonic death from inadequate cardiovascular development. Defective angiogenesis, pericardial effusion and underdeveloped heart looping morphogenesis coincide with alterations in cell cycling genes and genes for vasculogenesis. Significant alterations in the expression of cardiac developmental markers, however, were not detected. In addition, the qk^{k2} lethality appears to precede any discernable function in the embryonic neural tissue. However, adult carriers of the qk^{k2} allele show increased susceptibility to chemically induced seizures, demonstrating an effect of partial loss of quaking function in the nervous system.

The induction of the new qk^{e5} allele with ENU mutagenesis reveals that *quaking* has a more critical role in postnatal myelination than previously suspected from work on qk^{v}. Homozygous qk^{e5} animals have a *quaking* phenotype which progresses to severe ataxia in adult mice, as well as early onset seizures which lead to early death. The qk^{e5} molecular defect appears to be regulatory, resulting in low QKI-5 and absent QKI-6 and QKI-7 proteins in oligodendrocytes, similar to qk^{v} homozygotes. Although oligodendrocytes in both of these viable mutants appear to develop to late stages, they are deficient in their ability to properly myelinate.

Since *quaking* mutations result in such diverse phenotypes, it has been suggested that it has a general role in cellular development. If quaking, for instance, has a general function in cellular transport, the result of its loss of function in different tissues would depend on the potentially diverse RNAs to which *quaking* could bind. In the embryo this could, for example, mean transport of RNAs from the nucleus to stimulate angiogenic processes while in the brain it could result in transport of myelin protein RNAs to the site of active myelination. The functions of *quaking* in the embryo and in the central nervous system will be more clear as target RNAs of *quaking* proteins are identified.

The existing *quaking* allele series is impressive in its diversity of phenotypes resulting from alteration of different steps in the cellular pathway of *quaking* function (Figure 31). We now suggest that the qk^{k2} mutation alters RNA binding or protein interactions necessary for *quaking* function once RNA is bound. Also, we suggest that the qk^{e5} mutation is a severe regulatory mutation. This information combined with biochemical studies and continued examination of these *in vivo* models of lost *quaking* function will be useful in revealing the full range of *quaking* functions throughout development.

Future studies include the determination of *quaking* protein expression patterns in extra embryonic tissue during angiogenesis and the biochemical result of the qk^{k2} mutation on RNA binding. Also, studies on potential RNA targets of *quaking* both in vascular tissues and in the postnatal brain will be key to understanding *quaking* function. The phenotypes of the qk^{v} and qk^{e5} alleles have provide intriguing clues to where an oligodendrocyte specific regulatory region may be found. Determination of this region would allow insite into the alternative *quaking* transcription mechanisms and thus, the process of tissue specific gene regulation. Also, given the similarities in qk^{e5} and qk^{v} oligodendrocyte protein alterations but variability in their phenotypes, we hope to determination how these two mutant mice differ on a molecular/cellular level so we can identify critical events in oligodendrocyte development and function.

REFERENCES

Abovich, N., and Roshbash, M. (1997). Cross-intron bridging interactions in the yeast commitment complex are conserved in mammals. *Cell* **89,** 403-412.

Agger, R., and Freimuth, P. (1995). Purification and cDNA sequence of a murine protein homologous to the human p62 tyrosine phosphoprotein that associates with the Ras GTPase-activating protein p120 GAP. *Gene* **158,** 307-308.

Ainger, K., Avossa, D., Morgan, F., Hill, S. J., Barry, C., Barbarese, E., and Carson, J. H. (1993). Transport and localization of exogenous myelin basic protein mRNA microinjected into oligodendrocytes. *Journal of Cell Biology* **123,** 431-441.

Arning, G., Gruter, P., Bilbe, G., and Kramer, A. (1996). Mammalian splicing factor SF1 is encoded by variant cDNAs and binds to RNA. *RNA* **2,** 794-810.

Baehrecke, E. H. (1997). *Who* encodes a KH RNA binding protein that functions in muscle development. *Development* **124,** 1323-1332.

Baldwin, H. S., Shen, H. M., Yan, H. C., De Lisser, H. M., Chung, A., Mickanin, C., Trask, T., Kirschbaum, N. E., Newman, P. J., Albeda, S. M., and Buck, C. A. (1994). Platelet endothelial cell adhesion molecule-1 (PECAM-1/CD31): alternatively spliced, functionally distinct isoforms expressed during mammalian cardiovascular development. *Development* **120,** 2539-2553.

Barbarese, E. (1991). Spatial distribution of myelin basic protein mRNA and polypeptide in *quaking* oligodendrocytes in culture. *Journal of Neuroscience Research* **29,** 271-281.

Barlat, I., Maurier, F., Duchesne, M., Guitard, E., Tocque, B., and et al. (1997). A role for Sam68 in cell cycle progression antagonized by a spliced variant within the KH domain. *Journal of Biological Chemistry* **272,** 3129-3132.

Bartoszewicz, Z. P., Noronha, A. B., Fukita, N., Sato, S., Bo, L., Trapp, B. D., and Quarles, R. H. (1995). Abnormal expression and glycosylation of the large and small isoforms of myelin-associated glycoprotein in dysmyelinating *quaking* mutants. *Journal of Neuroscience Research* **41,** 27-38.

Bennett, W. I., Gall, A. M., Southard, J. L., and Sidman, R. L. (1971). Abnormal spermiogenesis in *quaking*, a myelin-deficient mutant mouse. *Biology of Reproduction* **5,** 30-58.

Berglund, J. A., Chua, K., Abovich, N., Reed, R., and Rosbash, M. (1997). The splicing factor BBP interacts specifically with the pre-mRNA branchpoint sequence UACUAAC. *Cell* **89,** 781-787.

Burd, C. G., and Dreyfuss, G. (1994). Conserved structures and diversity of functions of RNA-binding proteins. *Science* **265,** 615-621.

Burton, P. B. J., Yacoub, M. H., and Barton, P. J. R. (1999). Cyclin-dependent kinase inhibitor expression in human heart failure. *European Heart Journal* **20,** 604-611.

Campagnoni, A. T., and Macklin, W. B. (1988). Cellular and molecular aspects of myelin protein gene expression. *Molecular Neurobiology* **2,** 41-86.

Chen, T., and Richard, S. (1998). Structure-function analysis of *qkI*: a lethal point mutation in mouse *quaking* prevents homodimerization. *Molecular and Cellular Biology* **18,** 4863-4871.

Church, G., and Gilbert, W. (1984). Genomic Sequencing. *Proceedings of the National Academy of Sciences USA* **81,** 1991-1995.

Colman, D. R., Kreibich, G., Frey, A. B., and Sabatini, D. D. (1982). Synthesis and incorporation of myelin polypeptides into CNS myelin. *Journal of Cell Biology* **95,** 598-608.

Cox, G. A., Lutz, M., Yang, C., Biemesderfer, D., Bronson, R. T., Fu, A., Aronson, P. S., Noebels, J. L., and Frankel, W. N. (1997). Sodium/hydrogen exchanger gene defect in slow-wave epilepsy mutant mice. *cell* **91,** 139-148.

Cox, R. D., Hugill, A., Shedlovsky, A., Noveroske, J. K., Best, S., Justice, M. J., Lehrach, H., and Dove, W. F. (1999). Contrasting effects of ENU-induced embryonic lethal mutations of the *quaking* gene. *Genomics* **57,** 333-341.

Cruz-Alvarez, M., and Pellicer, A. (1987). Cloning of a full-length complementary DNA for an Artemia salina glycine-rich protein. Structural relationship with RNA binding proteins. *Journal of Biological Chemistry* **262,** 13377-13380.

Darnell, J. E., Jr., Kerr, I. M., and Stark, G. R. (1994a). Jak-STAT pathways and transcriptional activation in response to IFNs and other extracellular signaling proteins. *Science* **264,** 1415-1421.

Darnell, J. E. J., Kerr, I. M., and Stark, G. R. (1994b). Jak-STAT pathways and transcriptional activation in response to IFNs and other extracellular signaling proteins. *Science* **264,** 1415-1421.

Delassalle, A., Zalc, B., Lachapelle, F., Raoul, M., Collier, P., and Jacque, C. (1981). Regional distribution of myelin basic protein in the central nervous system of *quaking* and *jimpy* and normal mice during development and aging. *Journal of Neuroscience Research* **6,** 303-313.

Depre, C., Shipley, G. L., Chen, W., Han, Q., Doenst, T., Moore, M. L., Stepkowski, S., Davies, P. J. A., and Taegtmeyer, H. (1998). Unloaded heart in vivo replicates fetal gene expression of cardiac hypertrophy. *Nature Medicine* **4,** 1269-1275.

Doolittle, D. P., and Schweikart, K. M. (1977). Myelin deficient, a new neurological mutant in the mouse. *Journal of Heredity* **68,** 331-332.

Ebersole, T. A., Chen, Q., Justice, M. J., and Artzt, K. (1996). The *quaking* gene product necessary in embryogenesis and myelination combines features of RNA binding and signal transduction proteins. *Nature Genetics* **12,** 260-265.

Ebersole, T. A., Rho, O., and Artz, K. (1992). The proximal end of mouse chromosome 17: New molecular markers identify a deletion associated with *quaking viable. Genetics* **131,** 183-190.

Echelard, Y., Epstein, D. J., St-Jacques, B., Shen, L., Mohler, J., McMahon, J. A., and McMahon, A. P. (1993). *Sonic hedge hog,* a member of a family of putative signaling molecules, is implicated in the regulation of CNF polarity. *Cell* **75,** 1417-1430.

Ekker, S. C., Ungar, A. R., Greenstein, P., Von Kessler, D. P., Porter, J. A., Moon, R. T., and Beachy, P. A. (1995). Patterning activities of vertebrate hedgehog proteins in the developing eye and brain. *Curr Biol* **5,** 944-955.

Ericson, J., Muhr, J., Placzek, M., Lints, T., Jessell, T. M., and Edlund, T. (1995). *Sonic hedgehog* induces the differentiation of ventral forebrain neurons: a common signal for ventral patterning within the neural tube. *Cell* **81,** 747-756.

Ericson, J., Rashbass, P., Schedl, A., Brenner-Morton, S., Kawakami, A., van Heyningen, V., and Jessell, T. M. (1997). *Pax6* controls progenitor cell identity and neuronal fate in response to graded *Shh* signaling. *Cell* **90,** 169-180.

Ferrara, N., Carver-Moore, K., Chen, H., Dowd, M., Lu, L., O'Shea, K. S., Powell-Braxton, L., Hillan, K. J., and Moore, M. W. (1996). Heterozygous embryonic lethality induced by targeted inactivation of the *VEGF* gene. *Nature* **380,** 349-442.

Friedrich, V. L., Jr. (1974). The myelin deficit in *quaking* mice. *Brain Research* **82,** 168-172.

Fujita, N., Sato, S., Ishiguro, H., Inuzuka, T., Baba, H., Kurihara, T., Takahash, i. Y., and Miyatake, T. (1990). The large isoform of myelin-associated glycoprotein is scarcely expressed in the *quaking* mouse brain. *Journal of Neurochemistry* **55,** 1056-1059.

Fujita, N., Sato, S., Kurihara, T., Inuzuka, T., Takahashi, Y., and Miyatake, T. (1988). Developmentally regulated alternative splicing of brain myelin-associated glycoprotein mRNA is lacking in the *quaking* mouse. *FEBS Letters* **232,** 323-327.

Fumagalli, S., Totty, N. F., Hsuan, J. J., and Courtneidge, S. A. (1994). Target for Src in mitosis. *Nature* **368,** 871-4.

Fusco, L., and Vigevano, F. (1993). Ictal clinical electroencephalographic findings of spasms in West syndrome. *Epilepsia* **34,** 671-678.

Fyrberg, C., Becker, J., Barthmaier, P., Mahaffey, J., and Fyrberg, E. (1997). A *Drosophila* muscle-specific gene related to the mouse *quaking* locus. *Gene* **197,** 315-323.

Guyton, A. C., and Hall, J. E. (1996). "Textbook of Medical Physiology." W.B. Saunders Company, Philadelphia, PA.Hanahan, D. (1997). Signaling vascular morphogenesis and maintenance. *Science* **277,** 48-50.

Hanahan, D. (1997). Signaling vascular morphogenesis and maintenance. *Science* **277,** 48-50.

Hardy, R. J. (1998a). Molecular defects in the dysmyelinating mutant *quaking*. *Journal of Neuroscience Research* **51,** 417-422.

Hardy, R. J. (1998b). QKI expression is regulated during neuron-glial cell fate decisions. *Journal of Neuroscience Research* **54,** 46-57.

Hardy, R. J., and Friedrich, V. L., Jr. (1996). Oligodendrocyte progenitors are generated throughout the embryonic mouse brain, but differentiate in restricted foci. *Development* **122,** 2059-2069.

Hardy, R. J., Loushin, C. L., Friedrich, V. L., Jr., Chen, Q., and Ebersole, T. A. (1996). Glial cell type-specific expression of QKI proteins is altered in *quaking viable* mutant mice. *The Journal of Neuroscience* **16,** 7941-7949.

Heikinheimo, M., Lawshe, A., Shackleford, G. M., Wilson, D. B., and MacArthur, C. A. (1994). *Fgf-8* expression in the post-gastrulation mouse suggests roles in the development of the face, limbs and central nervous system. *Mechanisms of Development* **48,** 129-138.

Herrmann, B. G. (1991). Expression pattern of the *Brachyury* gene in whole-mount TWis/TWis mutant embryos. *Development* **113,** 913-917.

Hitotsumachi, S., Carpenter, D. A., and Russell, W. L. (1985). Dose-repetition increases the mutagenic effectiveness of *N*-ethyl-*N*-nitrosourea in mouse spermatogonia. *Proceedings of the National Academy of Sciences USA* **82,** 6619-6621.

Hogan, B., Beddington, R., Costantini, F., and Lacy, E. (1994). "Manipulating the Mouse Embryo." Cold Spring Harbor Press,

Hogan, E. L., and Greenfield, S. (1984). Animal models of genetic disorders in myelin. *In* "Myelin" (P. Morrell Ed.) Plenum Press, New York.

Hopper, A. F., and Heart, N. H. (1985). "Foundations of animal development." Oxford University Press, New York. Huang, J.-D., Cope, M. J. T. V., Mermall, V., Strobel, M. C., Kendrick-Jones, J., Russell, L. B., Mooseker, M. S., Copeland, N. G., and Jenkins, N. A. (1998a). Molecular Genetic Dissection of Mouse Unconventional Myosin-VA: Head Region Mutations. *Genetics* **148,** 1951-1961.

Huang, J.-D., Cope, M. J. T. V., Mermall, V., Strobel, M. C., Kendrick-Jones, J., Copeland, N. G., and Jenkins, N. A. (1998b). Molecular Genetic Dissection of Mouse Unconventional Myosin-VA: Head Region Mutations. *Genetics* **148,** 1951-1961.

Huang, J.-D., Mermall, V., Strobel, M. C., Russell, L. B., Mooseker, M. S., Copeland, N. G., and Jenkins, N. A. (1998b). Molecular Genetic Dissection of Mouse Unconventional Myosin-VA: Tail Region Mutations. *Genetics* **148,** 1963-1972.

Hunter, T., and Pines, J. (1994). Cyclins and cancer II: Cyclin D and CDK inhibitors come of age. *Cell* **79,** 573-582.

Jacque, C., Delassalle, A., Raoul, M., and Baumann, N. (1983). Myelin basic protein deposition in the optic and sciatic nerves of dysmyelinating mutants *quaking, jimpy,* *trembler*, MLD, and *shiverer* during development. *Journal of Neurochemistry* **41,** 1335-1340.

Jan, E., Motzny, C. K., Graves, L. E., and Goodwin, E. B. (1999). The STAR protein, GLD-1, is a translational regulator of sexual identity in *Caenorhabditis elegans*. *EMBO J* **18,** 258-69.

Jones, A., Francis, R., and Schedl, T. (1996). GLD-1, a cytoplasmic protein essential for oocyte differentiation, shows stage-and sex-specific expression during *Caenorhabditis elegans* germline development. *Developmental Biology* **180,** 165-183.

Jones, A. R., and Schedl, T. (1995). Mutations in *gld-1*, a female germ cell-specific tumor suppressor gene in *Caenorhabditis elegans*, affect a conserved domain also found in Src-associated protein Sam68. *Genes and Development* **9,** 1491-1504.

Justice, M. J. (1999). Mutagenesis of the mouse germline. *In* "Mouse Genetics and Transgenics: A Practical Approach" (I. Jackson and C. Abbott, Eds.), Oxford University Press, Oxford.

Justice, M. J., and Bode, V. C. (1986). Induction of new mutations in a mouse t-haplotype using ethylnitrosourea mutagenesis. *Genetical Research* **47,** 187-192.

Justice, M. J., and Bode, V. C. (1988). Three ENU-induced alleles of the murine *quaking* locus are recessive embryonic lethal mutations. *Genetical Research* **51,** 95-102.

King, D. P., Vitaterna, M. K., Chang, A. M., Dove, W. F., Pinto, L. H., Turek, F. W., and Takahashi, J. S. (1997a). The mouse *Clock* mutation behaves as an antimorph and maps within the *W19H* deletion, distal of *Kit*. *Genetics* **146,** 1049-1060.

King, D. P., Zhao, Y., Sangoram, A. M., Wilsbacher, L. D., Tanaka, M., Antoch, M. P., Steeves, T. D. L., Vitaterna, M. H., Kornhouser, J. H., Lowrey, P. L., Turek, F. W., and Takahashi, J. S. (1997b). Positional cloning of the mouse circadian *Clock* gene. *Cell* **89,** 641-653.

Kispert, A., and Herrmann, B. G. (1994). Immunohistochemical analysis of the *Brachyury* protein in wild-type and mutant mouse embryos. *Developmental Biology* **161,** 179-193.

Komuro, I., and Izumo, S. (1993). *Csx*: a murine homeobox-containing gene specifically expressed in the developing heart. *Proceedings of the National Academy of Sciences USA* **90,** 8145-8149.

Kondo, T., Furuta, T., Mitsunaga, K., Ebersole, T. A., Shichiri, M., Wu, J., Artzt, K., Yamamura, K., and Abe, K. (1999). Genomic organization and expression analysis of the mouse *qkI* locus. *Mammalian Genome* **10,** 662-669.

Kosobud, A. E., and Crabbe, J. C. (1990). Genetic correlations among inbred strain sensitivities to convulsions induced by 9 convulsant drugs. *Brain Research* **256,** 8-16.

Krämer, A. (1992). Purification of splicing factor SF1, a heat-stable protein that functions in the assembly of a presplicing complex. *Molecular and Cellular Biology* **12,** 4545-4552.

Laborda, J. (1991). cDNA used as an estradiol-independent mRNA control is the cDNA for human acidic ribosomal phosphoprotein PO. *Nucleic Acid Research* **19,** 3998.

Ladoux, A., and Frelin, C. (1993). Hypoxia is a strong inducer of vascular endothelial growth factor mRNA expression in the heart. *Biochemistry and Biophysics Research Communications***195**, 1005-1010

Lemke, G. (1986). Molecular biology of the major myelin genes. *Trends in Neurological Science* **9,** 266-270.

Levine, J. M., and Card, J. P. (1987). Light and electron microscopic localization of a cell surface antigen (NG2) in the rat cerebellum: association with smooth protoplasmic astrocytes. *Journal of Neuroscience* **7,** 2711-2720.

Levine, J. M., Stincone, F., and Lee, Y. S. (1993). Development and differentiation of glial precursor cells in the rat cerebellum. *Glia* **7,** 307-321.

Li, Z., Zhang, Y., Li, D., Feng, Y. (2000). Destabilization and mislocalization of myelin basic protein mRNAs in quaking dysmyelination lacking the QKI RNA-binding proteins. Journal of Neuroscience 20(13), 4944-4953

Lin, Q., Schwarz, J., Bucana, C., and Olson, E. N. (1997). Control of mouse cardiac morphogenesis and myogenesis by transcription factor *MEF2C. Science* **276,** 1404.

Lints, T. J., Parsons, L. M., Hartley, L., Lyons, I., and Harvey, R. P. (1993). *Nkx-2.5*: a novel murine homeobox gene expressed in early heart progenitor cells and their myogenic descendants. *Development* **119,** 419-431.

Marker, P. C., Seung, K., Bland, A. E., Russell, L. B., and Kingsley, D. M. (1997). Spectrum of *Bmp5* mutations from germline mutagenesis experiments in mice. *Genetics* **145,** 435-443.

Marti, E., Bumcrot, D. A., Takada, R., and McMahon, A. P. (1995). Requirement of 19K form of *Sonic hedgehog* for induction of distinct ventral cell types in CNS explants. *Nature* **375,** 322-325.

Mezquita, J., Pau, M., and Mezquita, C. (1998). Four isoforms of the signal-transduction and RNA-binding protein QKI expressed during chicken spermatogenesis. *Molecular reproduction and development* **50,** 70-78.

Mikoshiba, K., Okano, H., Tamura, T., and Ikenaka, T. (1991). Structure and function of myelin protein genes. *Annual Reviews in Neuroscience* **14,** 201-217.

Nishiyama, A. (1998). Glial progenitor cells in normal and pathological states. *Keio. Journal of Medicine* **47,** 205-208.

Noveroske, J. K., Weber, J. S., and Justice, M. J. (2000). The mutagenic action of *N*-ethyl-*N*-nitrosourea in the mouse. *Mammalian Genome* **11,** 478-483.

Pellmar, T. C., and Wilson, W. A. (1977). Synaptic mechanism of pentylenetetrazole: selectivity for chloride conductance. *Science* **197,** 912-914.

Peters, J., J., A. S., Loutit, J. F., and Glegg, J. B. (1985). A mouse *β-globin* mutant that is an exact model of hemoglobin Rainier in man. *Genetics* **110,** 709-721.

Pringle, N., and Richardson, W. D. (1993). A singularity of *PDGF alpha-receptor* expression in the dorsoventral axis of the neural tube may define the origin of the oligodendrocyte lineage. *Development* **117,** 525-533.

Privat, A., Jacque, C., Bourre, J. M., Dupouey, P., and Baumann, N. (1979a). Absence of the major dense line in myelin of the mutant mouse "*shiverer*". *Neuroscience Letters* **12,** 107-112.

Radice, G. L., Rayburn, H., Matsunami, H., Knudsen, K. A., Takeichi, M., and Hynes, R. O. (1997). Developmental defects in mouse embryos lacking *N-cadherin*. *Developmental biology* **181,** 64-78.

Ramanjaneyula, R., and Ticku, M. K. (1984). Interactions of pentamethylenetetrazole and tetrazole analogues with the picrotoxinin site of the benzodiazepine-GABA receptor-ionophore complex. *European Journal of Pharmacology* **98,** 337-345.

Readhead, C., Popko, B., Takahashi, N., Shine, D. H., Saavedra, R. A., Sidman, R. L., and Hood, L. (1987). Expression of a myelin basic protein gene in transgenic *shiverer* mice: Correction of the dysmyelinating phenotype. *Cell* **48,** 703-712.

Risua, W. (1997). Mechanisms of angiogenesis. *Nature* **386,** 671-674.

Ritter, S. J., and Davies, P. J. A. (1998). Identification of a *transforming growth factor-beta 1/bone morphogenetic protein 4 (TGF-beta 1/BMP4)* response element within the mouse tissue transglutaminase gene promoter. *Journal of Biological Chemistry* **273,** 12798-12806.

Roelink, H., Porter, J., Chiang, C., Tanabe, Y., Chang, D. T., Beachy, P. A., and Jessell, T. M. (1995). Floor plate and motor neuron induction by different concentrations of the amino-terminal cleavage product of *Sonic hedgehog* autoproteolysis. *Cell* **81,** 445-455.

Roth, J. R., Hunkeler, M. J., and Campagnoni, A. T. (1985). Expression of myelin basic protein genes in several dysmyelinating mouse mutants during early postnatal brain development. *Journal of Neurochemistry* **45.**

Ruiz i Altaba, A., Jessell, T. M., and Roelink, H. (1995). Restrictions to floor plate induction by hedgehog and winged-helix genes in the neural tube of frog embryos. *Molecular and Cellular Neuroscience* **6,** 106-121.

Russell, W. L., Kelly, E. M., Hunsicker, P. R., Bangham, J. W., Maddux, S. C., and Phipps, E. L. (1979). Specific-locus test shows ethylnitrosourea to be the most potent mutagen in the mouse. *Proceedings of the National Academy of Sciences USA* **76,** 5818-5819.

Salzer, J. L., Pedraza, L., Brown, M., Struyk, A., Afar, D., and Bell, J. (1990). Structure and function of the myelin-associated glycoproteins. *Annals of the New York Academy of Science* **605,** 29-43.

Sasaki, H., and Hogan, B. L. M. (1994). *HNF-3β* as a regulator of floor plate development. *Cell* **76,** 103-115.

Scherer, S. S., and Chance, P. F. (1995). Myelin genes: getting the dosage right. *Nature Genetics* **11,** 226-228.

Schumacher, A., Faust, C., and Magnuson, R. (1996). Positional cloning of a global regulator of anterior-posterior patterning in mice. *Nature* **383,** 250-253.

Shedlovsky, A., Guenet, J.-L., Johnson, L. L., and Dove, W. F. (1986). Induction of recessive lethal mutations in the *T/t-H-2* region of the mouse genome by a point mutagen. *Genetical Research* **47,** 135-142.

Shedlovsky, A., King, T. R., and Dove, W. F. (1988). Saturation germ line mutagenesis of the murine *t* region including a lethal allele at the *quaking* locus. *Proceedings of the National Academy of Sciences USA* **85,** 180-184.

Shedlovsky, A., McDonald, J. D., Symula, D., and Dove, W. F. (1993). Mouse models of human phenylketonuria. *Genetics* **134,** 1205-1210.

Sherr, C. J. (1994). G1 phase progression: cycling on cue. *Cell* **79,** 551-555.

Sherr, C. J., and Roberts, J. M. (1995). Inhibitors of mammalian G1 cyclin-dependent kinases. *Genes and Development* **9,** 1149-1163.

Shibuya, T., and Morimoto, K. (1993). A review of the genotoxicity of 1-ethyl-1-nitrosourea. *Mutation Research* **297**, 3 - 38.

Sidman, R. L., Dickie, M. M., and Appel, S. H. (1964). Mutant Mice (*quaking* and *jimpy*) with deficient myelination in the central nervous system. *Science* **144**, 309-311.

Singer, B., and Dosahjh, M. K. (1990). Site-directed mutagenesis for quantitation of base-base interactions at defined sites. *Mutation Research* **233**, 45-51.

Siomi, H., Choi, M., Siomi, M. C., Nussbaum, R. L., and Dreyfuss, G. (1994). Essential role for KH domains in RNA binding: impaired RNA binding by a mutation in the KH domain of *FMR1* that causes fragile X syndrome. *Cell* **77**, 33-39.

Subramanian, S. V., and Nadalginard, B. (1996). Early expression of the different isoforms of the *myocyte enhancer factor-2 (MEF2)* protein in myogenic as well as non-myogenic cell lineages during mouse embryogenesis. *Mechanisms in Development* **57**, 103-112.

Suri, C., Jones, P. F., Patan, S., Bartunkova, S., Maisonpierre, P. C., Davis, S., Sato, T. N., and Yancopoulos, G. D. (1996). Requisite role of angiopoietin-1, a ligand for the tie2 receptor, during embryonic angiogenesis. *Cell* **87**, 1171-1180.

Tanaka, H., Abe, K., and Kim, C. (1997). Cloning and expression of the *quaking* gene in zebrafish embryo. *Mechanisms of Development* **69**, 209-213.

Tanaka, M., Chen, Z., Bartunkova, S., Yamasaki, N., and Izumo, S. (1999). The cardiac homeobox gene *Csx/Nkx2.5* lies genetically upstream of multiple genes essential for heart development. *Development* **126,** 1269-1280.

Taylor, S. J., and Shalloway, D. (1994). An RNA-binding protein associated with Src through its SH2 and SH3 domains in mitosis. *Nature* **368,** 867-71.

Trapp, B. D., Andrews, S. B., Cootauco, C., and Quarles, R. H. (1989). The myelin-associated glycoprotein is enriched in multivesicular bodies and periaxonal membranes of actively myelinating oligodendrocytes. *Journal of Cell Biology* **109,** 2417-2426.

Trapp, B. D., Bernier, L., Andrews, S. B., and Colman, D. R. (1988). Cellular and Subcellular distribution of 2',3'-cyclic nucleotide 3'-phosphodiesterase and its mRNA in the rat central nervous system. *Journal of Neurochemistry* **51,** 859-868.

Trapp, B. D., Moeuch, T., Barbosa, E., Tennekoon, G., and Griffith, J. (1987). Spatial segregation of mRNA encoding myelin-specific proteins. *Proceedings of the National Academy of Sciences USA* **84,** 7773-7777.

Vernet, C., and Artzt, K. (1997). STAR, a gene family involved in signal transduction and activation of RNA. *Trends in Genetics* **13,** 479-484.

Vogel, E. W., and Natarajan, A. T. (1995). DNA damage and repair in somatic and germ cells *in vivo*. *Mutation Research* **330,** 183-208.

Vogel, E. W., Zijlstra, J. A., and Blijleven, W. G. H. (1983). Metabolic activation and mutagenic properties of procarcinogens in *Drosophila*. *In* "In Vitro Toxicity Testing of Environmental Agents, Current and Future Possibilities" (A. R. Kolber, T. K. Wong, L. D. Grant, R. S. De Woskin, and T. J. Hughes, Eds.), pp. 215A-232A. Plenum Press, New York.

Walther, C., and Gruss, P. (1991). *Pax6*, a murine paired box gene, is expressed in the developing CNS. *Development* **113,** 1435-1449.

Warrington, A. E., Barbarese, E., and Pfeiffer, S. E. (1993). Differential myelinogenic capacity of specific developmental stages of the oligodendrocyte lineage upon transplantation into hypomyelinating hosts. *Neuroscience Research* **34,** 1-13.

Warrington, A. E., and Pfeiffer, S. E. (1992). Proliferation and differentiation of O4+ oligodendrocytes in postnatal rat cerebellum: analysis in unfixed tissue slices using anti-glycolipid antibodies. *Journal of Neuroscience Research* **33,** 338-353.

Wilkinson, D. G., Bhatt, S., and Herrmann, B. G. (1990). Expression pattern of the mouse *T* gene and its role in mesoderm formation. *Nature* **343,** 657-659.

Willie, A., Ng, I. L., Grupp, L., Subramaniam, A., and Robbins, J. (1991). Cardiac myosin heavy chain mRNA expression and myocardial function in the mouse heart. *Circulation Research* **68,** 1742-1750.

Wu, J., Zhou, L., Tonissen, K., Tee, R., and Artzt, K. (1999). The STAR protein *quaking*I-5 (QKI-5) has a novel nuclear localization signal and shuttles between the nucleus and the cytoplasm. *Journal of Biological Chemistry* **274,** 29202-29210.

Xue, Y., Gao, X., Lindsell, C. E., Norton, C. R., Chang, B., Hicks, C., Gendron-Maguire, M., Rand, E. B., Weinmaster, G., and Gridley, T. (1999). Embryonic lethality and vascular defects in mice lacking the notch ligand *jagged1. Human Molecular Genetics* **8,** 723-730.

Zaffran, S., Astier, M., Gratecos, D., and Semeriva, M. (1997). The *held out wings* (*how*) *Drosophila* gene encodes a putative RNA-binding protein involved in the control of muscular and cardiac activity. *Development* **124,** 2087-2098.

Zeller, R., Bloch, K. D., Williams, B. S., Arceci, R. J., and Seidman, C. E. (1987). Localized expression of the atrial natriuretic factor gene during cardiac embryogenesis. *Genes and Development* **7,** 693-698.

Zhang, D., Gaussin, V., Taffet, G. E., Belaguli, N. S., Yamada, M., Schwartz, R. J., Michael, L. H., Overbeek, P. A., and Schneider, M. D. (2000). *TAK1* is activated in the myocardium after pressure overload and is sufficient to provoke heart failure in transgenic mice. *Nature Medicine* **6,** 556-563.

Zhang, P., Liegeosis, N. J., Wong, C., Finegold, M., Hou, H., Thompson, J. C., Silverman, A., Harper, J. W., DePinho, R. A., and Elledge, S. J. (1997). Altered cell differentiation and proliferation in mice lacking p57KIP2 indicates a role in Beckwith-Wiedemann syndrome. *Nature* **387,** 151-158.

Zijlstra, J. A., Brussee, J., A., v. d. G., and Vogel, E. W. (1989). Importance of multiple hydroxylated metabolites in hexamethyl-phosphoramide (HMPA)-mediated mutagenesis in *Drosophila melanogaster. Mutation Research* **212,** 193-211.

Zijlstra, J. A., Vogel, E. W., and Breimer, D. D. (1987). Pharmacological aspects of mutagenicity research in *Drosophila melanogaster. Reviews in Biochemistry and Toxicology* , 121-154.

Zorn, A. M., and Krieg, P. A. (1997). The KH domain protein encoded by *quaking* functions as a dimer and is essential for notochord development in *Xenopus* embryos. *Genes and Development* **11,** 2176-2190.

APPENDIX

Figure 1: Mutagenic action of *N*-ethyl-*N*-nitrosourea A) Structure ENU with its transferable ethyl group highlighted in red. B) ENU adduct formation and mispairing of O^4-ethylthymine. Arrows indicate deoxyribose attachment sights.

A

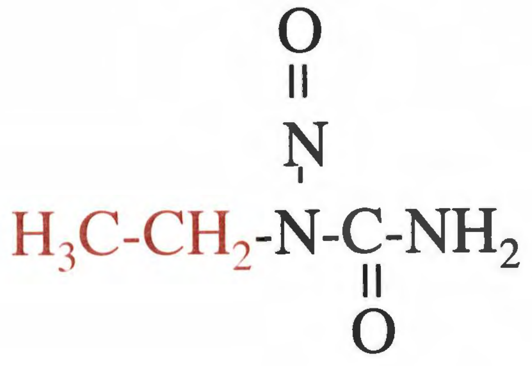

$H_3C\text{-}CH_2\text{-}N(N{=}O)\text{-}C({=}O)\text{-}NH_2$

B

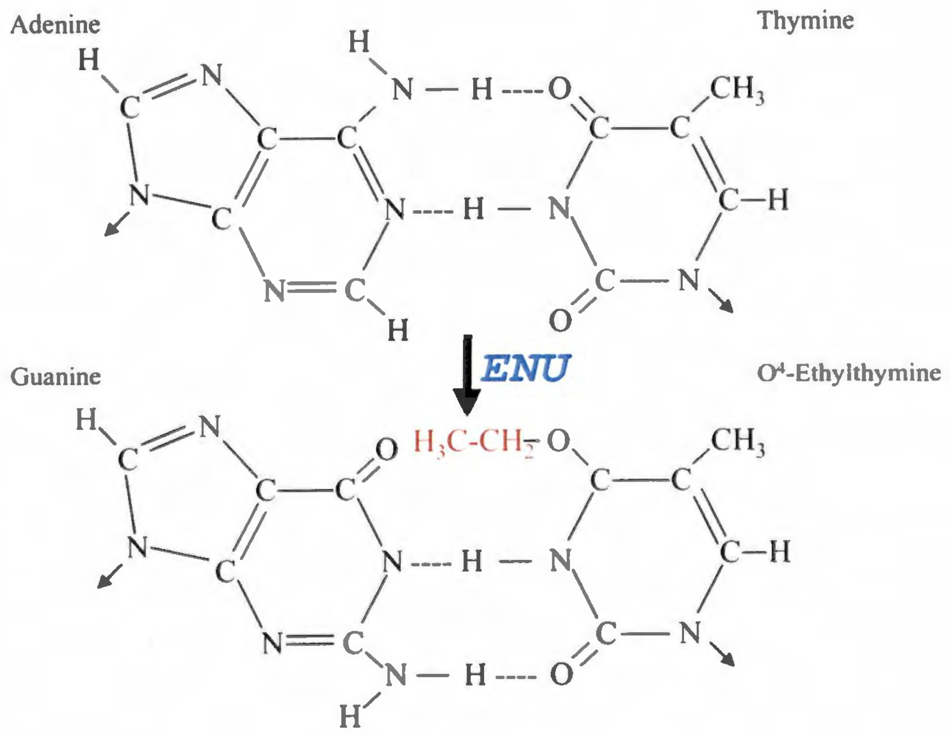
Adenine
Thymine
ENU
Guanine
O⁴-Ethylthymine

Figure 2: Mispairing of ENU ethylated bases. Mispairing results in a base pair substitution after two rounds of DNA replication. Thymine is in red to indicate the presence of the O^4-ethyl adduct. Blue letters indicate base substitutions.

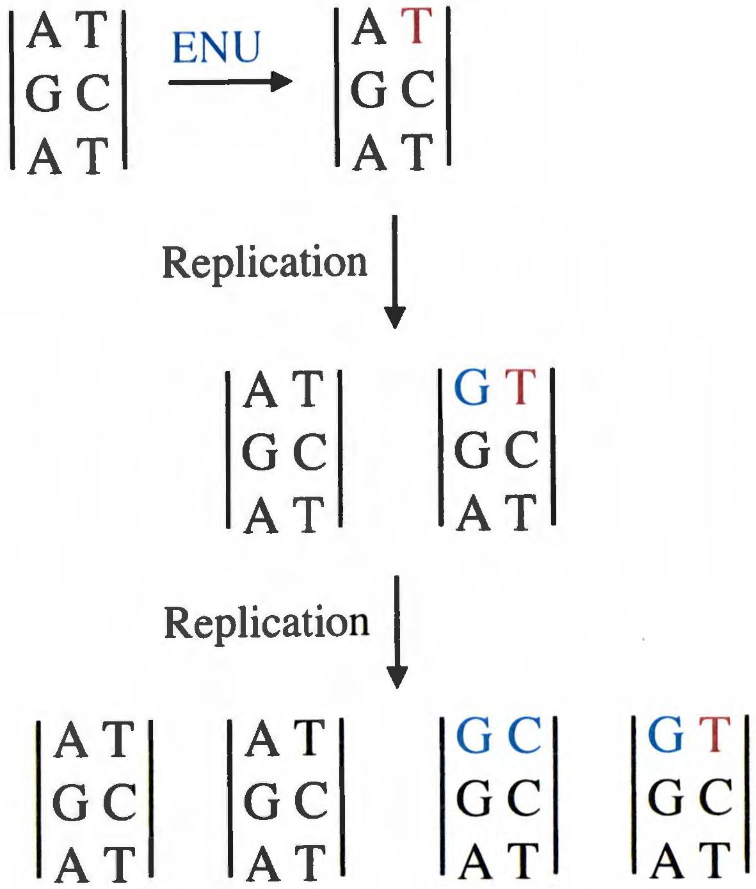
A T
G C
A T
ENU
A T
G C
A T
Replication
A T
G C
A T
G T
G C
A T
Replication
A T
G C
A T
A T
G C
A T
G C
G C
A T
G T
G C
A T

Figure 3: Structure of the *quaking* protein product QKI. The STAR domain consists of the KH (RNA binding) domain and its flanking QUA1 and QUA2 domains. The RG boxes are also indicative of RNA binding proteins. The tyrosine tail and proline rich regions (green) which contain SH3 binding sites are indicative of downstream function in a signal transduction pathway. QKI isoforms differ only in the carboxy terminus. QKI structure is according to Ebersole et al., (1996) Nature Genetics 12, p260.

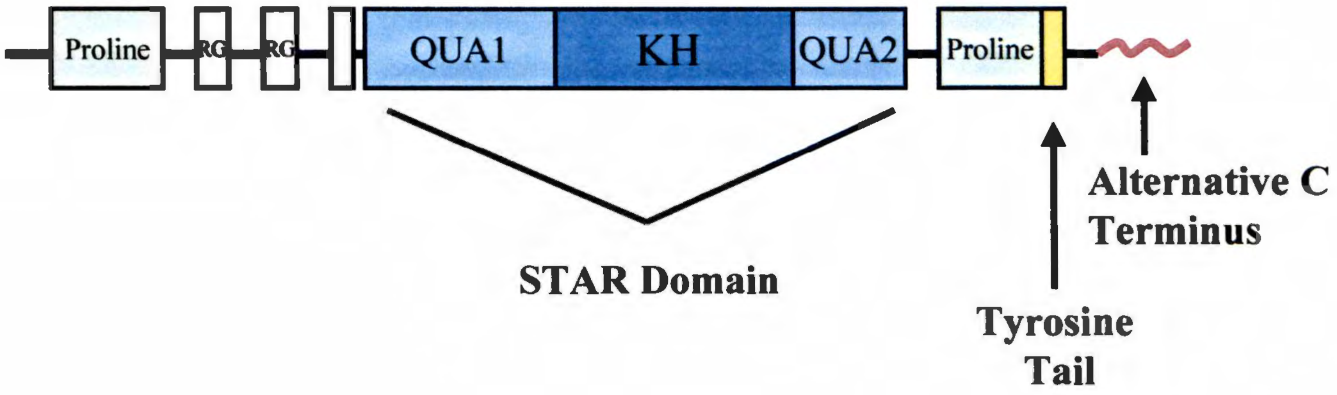
Proline
RG
RG
QUA1
KH
QUA2
Proline
STAR Domain
Alternative C Terminus
Tyrosine Tail

Table 1: Expression and functional evolution of *quaking*

	Drosophila	Zebrafish	*Xenopus*	Mouse	Human
Homolog	*how*	*zqk*	*Xqua*	*qkI*	*Hqk*
Embryonic Expression	Mesoderm Heart	Neural Ecto Dorsal Meso Heart	Neural Ecto Dorsal Meso Heart	Neural Ecto Heart	Neural Ecto Heart
Adult Expression	Muscle Heart	Brain Heart	Brain Heart	Brain Heart	Brain Heart
Mutants	Embryo Lethal OR Held Out Wings	?	Embryo Lethal Reduced Head and Notochord	Embryo Lethal OR Dysmyelination	?

Figure 4: Genomic structure and transcripts of the *quaking* gene. Top line: Exon-intron genomic structure of *quaking*. The highly conserved regions of the STAR domain are indicated above and the green arrow indicates the translation start site. Below the genomic structure, with names indicated on the left, are the alternative transcripts of *quaking*. Like colored boxes indicate like sequence and red arrows designate the translation stop sites. qkI-5a codes for QKI-5 protein, qkI-5b and qkI-6 both code for QKI-6 and qkI-7 codes for the QKI-7 isoform. Transcripts are according to Kondo et al., (1999) Mammalian Genome 10, p 262.

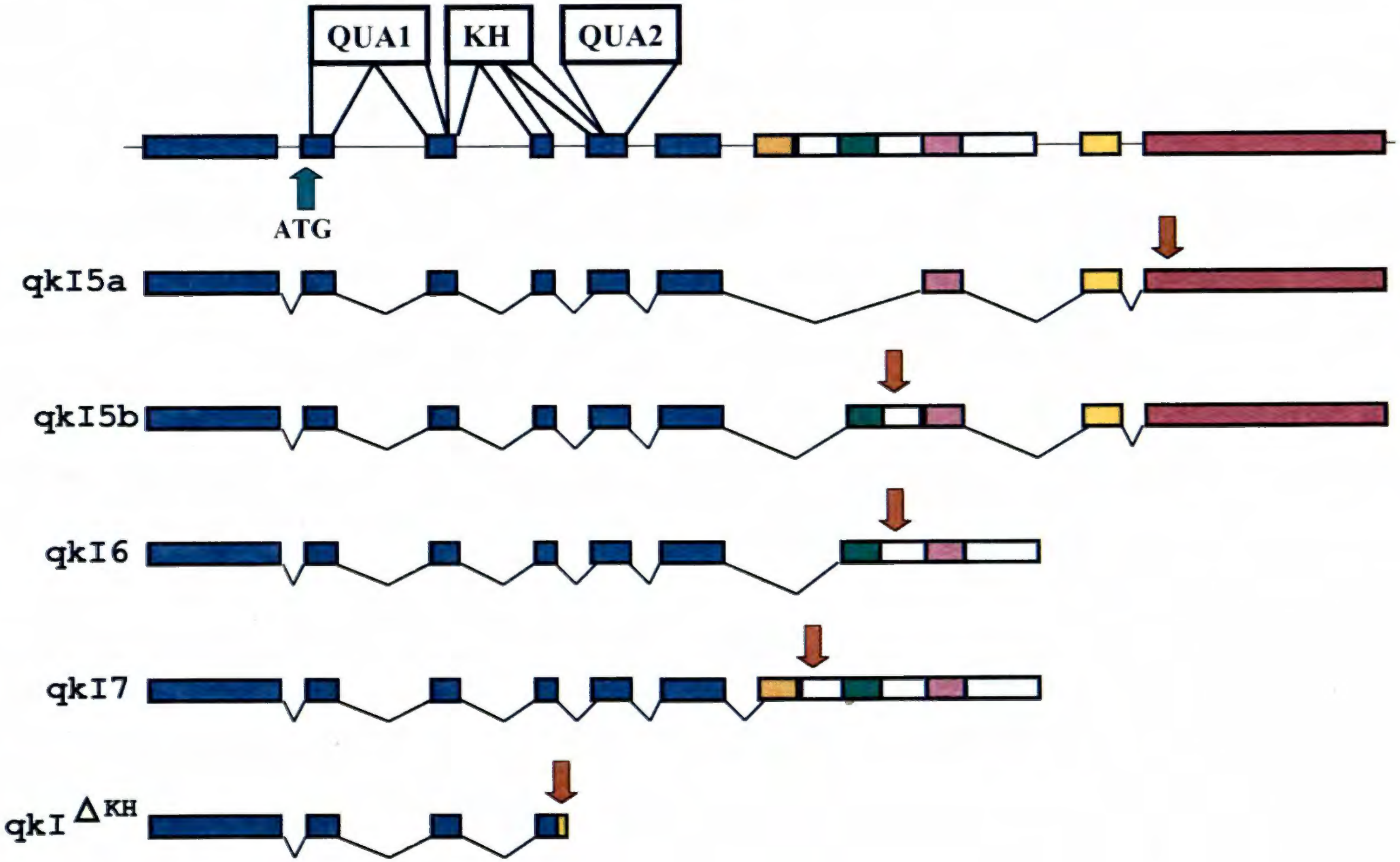
QUA1
KH
QUA2
ATG
qkI5a
qkI5b
qkI6
qkI7
$qkI^{\Delta KH}$

Figure 5: The Model of *quaking* function. Transcription and translation of *quaking* RNA is followed by subsequent dimerization of QKI proteins. Signal transduction activation may be required for *quaking* function in RNA transport, splicing and suppression of translation. Proper function in embryonic cells and oligodendrocytes results in normal embryo development and myelination in each of the organisms in which *quaking* homologues have been cloned.

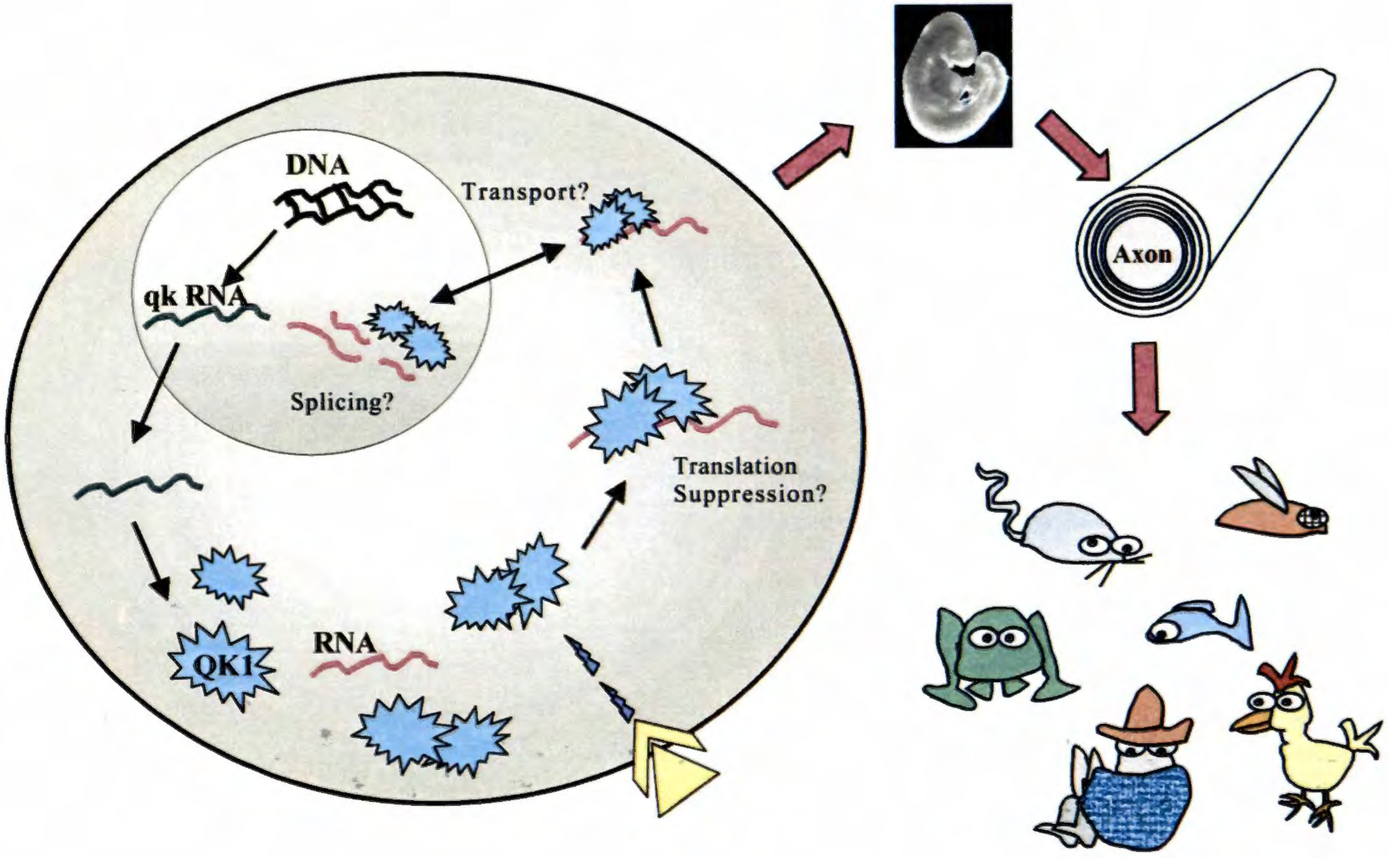
DNA
qk RNA
Transport?
Splicing?
Translation
Suppression?
QK1
RNA
Axon

Figure 6: Molecular defect in the *qk*^{k2} allele. A) Sequencing revealed a T to A transversion in homozygous *qk*^{k2} cDNA. B) The resulting mutant QKI protein contains a valine to glutamic acid change at amino acid position 157 which lies in the common KH (RNA) binding domain. The newly sequenced wild-type transcript qkIΔQUA2 results in the truncated protein QKIΔQUA2. This truncated isoform terminates after the unique four amino acids, FFFA, in the QUA2 domain.

A

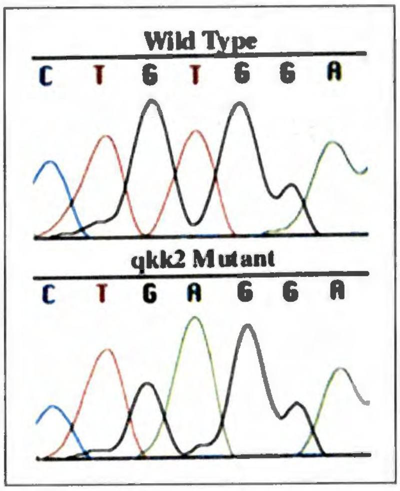
Wild Type
C T G T G G A
qkk2 Mutant
C T G A G G A

B

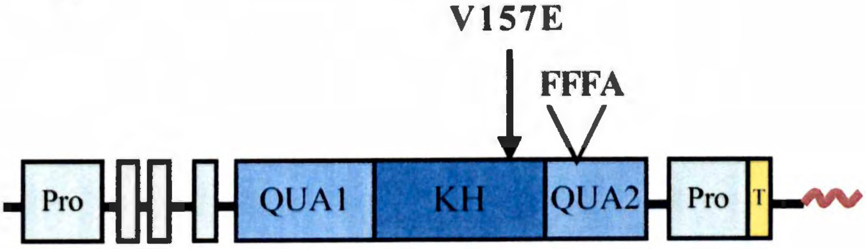
V157E
FFFA
Pro
QUA1
KH
QUA2
Pro
T

Figure 7: Embryo lethality of the *qk*^{k2} allele. A) Wild-type and homozygous *qk*^{k2} embryos at E9.5 of development. The qkk2 mutants commonly display open head folds (white arrow) and kinky neural tubes (green arrow). At E10.5 of development, wild-type embryos (B) have tightly looped hearts (black arrow) while homozygous *qk*^{k2} embryos (C), have less compact hearts and pericardial effusion. Mutants at this late stage often display this general puffy distorted appearance.

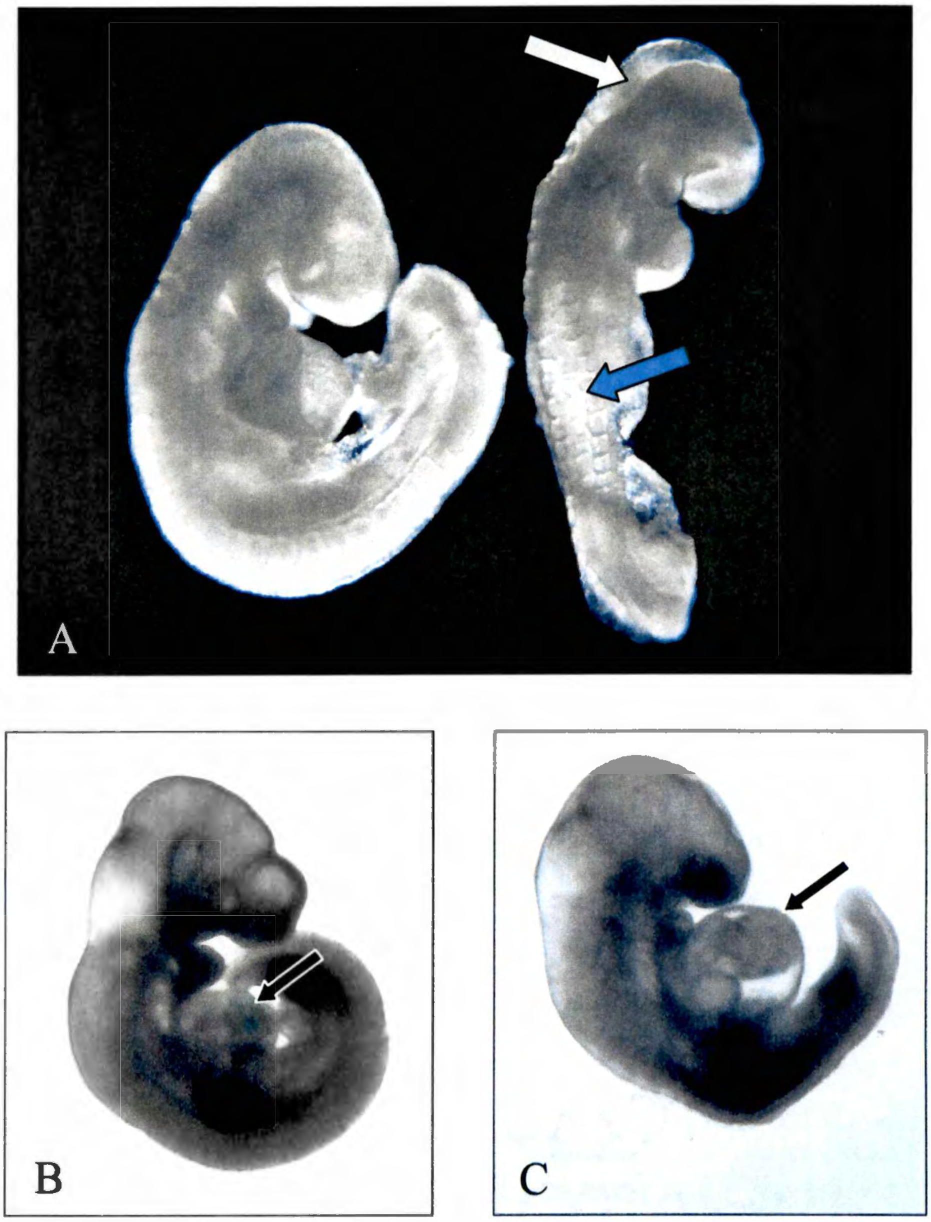
A
B
C

Figure 8: Vascular differentiation defects in *qk*^{k2} mutants. Wild-type (A) and homozygous *qk*^{k2} mutant (B) embryos dissected at E9.5 show decreased extra embryonic blood vessels on the yolk sac. E10.5 yolk sacs stained with antibodies against the vascular endothelial cell maker PECAM-1 show that the large vitelline vessel network on wild-type yolk sacs (C) is completely absent in *qk*^{k2} homozygotes (D). Less strikingly, but still apparent, vessel differentiation within the embryo itself is affected. This is observable in the brain of wild-type embryos (E) which have a more extensive vessel network (arrows) than that of the *qk*^{k2} mutants (F).

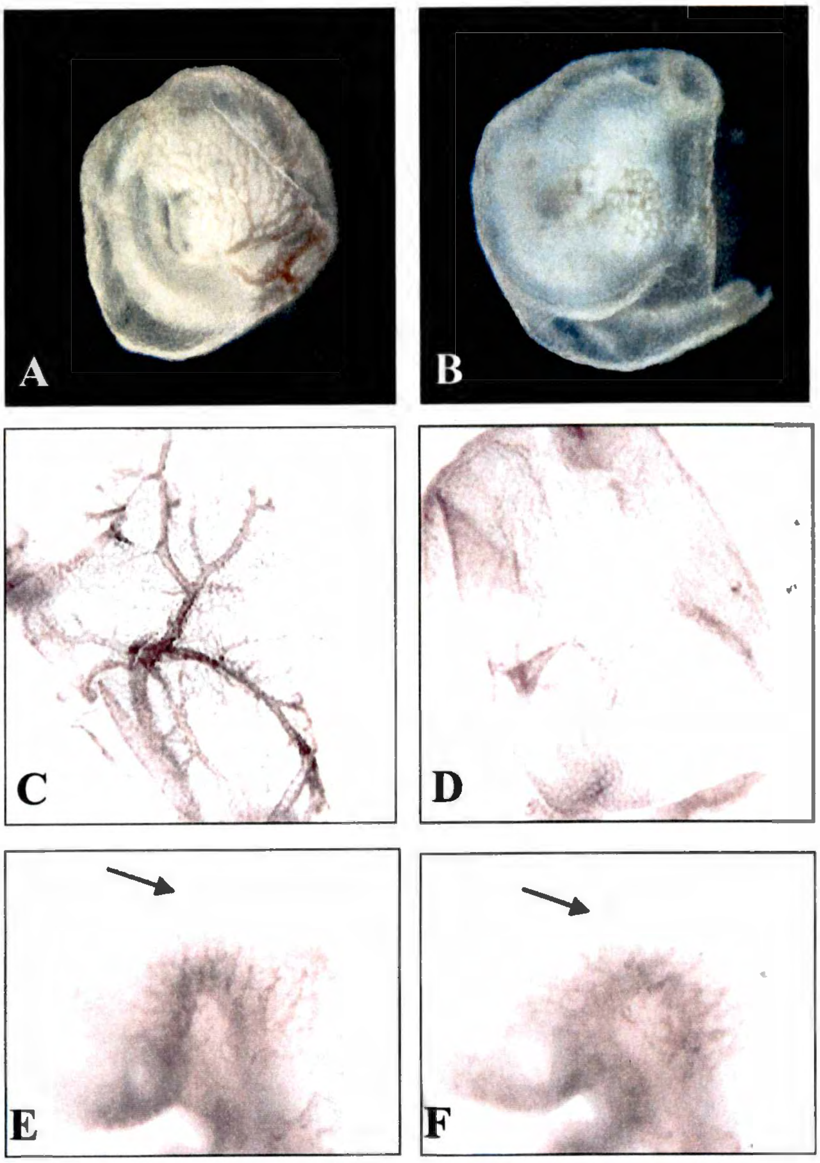
A
B
C
D
E
F

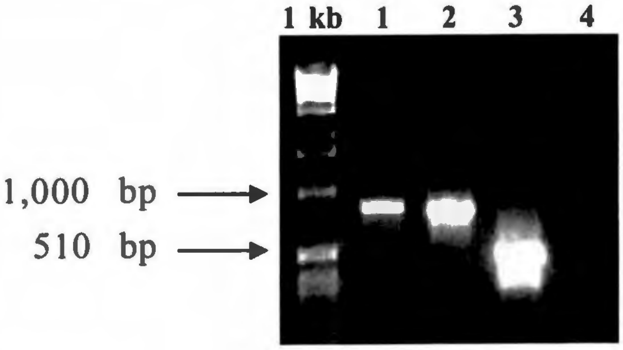

Figure 9: Expression of *quaking* in the yolk sac. Total RNA from yolk sacs were reverse transcribed with oligo d(T) and the resulting cDNA was amplified with *quaking* specific primers. A 1 kb ladder was used as a size standard. Lane 1 shows the expression of the expected 661 base pair *quaking* product at E8.5. Lane 2 is the same amplified product but obtained from yolk sac at E9.5. Lane 3 is a positive viral cDNA control and lane 4 is a negative control from samples without reverse transcriptase to ensure amplification was not from genomic DNA.

Figure 10: Histological sections of E10.5 embryos. Transverse sections stained with hemotoxylin and eosin show that wild-type (A) and qk^{k2} homozygous mutants (B) consistently differ only in the degree of heart looping. Wild-type hearts have four distinct chambers at this time (right and left ventricle and right and left aorta indicated as RV, LV, RA, and LA respectively). In the qk^{k2} mutants, these regions can be seen as one large cavity. High magnification of wild-type (C) and mutant (D) hearts shows that the histological association of cardiac cells is normal in qk^{k2} mutants. The abnormal fluid accumulation between the pericardium (arrows) and the inner myocardium in qk^{k2} mutants is lost during fixation.

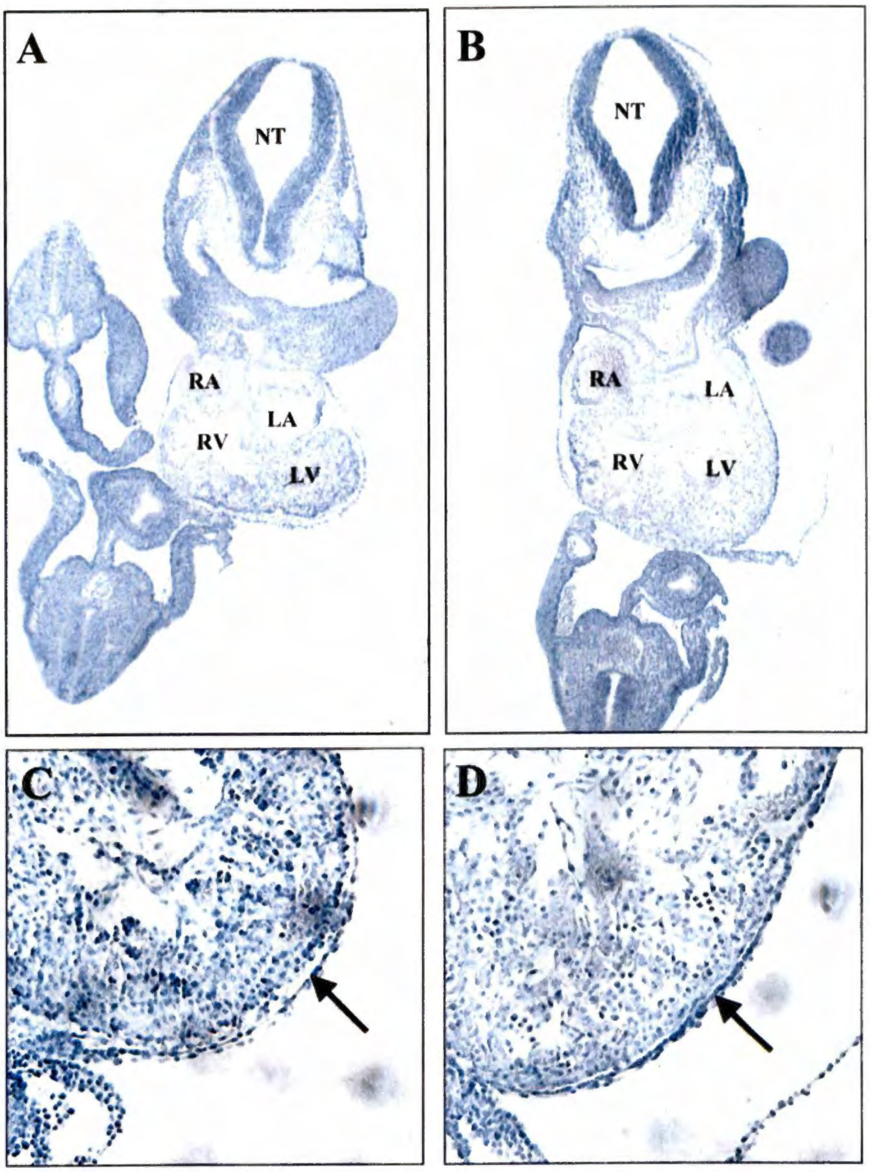
A
NT
RA
LA
RV
LV
B
NT
RA
LA
RV
LV
C
D

Figure 11: Expression of heart markers during embryo development. Whole mount *in situ* hybridization at E9.5 shows that *Nkx2.5*, a marker of cardiac looping, is expressed similarly in wild-type (A) and *qk*^{k2} mutants (B). Both right and left sides of the heart are shown. Immunohistochemistry of transverse sections from E10.5 wild-type (C) and *qk*^{k2} homozygotes (D) show α-sarcomeric actin protein is present in *qk*^{k2} mutants.

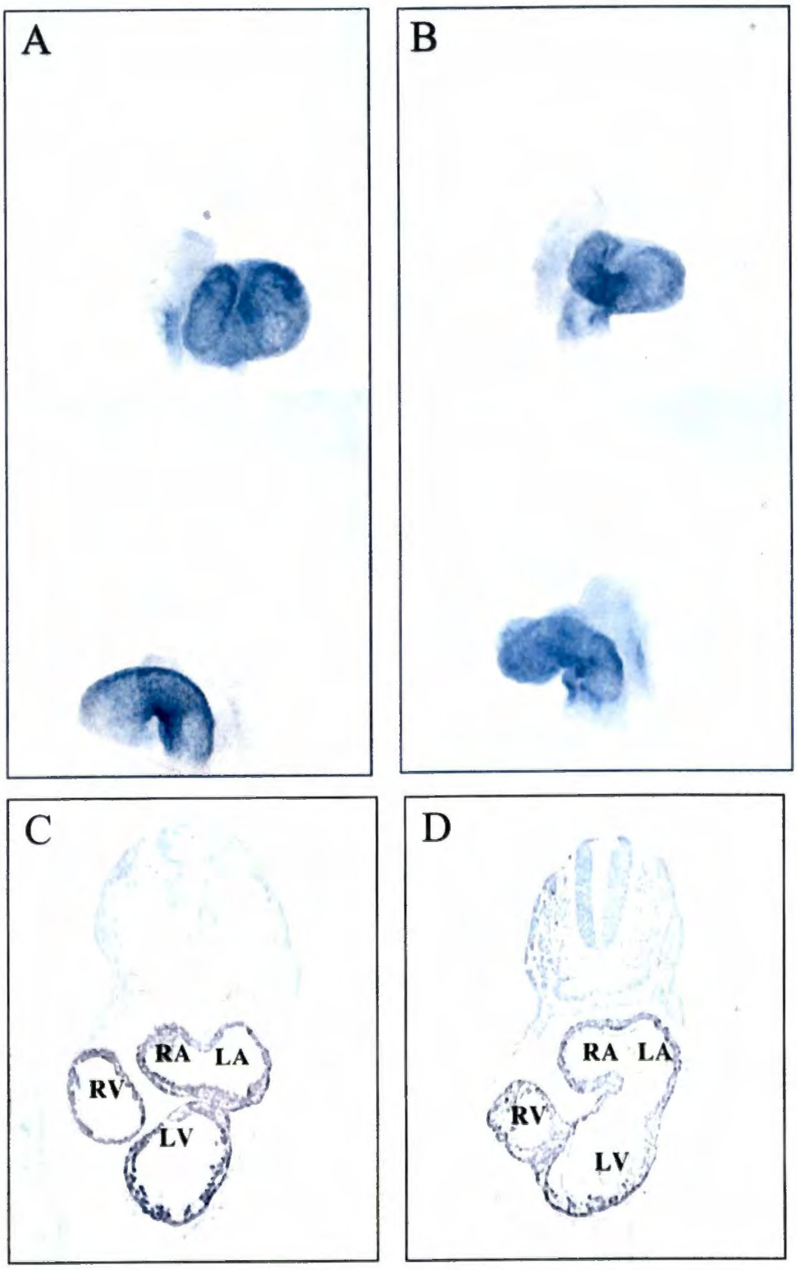
A
B
C
RA
LA
RV
LV
D
RA
LA
RV
LV

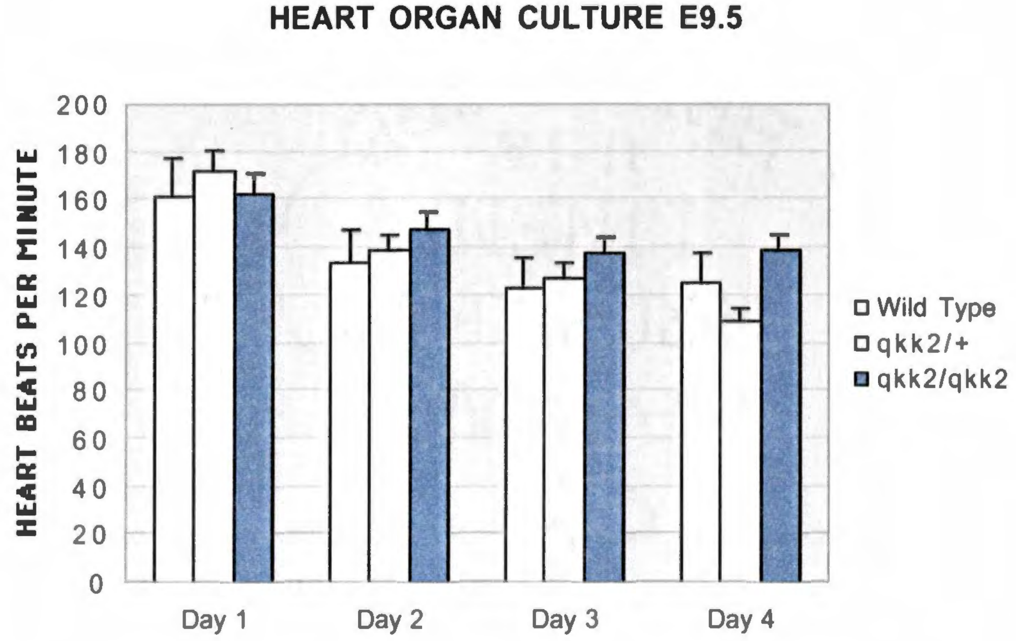

Figure 12: Embryonic heart rates in organ culture. Whole hearts were place in organ culture and the average heart beats per minute were determined each day. There were no significant differences in the average beating rates of wild-type (N=6), heterozygotes (N=10) and *qk*^{k2} homozygotes (N= 7).

Figure 13: Cardiac gene expression by quantitative RT-PCR. For each experiment, expression is reported as the number of transcripts of interest per number of internal control *36B4* transcripts. The cardiac differentiation genes *Anf* (A) and *βMhc* (B) are both expressed at similar levels in wild-type, heterozygous and qk^{k2} homozygous hearts. In contrast, *Angp1* (C) and *Mef2c* (D) are expressed at higher levels at E9.5 in wild-type hearts than qk^{k2}/ qk^{k2} or qk^{k2}/+ hearts. *Vegf* (E) is overexperssed in qk^{k2}/ qk^{k2} hearts by E10.5 of development.

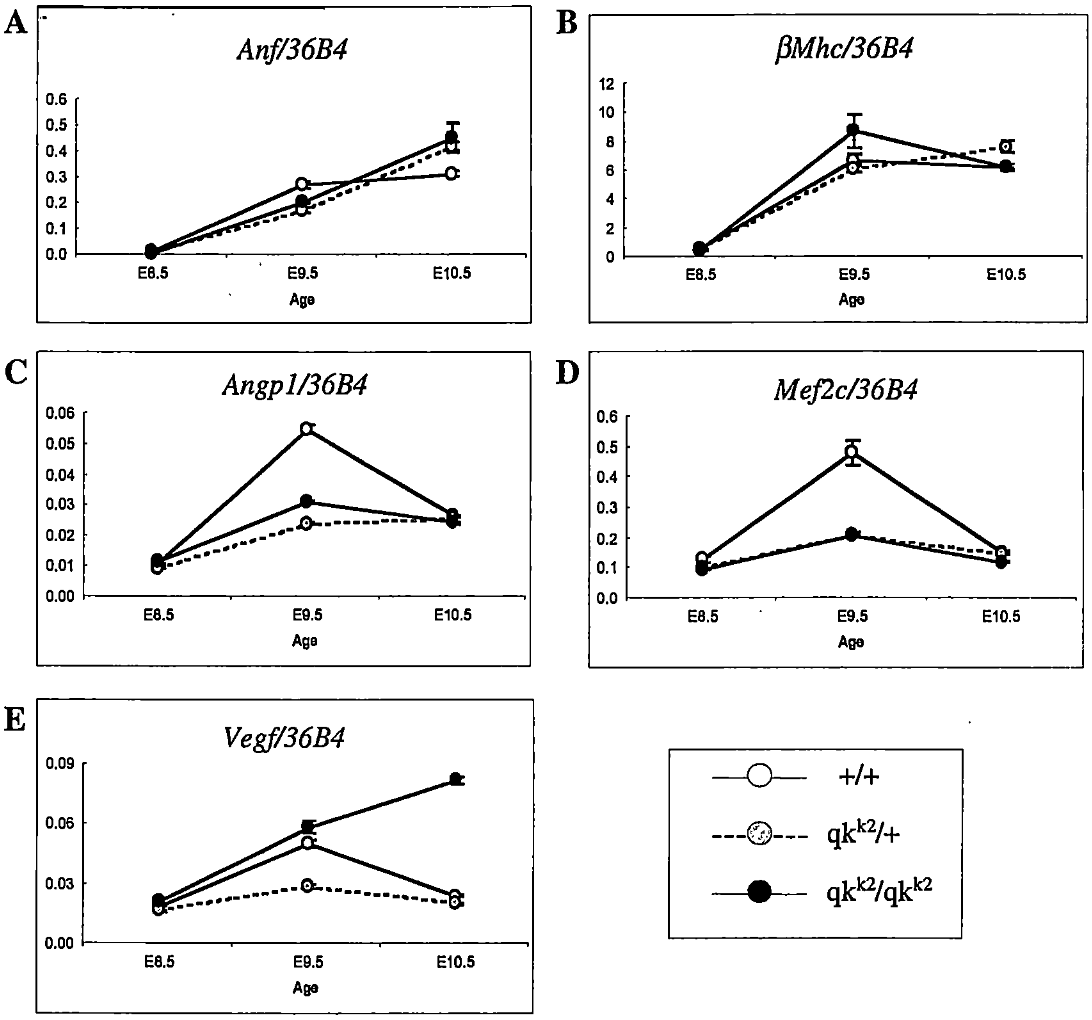
A
Anf/36B4
0.6
0.5
0.4
0.3
0.2
0.1
0.0
E8.5
E9.5
E10.5
Age
B
βMhc/36B4
12
10
8
6
4
2
0
E8.5
E9.5
E10.5
Age
C
Angp1/36B4
0.06
0.05
0.04
0.03
0.02
0.01
0.00
E8.5
E9.5
E10.5
Age
D
Mef2c/36B4
0.6
0.5
0.4
0.3
0.2
0.1
0.0
E8.5
E9.5
E10.5
Age
E
Vegf/36B4
0.09
0.06
0.03
0.00
E8.5
E9.5
E10.5
Age
+/+
$qk^{k2}/+$
qk^{k2}/qk^{k2}

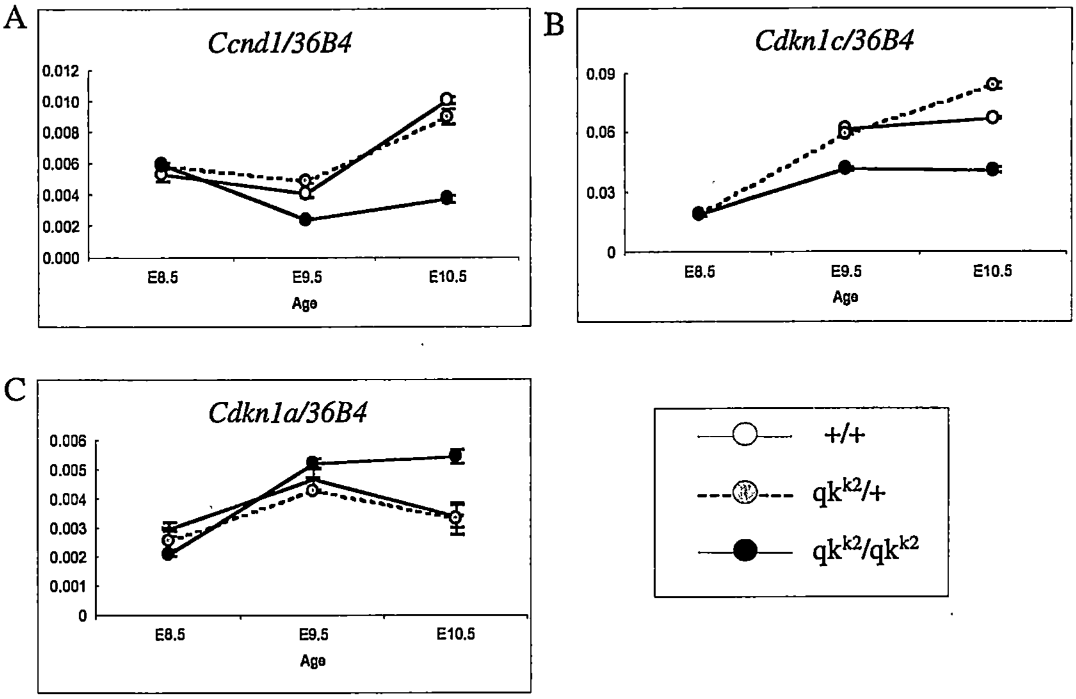

Figure 14: Cell cycle gene expression by quantitative RT-PCR. For each experiment, expression is reported as the number of transcripts of interest per number of internal control *36B4* transcripts. The the cell cycle inducer *Ccnd1* (A) and cell cycle inhibitor *Cdkn1c* (B) are both reduced in *qk*^{k2} mutant hearts by E10.5. The cell cycle inhibitor *Cdkn1a* (C) is increased in *qk*^{k2} mutants by E10.5.

Table 2. Whole mount *in situ* genetic markers

Gene	E9.5 Expression	Function	References
Nkx2.5	Heart	Cardiac development and looping	(Komuro and Izumo, 1993; Lints *et al.*, 1993; Tanaka *et al.*, 1999)
Shh	Notochord Brain floor plate	Ventral neuron differentiation	(Ericson *et al.*, 1995; Marti *et al.*, 1995; Roelink *et al.*, 1995)
Foxa2	Ventral neural tube Brain floor plate	Floor plate development Ventral patterning and axon guidance	(Ruiz *et al.*, 1995; Sasaki and Hogan, 1994)
Fgf8	Forebrain and mid-hind brain junction Prospective limb	Embryonic development	(Ericson *et al.*, 1997; Heikinheimo *et al.*, 1994)
Pax6	Dorsal neural tube and diencephalon Eye and forebrain	Neuronal and glial cell differentiation	(Ekker *et al.*, 1995; Walther and Gruss, 1991)
T	Notochord Posterior embryo Primitive streak	Mesoderm formation Notochord differentiation	(Herrmann, 1991; Kispert and Herrmann, 1994; Wilkinson *et al.*, 1990)

Figure 15: Whole mount *in situ* hybridization at E9.5 with *Shh, Fgf8* and *Foxa2*. *Shh* expression, seen in the notochord and brain floor plate in wild-type embryos (A), is similar to that observed in *qk*^{k2} homozygotes (B) at E9.5 arrest. Several *qk*^{k2} homozygotes that were delayed slightly earlier did display a shortened domain of expression in the brain floor plate (D) when compared to aged matched wild-type embryos (C). *Fgf8* expression in the forebrain and mid/hind brain junction is similar in wild-type (E) and *qk*^{k2}/ *qk*^{k2} embryos (F) as well as expression in the prospective limb region, first brachial arch and tail. *Foxa2* is expressed in the developing brain floor plate and ventral neural tube in wild-type embryos (G). This pattern is the same as that seen in homozygous *qk*^{k2} mutants (H). Boxed inserts show neural tube cross sections which exhibit the ventral restricted expression pattern of *Foxa2*.

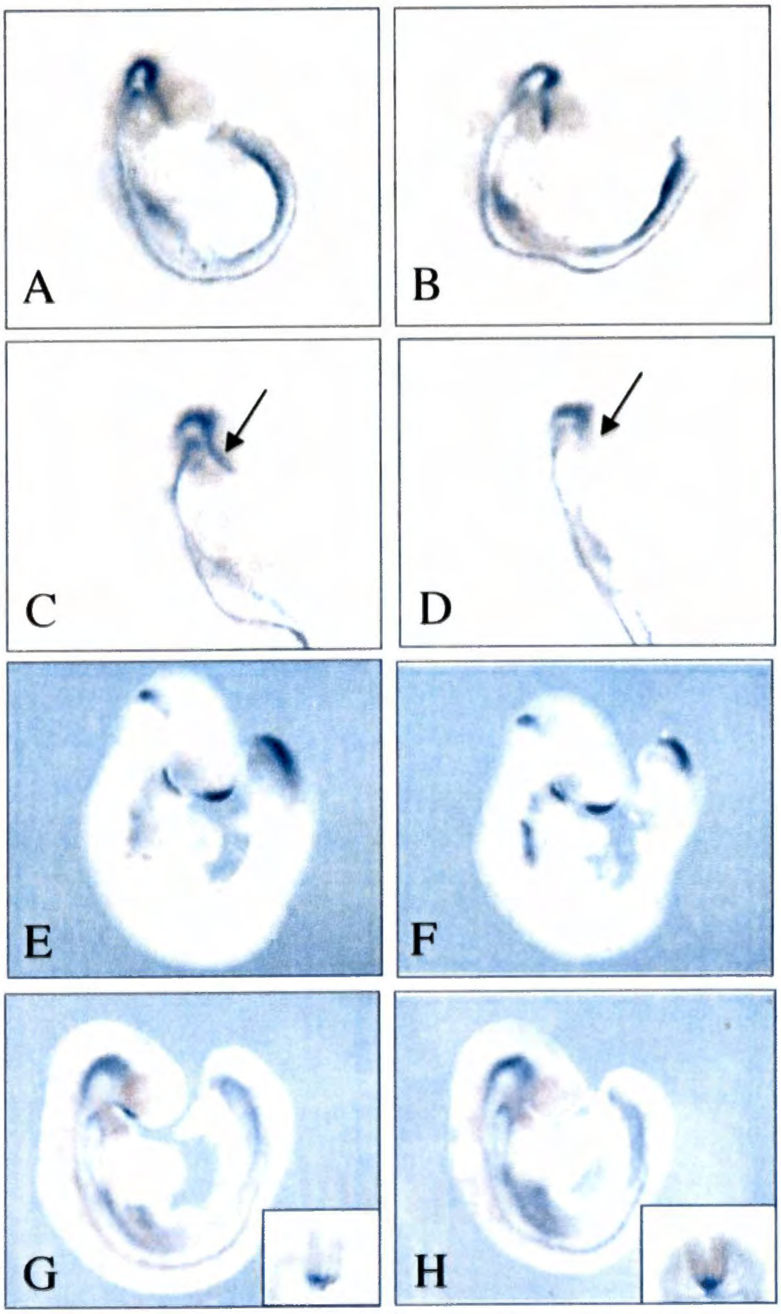
A
B
C
D
E
F
G
H

Figure 16: Whole mount *in situ* hybridization at E9.5 with *Pax6* and *T*. Expression of *Pax6* in wild-type (A) and qk^{k2} homozygous embryos (B) shows similar patterns in the forebrain, hindbrain, and the dorsal neural tube. Expression is also seen in the developing eye and dorsal diencephalon (insert). *T* expression in the notochord and tail of wild-type embryos (C) is similar to that observed in $qk^{k2}/\ qk^{k2}$ embryos (D).

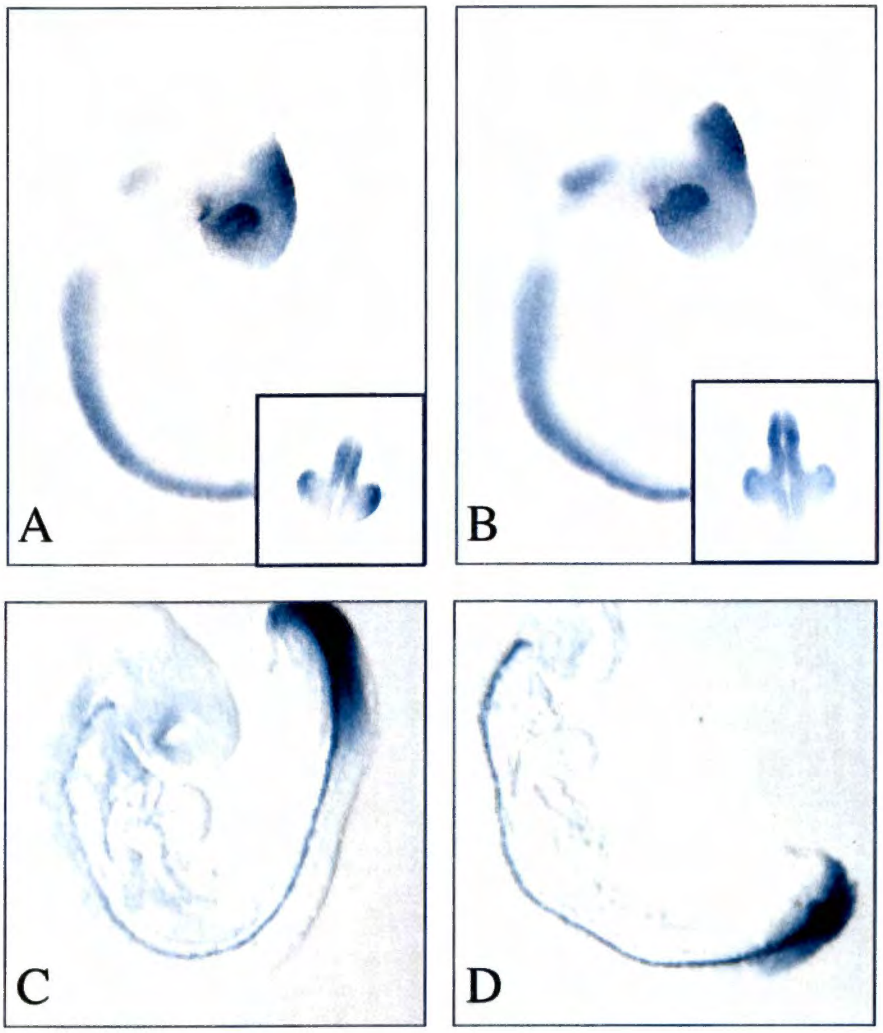
A
B
C
D

Table 3. Pentylenetetrazole seizure susceptibility

	Seizure	No Seizure
Wild Type (+/+)	7 (21%)	26 (79%)
Heterozygotes (*qk*^{k2}/+)	38 (84%)	7 (16%)

$p < 0.05$

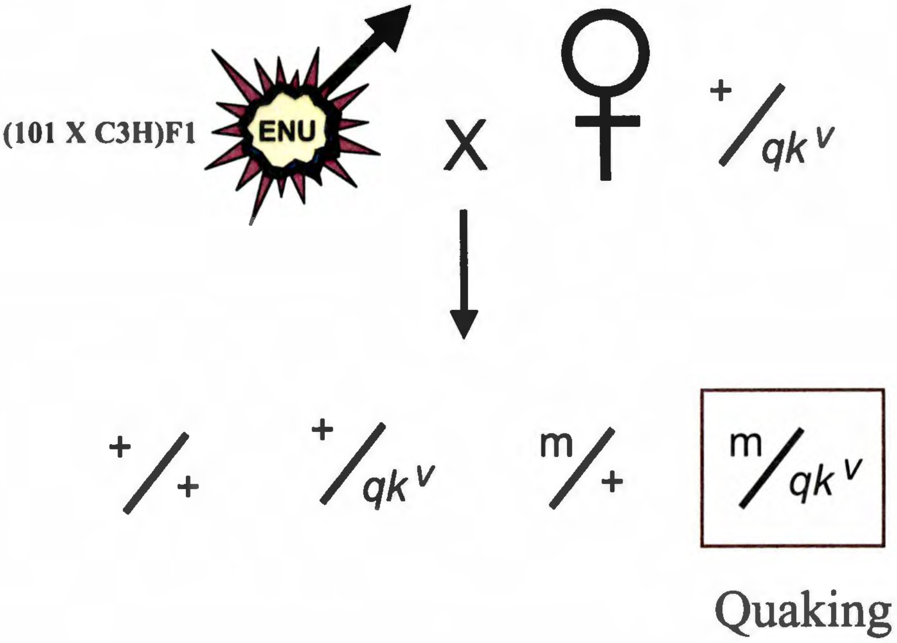
(101 X C3H)F1
ENU
X
+/qk v
+/+
+/qk v
m/+
m/qk v
Quaking

Figure 17: ENU mutagenesis screen for new *qkI* alleles. ENU mutagenized males were crossed with *qk*^{v} heterozygous females and offspring were screened for a quaking-like phenotype. Potential compound heterozygotes (boxed) of a new *qkI* mutation (m) with *qk*^{v} were subsequently tested for heritability and allelism to *quaking*.

Figure 18: *Quaking* allelism test crosses. The compound heterozygote mouse (boxed) selected from the ENU screen was mated to A) wild-type B) *qk*^{v} heterozygotes and C) *qk*^{v} homozygotes. The phenotypes of the offspring shown revealed the new mutation (m) was recessive and allelic to *quaking*. The presence of the *qk*^{v} allele could be determined by Southern blot genotyping.

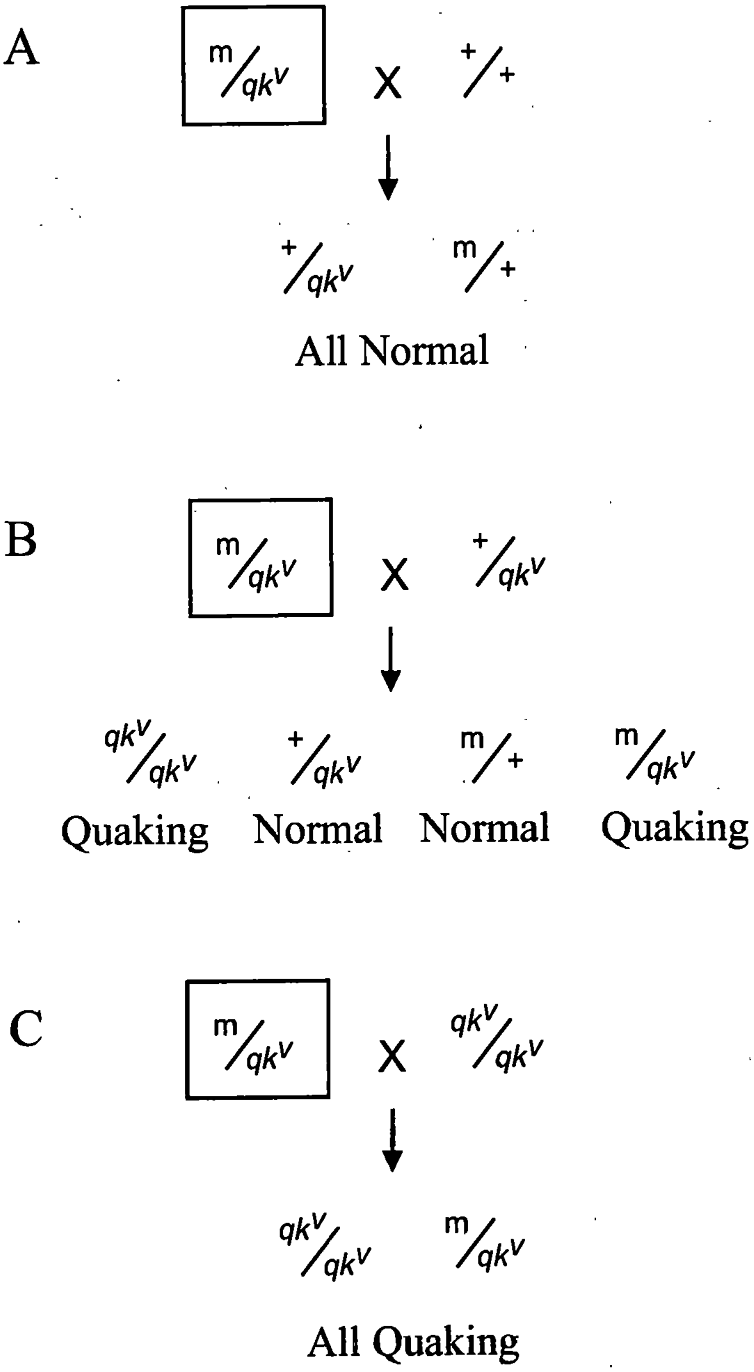
A
m/qkV
X
+/+
+/qkV
m/+
All Normal
B
m/qkV
X
+/qkV
qkV/qkV
+/qkV
m/+
m/qkV
Quaking
Normal
Normal
Quaking
C
m/qkV
X
qkV/qkV
qkV/qkV
m/qkV
All Quaking

Table 4. Homozygous and compound heterozygous phenotypes of *qk*^{e5}

Parental Cross	Offspring Phenotype		Total	Relative Phenotype Severity**
	Quake/Seize	Normal		
qk^{e5}/+ X qk^{e5}/+	82 (29%)	199 (71%)	281	++++
qk^{e5}/+ X qk^{kt1}/+	47 (41%)*	66 (59%)	113	++
qk^{e5}/+ X qk^{k2}/+	54 (21%)	200 (79%)	254	++
qk^{e5}/+ X qk^{v}/+	72 (26%)	200 (74%)	272	+++

*48% recovery of compound heterozygotes is expected due to *t*-chromatin transmission ratio distortion in qk^{kt1}/+ males.

**Phenotype severity is relative to the qk^{v}/qk^{v} phenotype designated "+"

Figure 19: Histology of *qk*^{e5} homozygous brains. Coronal sections stained with hemotoxylin and eosin show the brain morphology of wild-type mice (A) is preserved in *qk*^{e5} homozygotes (B) with the exception that *qk*^{e5} mutants can commonly display enlarged ventricles (white arrows). Luxol fast blue staining for myelin lipids shows the intense staining of the corpus callosum (CC) and anterior commissure (AC) in wild-type mice (C), is absent in *qk*^{e5} mutants (D).

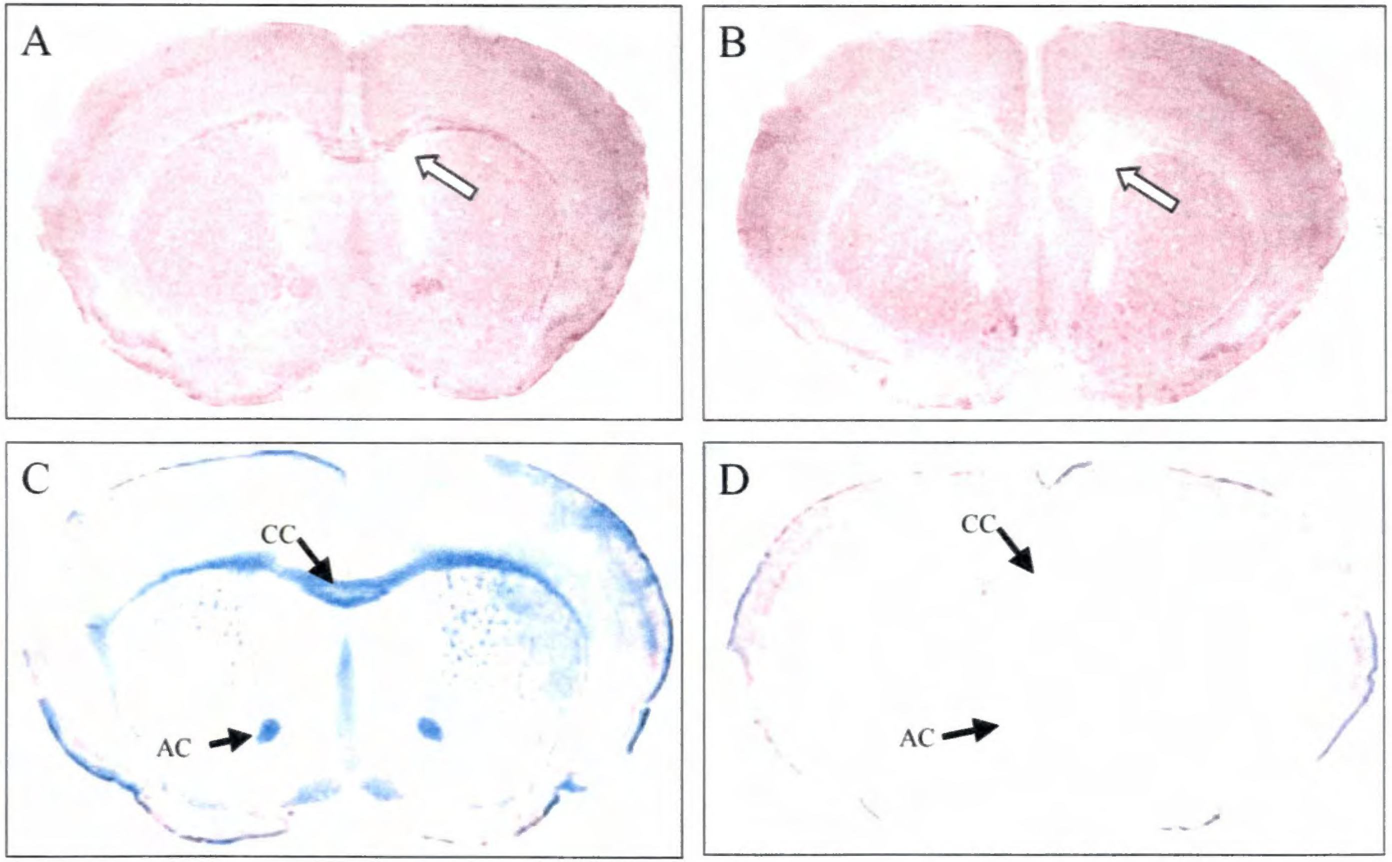
A
B
C
CC
AC
D
CC
AC

Figure 20: Dysmyelination in *qk*^{e5} homozygotes. Transmission electron mycroscopy of the corpus callosum reveals thick abundant myelin sheathes (arrows) present in wild-type brain (A). These thick sheaths are completely absent in the brain of *qk*^{e5}/*qk*^{e5}, which contain only the occasional thinly myelinated axon (B). Although the myelin sheaths are thin in *qk*^{v} /*qk*^{v} brain (C) there are visibly more myelinated axons than in *qk*^{e5}/*qk*^{e5}. X = 10,500. Luxol fast blue staining in the corpus collosum (inset) shows the intense myelin staining in the wild-type brain is completely absent in both *qk*^{e5}/*qk*^{e5} and *qk*^{v} /*qk*^{v} brains.

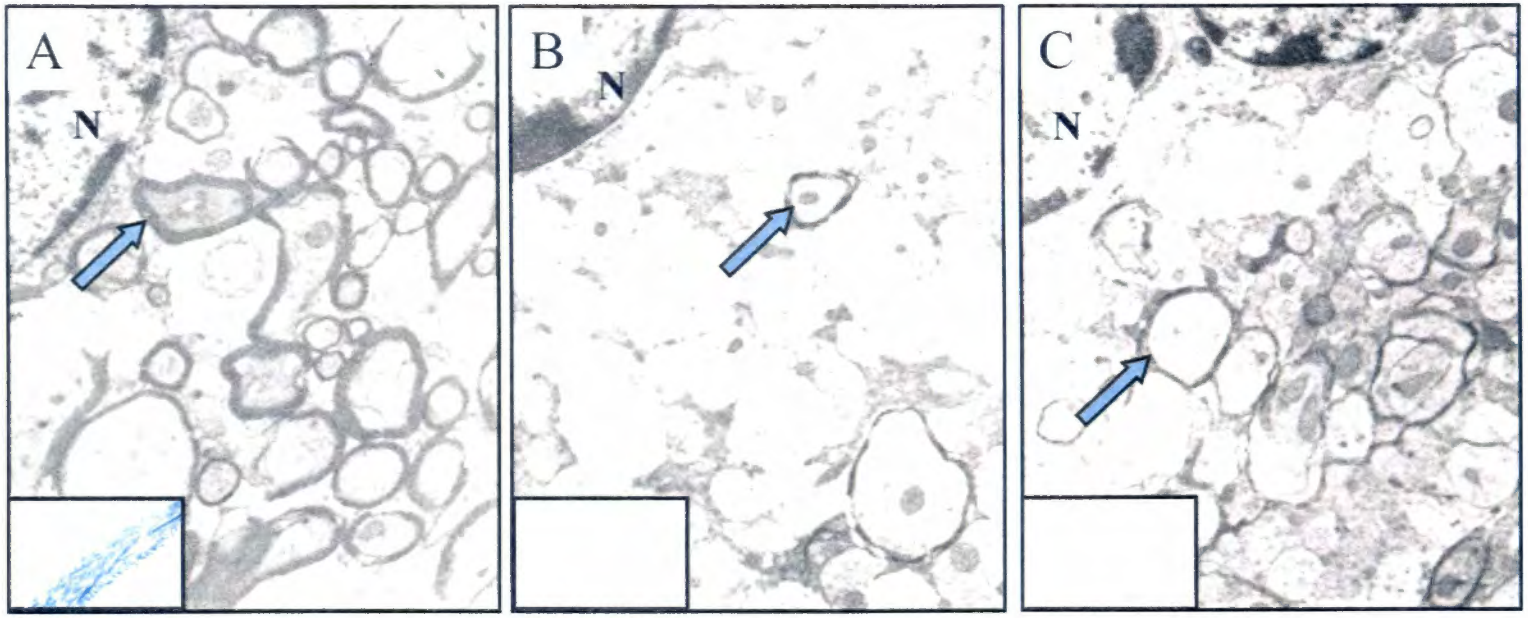
A
N
B
N
C
N

Figure 21: Electroencephalogram recording apparatus. Surface cortex EEG signals were recorded from mice via subdural electrodes attached to a microminiature connector on the skull surface. Electrical signals were synchronized with video camera images and recorded on VHS as a split screen image.

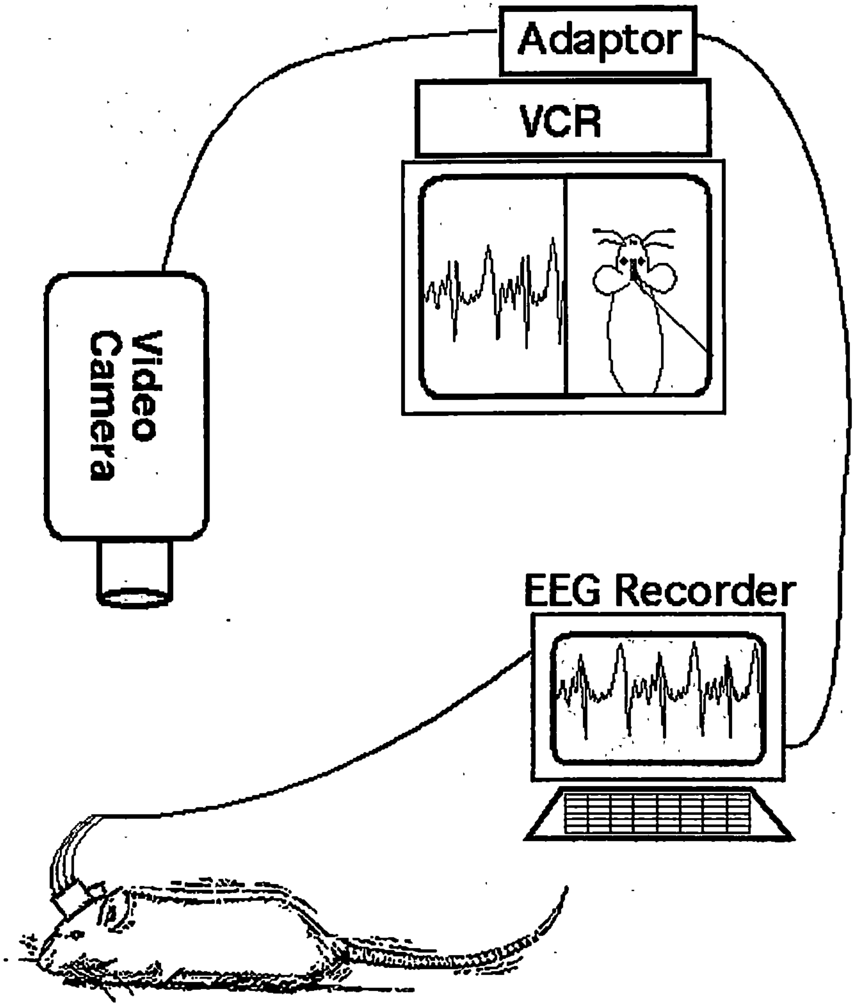
Adaptor
VCR
Video Camera
EEG Recorder

Figure 22: Cortical surface electroencephalogram recordings. EEG recordings of qk^{e5}/qk^{e5} mice during normal activity (A) often reveal interictal spiking events, which do not correlate to any abnormal behavior. During qk^{e5}/qk^{e5} seizure episodes (B) electrical impulses increase in frequency and decrease in amplitude. This is in contrast to a classic epileptic seizure pattern (C), which usually displays increased frequency and increased amplitude of electrical output. A typical wild-type electrical pattern from wild-type mice (D) is shown as a control. Arrows indicate the beginning of the behavioral seizure.

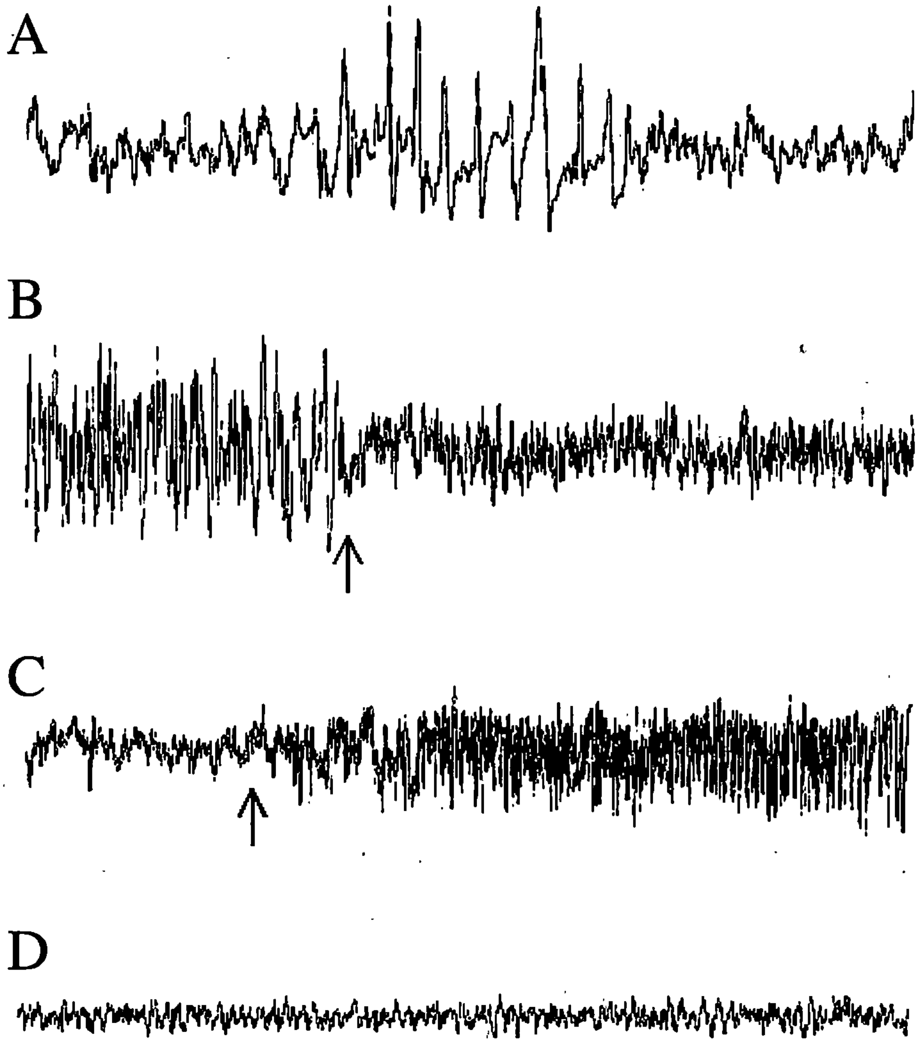
A
B
C
D

Table 5. Pentylenetetrazole seizure susceptibility at 42.5 mg/kg

	Seizure	No Seizure
Wild Type (+/+)	7 (23%)	23 (77%)
Heterozygotes (*qk*^{e5}/+)	7 (23%)	23 (77%)

p>0.05

Table 6. Pentylenetetrazole seizure susceptibility at 45.5 mg/kg

	Seizure	No Seizure
Wild Type (+/+)	10 (34%)	19 (66%)
Heterozygotes (*qk*^{e5}/+)	11 (38%)	18 (62%)

p >0.05

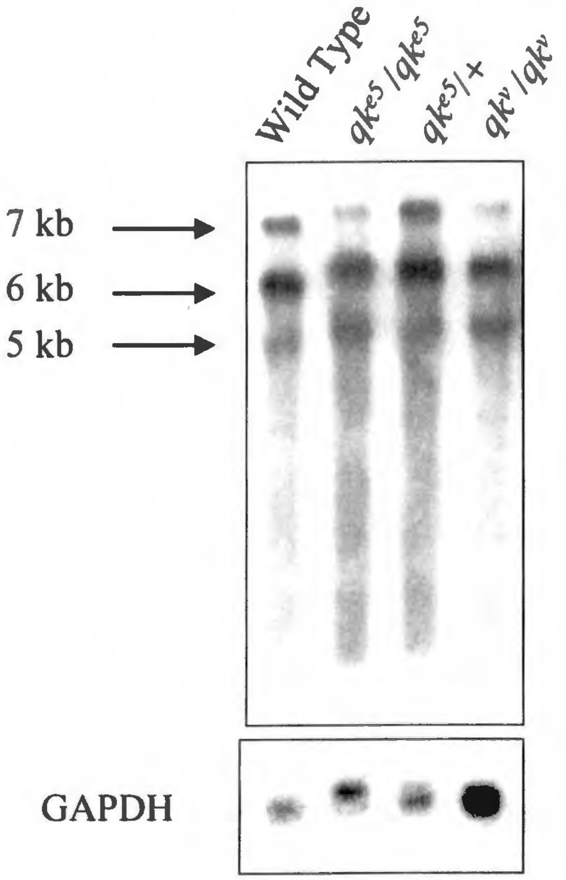
Wild Type
qk^{e5}/qk^{e5}
$qk^{e5}/+$
qk^{v}/qk^{v}
7 kb
6 kb
5 kb
GAPDH

Figure 23: Adult brain *qkI* expression. Northern blotting of whole brain mRNA was probed with 1-QUA2, a 3' cDNA fragment from the common coding region of *quaking*. All three transcript sizes qkI-5, qkI-6 and qkI-7 are present in qk^{e5} homozygous brains. A slight decrease in the level of the qkI-6 and qkI-7 kb transcripts is evident in qk^{e5}/qk^{e5} brain, similar to that seen in qk^{v}/qk^{v}. The GAPDH probe was used as a control for loading and migration.

Figure 24: Oligodendrocyte development. Oligodendrocytes at all stages of development are present in the central nervous system from mid-gestation through adulthood. Expression of the oligodendrocyte markers condroitin sulfate proteoglycan 2 (NG2/Cspg2), platelet derived growth factor alpha receptor (PDGFαR), sulphatide/seminolipid antigen (O4), 2',3'-cyclic nucleotide 3'-phosphodiesterase (CNP), and myelin basic protein (MBP) as well as QKI expression is indicated for each stage of differentiation.

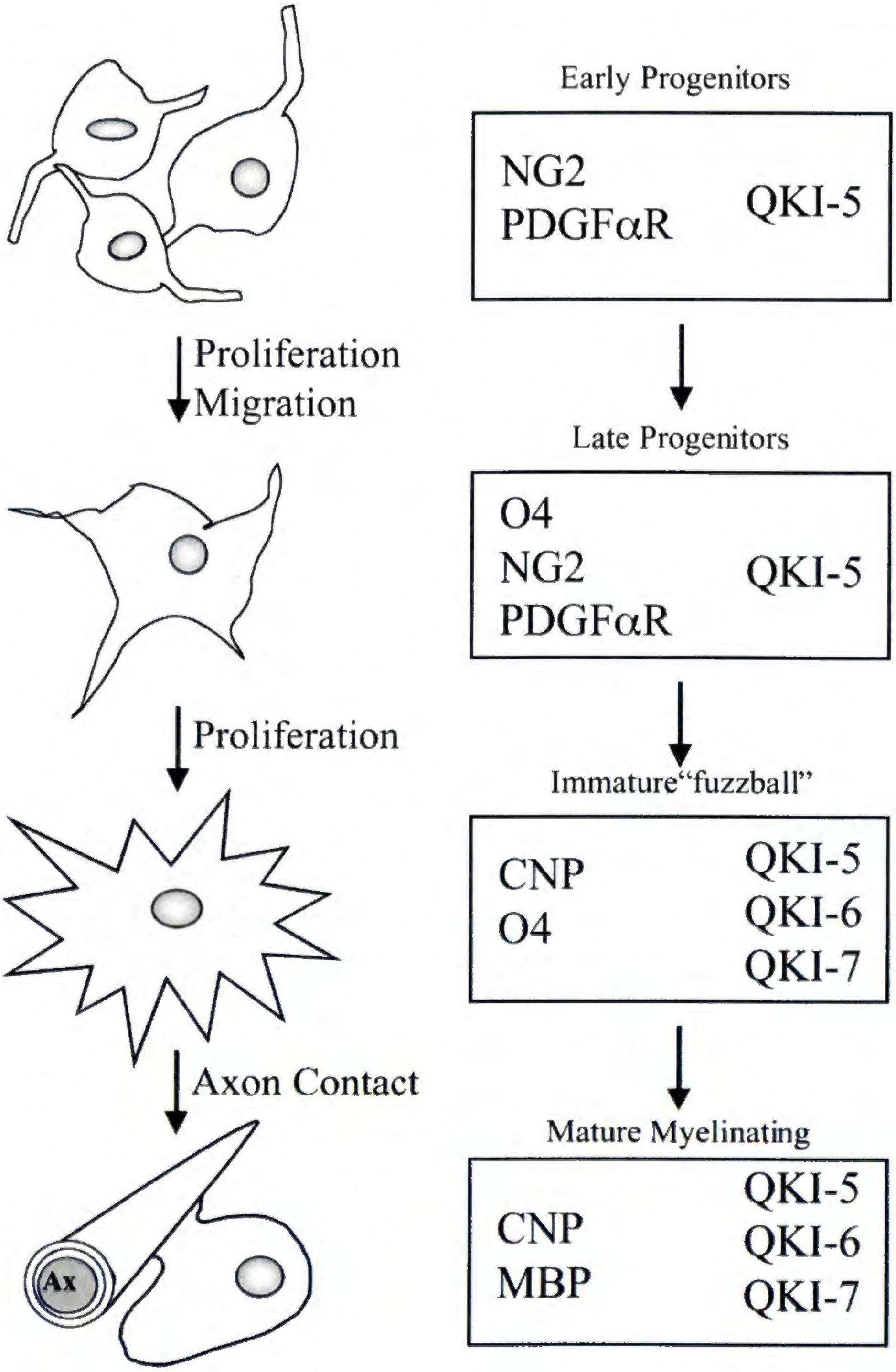
Early Progenitors
NG2
PDGFαR
QKI-5
Proliferation
Migration
Late Progenitors
O4
NG2
PDGFαR
QKI-5
Proliferation
Immature"fuzzball"
CNP
O4
QKI-5
QKI-6
QKI-7
Axon Contact
Mature Myelinating
Ax
CNP
MBP
QKI-5
QKI-6
QKI-7

Figure 25: Postnatal brain QKI-5 and O4 expression. Antibodies against QKI-5 protein (green) and the lipid antigen O4 (red) in the brain cortex at P7. A) Wild-type O4 positive oligodendrocytes (arrows) express high levels of QKI-5 in the nucleus. O4 negative cells are either astrocytes, or early oligodendrocyte progenitors. B) O4 positive oligodendrocytes in qk^{e5}/qk^{e5} mice express QKI-5 at low levels similar to O4 negative astrocytes and early oligodendrocyte progenitors.

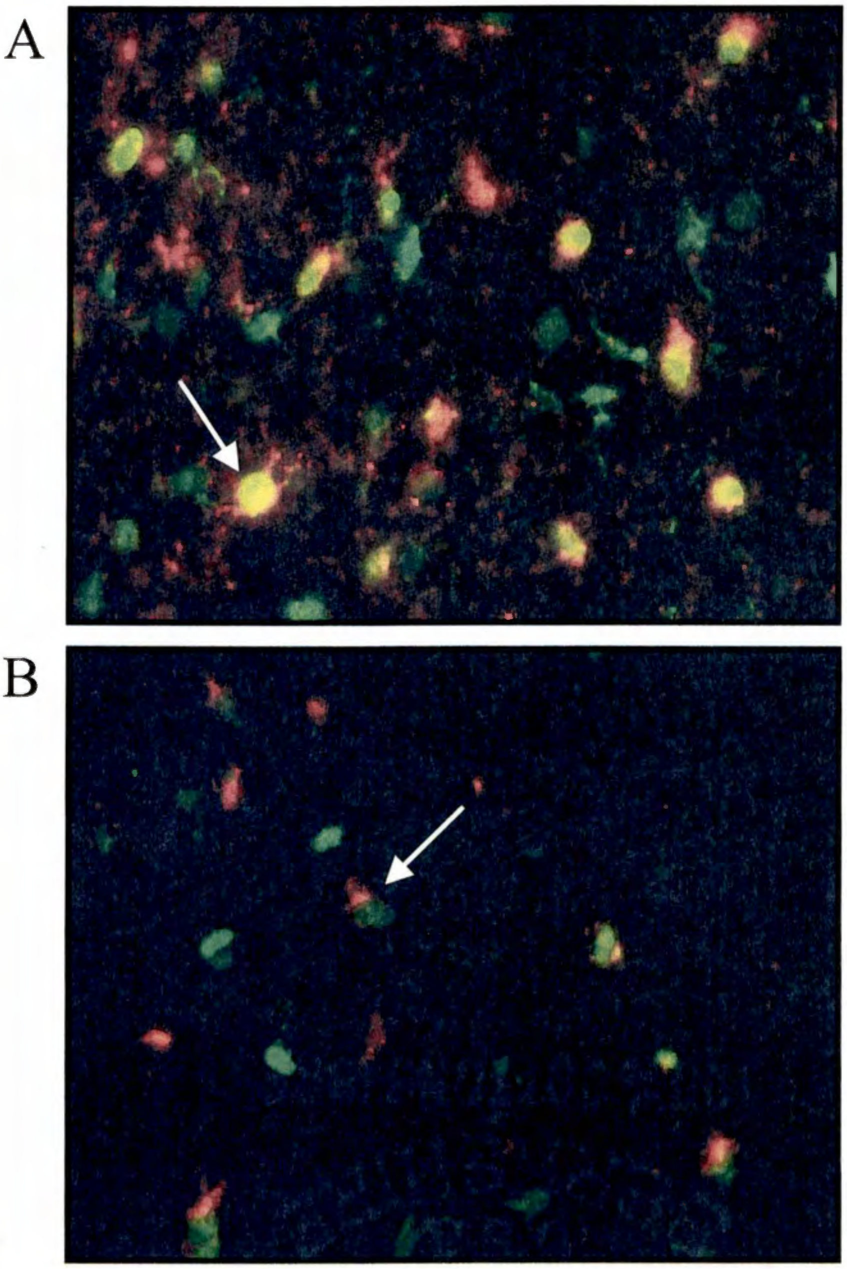
A
B

Figure 26: Postnatal brain QKI-6 and MBP expression. Antibodies against QKI-6 (green) and myelin protein MBP (red) in the brain cortex at P7. A) Wild-type brain contains oligodendrocytes expressing high levels of cytoplasmic QKI-6 (arrow) and the myelin protein MBP is abundant. B) QKI-6 positive oligodendrocytes are absent in *qk*^{e5}/*qk*^{e5} brain but low QKI-6 expression is present in astrocytes as confirmed with antibodies against GFAP (data not shown). MBP is present but at severely reduced levels.

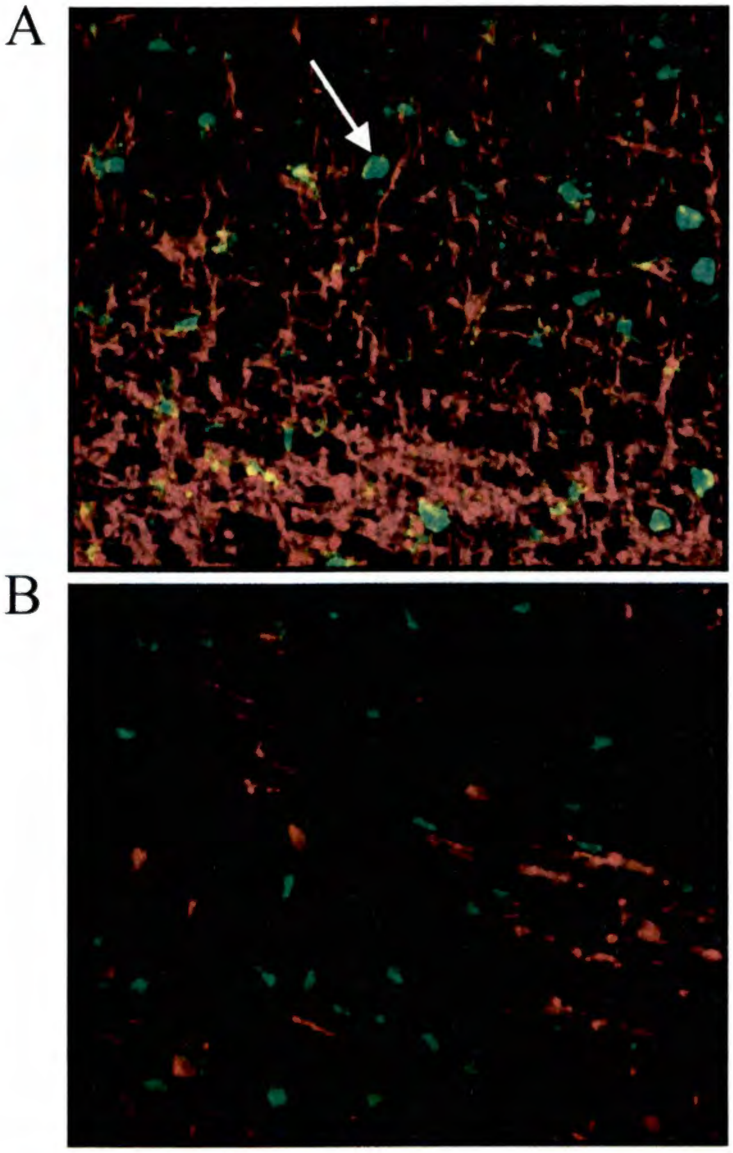
A
B

Figure 27: Postnatal brain QKI-7 and O4 expression. Antibodies against QKI-7 (green) and O4 (red) in the brain cerebellum at P7. A) Wild-type brain contains O4 positive and QKI-7 positive oligodendrocytes (arrows) which together appear yellow. B) O4 positive oligodendrocytes in qk^{e5}/qk^{e5} brain are devoid of any QKI-7 expression. QKI-7 continues to be expressed at low levels in astrocytes.

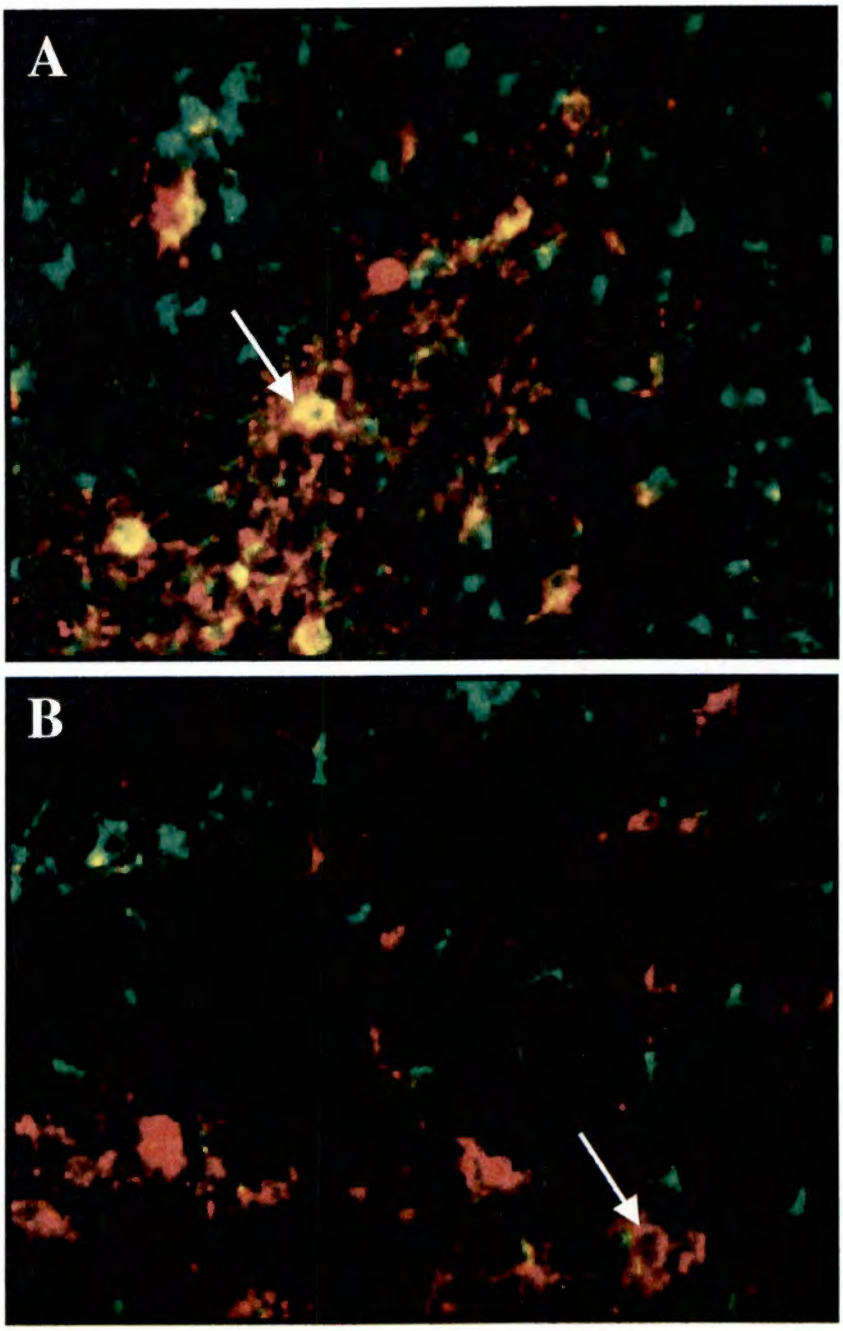
A
B

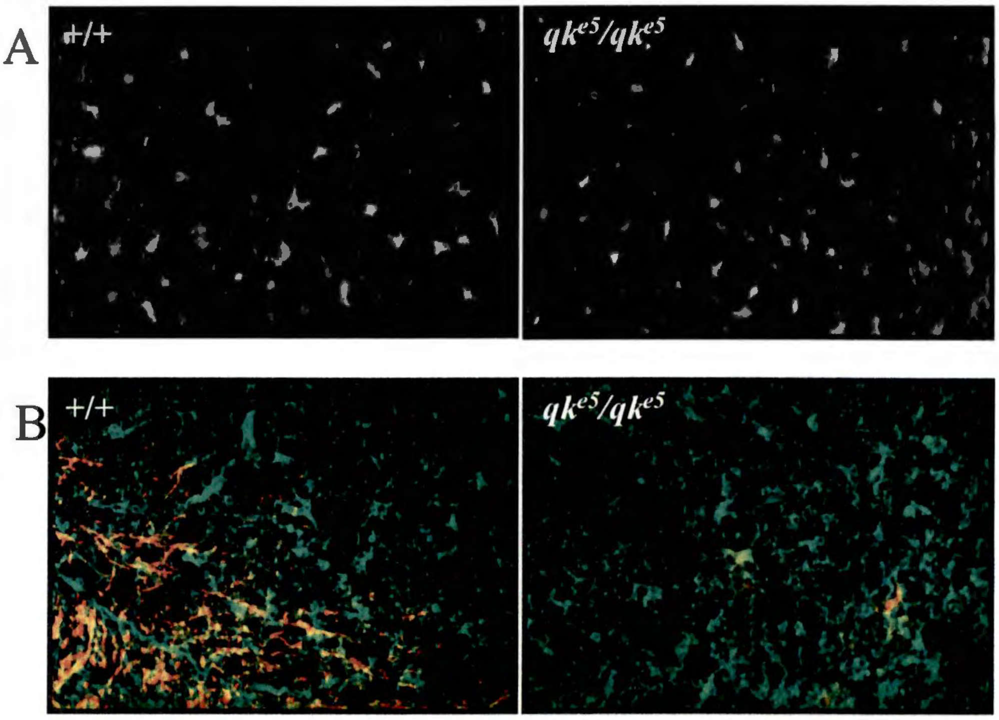

Figure 28: Postnatal brain PDGFαR and NG2 expression. A) Antibodies against PDGFαR in P7 cortex show this early glial marker is expressed in both wild-type and qk^{e5}/qk^{e5}. B) Antibodies against NG2 (green) and MBP (red) in P7 cortex show that NG2 is present at similar levels in wild-type and qk^{e5} mutant while MBP is severely decreased in qk^{e5}/qk^{e5} mutants.

Figure 29: Postnatal brain QKI-5 and CNP expression. Antibodies against QKI-5 (green) and the myelin protein CNP (red) in P14 cerebellum. A) Wild-type brains show abundant oligodendrocytes expressing QKI-5 at high levels compared to the low levels in astrocytes. Staining of CNP in myelin is abundant. B) Brains of qk^{e5}/qk^{e5} mice are devoid of oligodendrocytes expressing high levels of QKI-5. CNP is present but scarce in these mutants. C) Brains of qk^{v}/qk^{v} mice are also devoid of cells expressing QKI-5 at high levels and although they express CNP at higher levels than qk^{e5} mutants, there is still a severe reduction compared to wild-type.

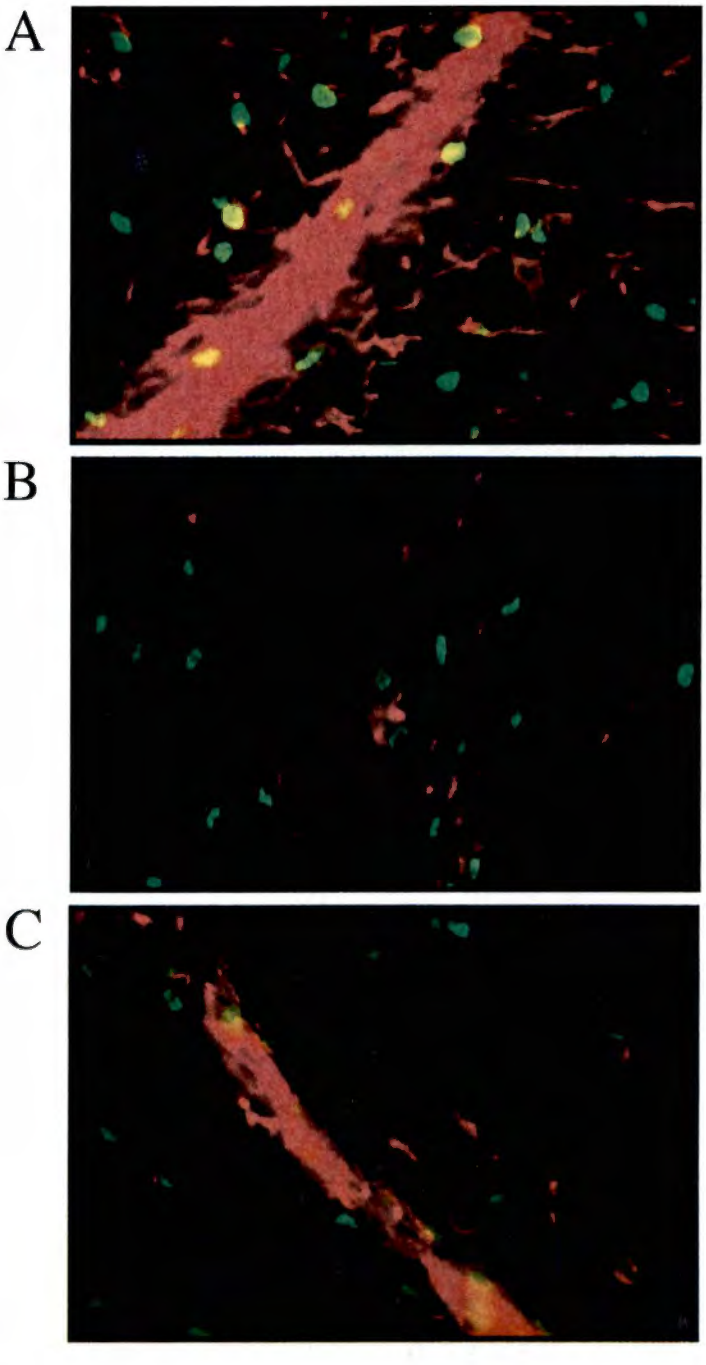
A
B
C

Figure 30: Postnatal brain QKI expression. In wild-type mouse oligodendrocytes, QKI-5 is localized to the nucleus and QKI-6 and QKI-7 are localized to the cytoplasm. In the viable *qk*^{v} /*qk*^{v} and *qk*^{e5}/*qk*^{e5} mice, QKI-5 is reduced and QKI-6 and QKI-7 are absent from oligodendrocytes.

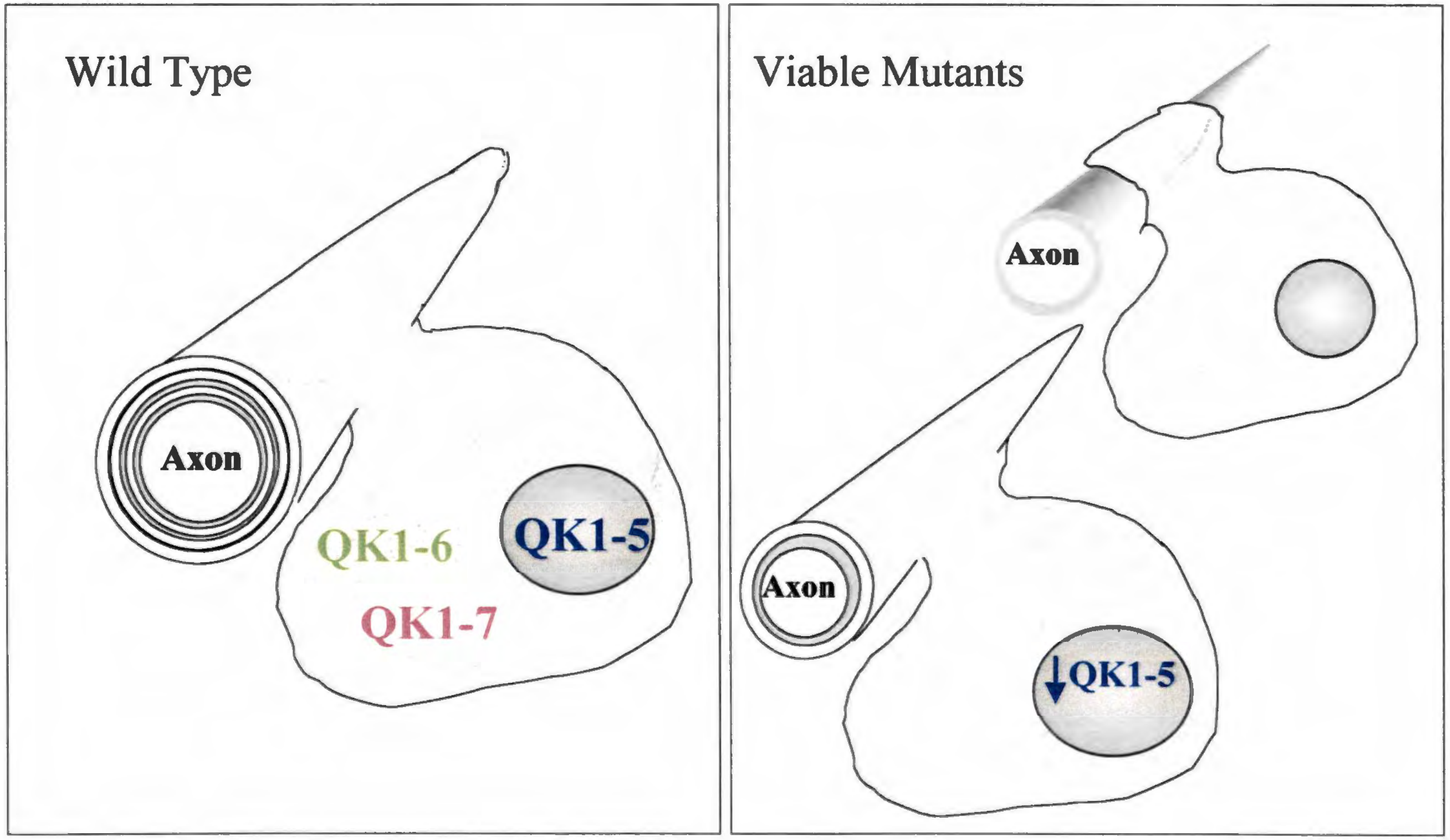
Wild Type
Axon
QK1-6
QK1-5
QK1-7
Viable Mutants
Axon
Axon
↓QK1-5

Figure 31: The *quaking* mutant allele series. Each of the six mutant alleles is unique in the way it affects *quaking* function. qk^{l-1} is a loss of the nuclear isoform, qk^{k2} likely affects RNA binding, $qk^{kt3/4}$ prevents dimerization, qk^{e5} is a severe regulatory mutation and qk^{v} is a mild regulatory mutation. The affect of qk^{kt1} remains to be determined.

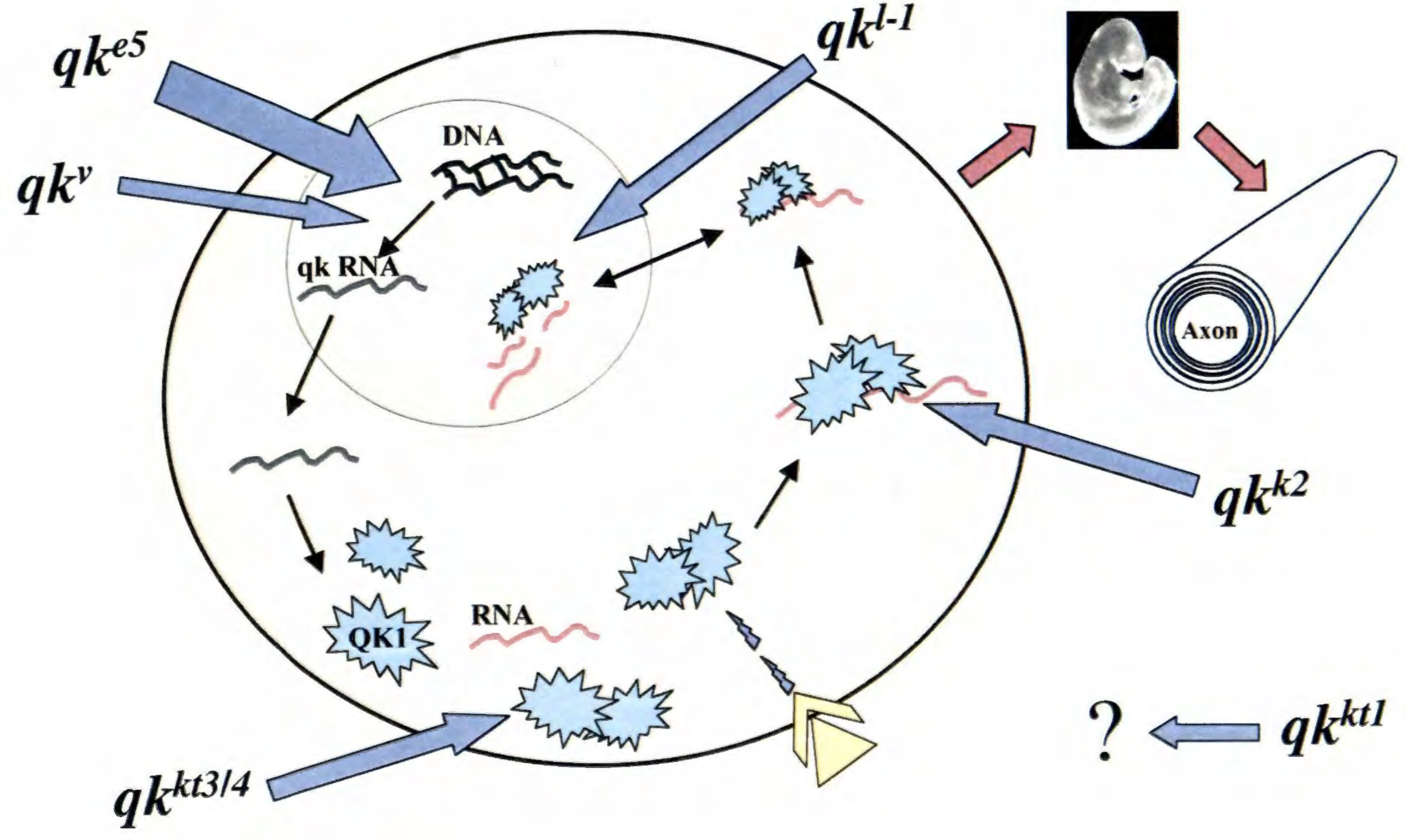
qk^{e5}
qk^{v}
DNA
qk RNA
qk^{l-1}
QK1
RNA
Axon
qk^{k2}
$qk^{kt3/4}$
?
qk^{kt1}

VITA

Janice K. Noveroske was born in Concord, California on August 3, 1968. She was raised in Midland, Michigan where she attended Midland Public Schools and graduated from Midland High School in June 1986. She pursued an undergraduate degree at both Delta College and Michigan State University, receiving a Bachelor of Science degree in Zoology from Michigan State University in June 1992. In August 1992 she entered the University of Tennessee, Knoxville where she received a Master of Science degree in Zoology in May 1995. Janice received a Doctor of Philosophy degree in Zoology through the University of Tennessee, Knoxville in December 2000 and is pursuing post-doctoral research in mammalian development.